UNIVERSITY OF KWAZULU-NATAL ™

INYUVESI YAKWAZULU-NATALI

SMART REAL-TIME SCHEDULING OF GENERATION UNITS IN AN ELECTRICITY MARKET CONSIDERING ENVIRONMENTAL ASPECTS AND PHYSICAL CONSTRAINTS OF GENERATORS

By

Arman Goudarzi

A thesis submitted in fulfilment of the academic requirements for the degree of Doctor of Philosophy in Electrical Engineering at the School of Engineering, University of KwaZulu-Natal

Supervisor: Dr Andrew G Swanson

Co-Supervisor: Dr John Van Coller

16 March 2017

COLLEGE OF AGRICULTURE, ENGINEERING AND SCIENCE

DECLARATION 1 - PLAGIARISM

I, Arman Goudarzi, declare that:

(i) The research presented in this thesis, except where otherwise indicated, and is my original work.

(ii) This thesis has not been submitted for any degree or examination at any other university.

(iii) This thesis does not contain other persons' data, pictures, graphs or other information, unless specifically acknowledged as being sourced from other persons.

(iv) This thesis does not contain other persons' writing, unless specifically acknowledged as being sourced from other researchers. Where other written sources have been quoted, then: a) their words have been re-written but the general information attributed to them has been referenced; b) where their exact words have been used, their writing has been placed inside quotation marks, and referenced.

(v) Where I have reproduced a publication of which I am an author, co-author or editor, I have indicated in detail which part of the publication was actually written by myself alone and have fully referenced such publications.

(vi) This thesis does not contain text, graphics or tables copied and pasted from the internet, unless specifically acknowledged, and the source being detailed in the thesis and in the References sections.

Arman Goudarzi Date

……

As the candidate's supervisor I agree/do not agree to the submission of this thesis.

Dr Andrew G Swanson Date

……

Dr John Van Coller Date

……

COLLEGE OF AGRICULTURE, ENGINEERING AND SCIENCE

DECLARATION 2 – PUBLICATIONS

Details of contributions to publications that form part and/or include research presented in this thesis (include publications in preparation, submitted, *in press* and published and give details of the contributions of each author to the experimental work and writing of each publication).

Publication 1: South African Universities Power Engineering Conference, Vol. 22, pp. 212-217, 2014.
Conference Title: Comparison of Evolutionary Optimization Techniques on Economic Load Dispatch with Transmission Line Constraints.
Authors: Arman Goudarzi, Akshay Kumar Saha

Publication 2: Computational Intelligence Applications in Smart Grid (CIASG), IEEE, pp. 1-7, 2014.
Conference Title: Intelligent Analysis of Wind Turbine Power Curve Models.
Authors: Arman Goudarzi, Innocent E. Davidson, Afshin Ahmadi, Ganesh K. Venayagamoorthy

Publication 3: SAIEE Africa Research Journal, Vol. 107, N0. 3, pp. 146-166, 2016.
Journal Title: Non-Convex Optimisation of Combined Environmental Economic Dispatch through Cultural Algorithm with Considering Physical Constraints of Generation units and Price Penalty Factors.
Authors: Arman Goudarzi, Afshin Ahmadi, Andrew G. Swanson, John Van Coller

Publication 4: Energy, Vol. 113, pp. 338-354, 2016.
Journal Title: Evaluating the impact of sub-hourly unit commitment method on spinning reserve in presence of intermittent generators.
Authors: Mehdi Kazemi, Pierluigi Siano, Debora Sarno, Arman Goudarzi
Contributions: Partial contribution in conceptual and mathematical formulation of the proposed methodology, programming of the proposed algorithms and writing.
Amount of contribution: 40 percent.

Publication 5: Applied Energy, Vol. 189, pp. 667-696, 2017.
Journal Title: Smart Real-Time Scheduling Of Generation units in an Electricity Market Considering Environmental Aspects and Physical Constraints of Generators.
Authors: Arman Goudarzi, Andrew G. Swanson, John Van Coller, Pierluigi Siano

Publication 6: Texas Power and Energy Conference (TPEC), 2017, accepted.
Conference Title: Non-Convex Optimization of Combined Environmental Economic Dispatch through the Third Version of the Cultural Algorithm (CA3).
Authors: Arman Goudarzi, Andrew G. Swanson, Fatemeh Tooryan, Afshin Ahmadi

Arman Goudarzi Date

……

Acknowledgements

Thank the almighty God for seeing me through all times.

To my lovely family and friends.

Abstract

The complexity of the electric power system increases with the deployment of new electricity market structures, integration of renewable energy, distributed generation, the injection of electric vehicles and other controllable loads. With these changes the need for optimal allocation of generation units becomes more important. However, this leads to an increase in uncertainty and erratic behaviour of the power system. Therefore, for the reliable operation of the system, modifications to current methods for power grid management models need to be identified and applied including economic load dispatch (ELD), unit commitment (UC) and optimal power flow (OPF). The main focus of this thesis is to develop fundamental theories and accurate analysis tools for smart real-time scheduling of generation units, specifically in the framework of the current and future requirements of the power network for optimal management of the generating resources. The main issues which are related to smart scheduling of generators are addressed in various scenarios based on the static and dynamic conditions of the system. Improvements have been obtained in terms of energy and cost efficiency through the proposed approaches and algorithms. The existing techniques and state of the art techniques have been mathematically enhanced through the proposed methodology in terms of time efficiency for analysis of large-scale of the power system while obtaining more cost-efficient results.

The foundation of this thesis is based on three studies, where each study analysed and investigated a single issue related to smart scheduling of the generation units from different point of view. The first study focusses on classical ELD due to the increased the environmental concern of rising levels of greenhouse gasses such as carbon oxide (CO), carbon dioxide (CO_2) and nitrogen dioxide (NO_x). The main emphasis of the analysis was on the optimal regulation of NO_x. The classical ELD was upgraded into a more challenging and multi-objective problem the so-called combined environmental economic dispatch (CEED). The study used a new technique to convert the resultant multi-objective problem into a single objective problem by means of price penalty factors (PPFs), where an optimization algorithm was utilized to find the most optimum solution. To simulate the complication of the real world constraints of the power system as well as the generation units the following constraints including the valve-point effect, emission costs, the prohibited operation zone, the ramp rate limit, and the transmission losses were taken into account.

The focus of the second study was to find a real-time solution for CEED in an electricity market environment considering the instantaneous changes of load demand due to the dynamic behaviour of power system and various demand response programs (DRPs) proposed by the system operator. The practical constraints of generating unit's constraints have been considered to emulate the complexity of the power system. A hybrid mathematical approach based on the

least square support vector machine (LSSVM) and the third version of cultural algorithm (CA3), which was formulated in the first paper, was proposed to solve the problem. A number of test cases were used to investigate the practicality of the method and the results of the proposed method were compared to other prominent recently developed methods.

The third study proposed a solution for UC problem while the two worldwide integrated renewable energies (wind and solar) are embedded into system. To find a solution for real-time scheduling of the generation units considering the intermittency of distributed energy resources and the physical constraints of the thermal generators, the proposed solution has been formulated on a sub-hourly basis, where the time resolutions are divided into 60, 30, 15, 10 and 5 minutes. In this study, a unique version of dynamic programming (DP) has been employed to deal with UC problem which a simple version of quadratic programming (QP) based on formulation of mixed integer quadratic programming (MIQP) which has been presented in the second study has been utilized to solve ELD.

After applying the proposed methods of study on different test cases through to several scenarios, the results shows the outperformance of the methodologies of the study over the other well-known methods and confirms the efficiency and practicality of the proposed methodologies for real-time dispatching of generation resources in an electricity market.

Table of Contents

DECLARATION 1 - PLAGIARISM ii
DECLARATION 2 – PUBLICATIONS iii
Acknowledgements iv
Abstract v
Table of Contents vii
List of Figures ix
List of Tables xii
Nomenclature xiv
1. Chapter 1 xviii
Introduction 1
1.1 Background of the study 1
1.2 Aims of the study 2
1.3 Contributions of the study 3
1.4 Layout of the study 4
2. Chapter 2 5
2.1 Introduction 6
2.2 Problem Formulation 9
2.2.1 Combined environmental economic dispatch (CEED) 9
2.3 Evaluation of generation levels 14
2.4 Cultural algorithms 15
2.4.1 The basic concepts of cultural algorithm 15
2.4.2 Belief space 16
2.5 Results and discussion 20
2.5.1 Case 1 21
2.5.2 Case 2 26
2.5.3 Case 3 30
2.6 Conclusions 35
2.7 References 36
3. Chapter 3 40
3.1 Introduction 41
3.2 Problem formulation 47
3.2.1 Time window for the wholesale electricity market operation 47
3.2.2 Combined environmental economic dispatch (CEED) 48
3.3 The third version of Cultural Algorithm (CA3) 52
3.4 Least square support vector machine (LSSVM) 55

3.5 Evaluation of prediction performance 60
3.6 Results and discussion 61
3.6.1 Test Case 1 64
3.6.2 Test Case 2 69
3.6.3 Test Case 3 76
3.6.4 Test Case 4 82
3.6.5 Test Case 5 86
3.7 Conclusions 89
3.8 References 91
3.9 Appendix 96
3.9.1 Appendix A 96
3.9.2 Appendix B 97
3.9.3 Appendix C 98
4. Chapter 4 101
4.1 Introduction 102
4.2 Problem formulation 105
4.2.1 Statement of the problem 105
4.2.2 System constraints 107
4.2.3 Diesel unit constraints 108
4.2.4 Renewable system constraints 109
4.3 Proposed method for unit commitment (UC) 111
4.3.1 Initial diesel UC and ELD 114
4.3.2 Diesel UC and ED incorporating wind and PV power 116
4.3.3 Modelling choices and input data 118
4.4 Numerical experiments 120
4.4.1 Case study 1: Ten-unit thermal system UC and ELD with and without WT and PV power plants 121
4.4.2 Case study 2: IEEE 118-Bus test system thermal system UC and ELD with and without WT and PV power plants 126
4.5 Conclusions 130
4.6 References 132
5. Chapter 5 135
5.1 Conclusions 136
5.2 Recommendations 137

List of Figures

2.1 Fuel cost function curve for CEED with valve-point loading effect……..10

2.2 Operation of generation units when considering ramp rate limits…….12

2.3 Fuel cost function curve with prohibited operating zones…….12

2.4 Illustration of conceptual framework of cultural algorithm based on the two spaces……15

2.5 Best obtained solution in the search space for case 1…….22

2.6. a Convergence process of CEED cost through the Max-Max PPF (5 generation units)…...23

2.6.b Convergence process of CEED cost through the Max-Min PPF (5 generation units)……23

2.6.c Convergence process of CEED cost through the Min-Max PPF (5 generation units)……23

2.6.d Convergence process of CEED cost through the Min-Min PPF (5 generation units)…….24

2.7 Best obtained solution in the search space for case 2…….26

2.8.a Convergence process of CEED cost through the Max-Max PPF (20 generation units)…..27

2.8.b Convergence process of CEED cost through the Max-Min PPF (20 generation units)…..27

2.8.c Convergence process of CEED cost through the Min-Max PPF (20 generation units)…..27

2.8.d Convergence process of CEED cost through the Min-Min PPF (20 generation units)…..28

2.9 Best obtained solution in the search space for case 3…….31

2.10.a Convergence process of CEED cost through the Max-Max PPF (50 generation units)…31

2.10.b Convergence process of CEED cost through the Max-Min PPF (50 generation units)…31

2.10.c Convergence process of CEED cost through the Min-Max PPF (50 generation units)…32

2.10.d Convergence process of CEED cost through the Min-Min PPF (50 generation units)…32

3.1 Time frame of the electricity market operation……..48

3.2 Conceptual framework of cultural algorithm based on the two spaces……..53

3.3 General network structure of LSSVM-CA3……...58

3.4 flow chart process of LSSVM-CA3……...59

3.5 Daily load curve for 15 units system……..64

3.6.a Convergence process of LSSVM-CA3 adjusting parameters (first predicted load point, 1600 MW)……65

3.6.b Convergence process of LSSVM-CA3 adjusting parameters (second predicted load point, 2475 MW)……65

3.7.a Residual representation for the first predicted load point (1600 MW)……67

3.7.b Residual representation for the second predicted load point (2475 MW)……...68

3.8.a Evaluation of RMSE and MAE for the first predicted load point (1600 MW)……...68

3.8.b Evaluation of RMSE and MAE for the second predicted load point (2475 MW)……..69

3.9 Daily load curve for 40 units system……..70

3.10 Total generation cost of the day for the 40 units system……..70

3.11.a Convergence process of LSSVM-CA3 adjusting parameters (first predicted load point, 7550 MW)…….71

3.11.b Convergence process of LSSVM-CA3 adjusting parameters (second predicted load point, 8260 MW)……71

3.12.a Residual representation for the first predicted load point (7500 MW)……..74

3.12.b Residual representation for the second predicted load point (8260 MW)…….74

3.13.a Evaluation of RMSE and MAE for the first predicted load point (7500 MW)…….75

3.13.b Evaluation of RMSE and MAE for the second predicted load point (8260 MW)……75

3.14 Daily load curve for 140 units system……..76

3.15.a Convergence process of LSSVM-CA3 adjusting parameters (first predicted load point, 36500 MW)……...77

3.15.b Convergence process of LSSVM-CA3 adjusting parameters (second predicted load point, 41800 MW)……..77

3.16.a Residual representation for the first predicted load point (36500 MW)……79

3.16.b Residual representation for the second predicted load point (41800 MW)……...80

3.17.a Evaluation of RMSE and MAE for the first predicted load point (36500 MW)……...80

3.17.b Evaluation of RMSE and MAE for the second predicted load point (41800 MW)……..81

3.18 Evaluation of NRMSE for all the studied cases……...81

3.19.a Residual representation for the first predicted load point (125000 MW) of case 4, Training Phase…….83

3.19.b Residual representation for the first predicted load point (125000 MW) of case 4, Testing Phase……83

3.20.a Residual representation for the second predicted load point (139000 MW) of case 4, Training Phase……..84

3.20.b Residual representation for the second predicted load point (139000 MW) of case 4, Testing Phase……84

4.1 Autonomous hybrid system……..105

4.2 UC via forward DP……...112

4.3 Overall schematic of proposed method……113

4.4 Approximation (solid) of the quadratic cost function (dashed) vs. power output……117

4.5 Performance curve of the Enercon 330 turbine……119

4.6 PV efficiency vs. radiation……...119

4.7 Hourly generators' behavior and required reserve……123

4.8 Hourly contributions of diesel and renewable power plants ……...124

4.9 Comparison of hourly available and required spinning reserves after applying renewable power……..124

4.10 Hourly generators' behaviour and required reserve……128

4.11 Hourly contributions of diesel and renewable power plants……..128

4.12 Comparison of hourly available and required spinning reserves after applying renewable power……..129

List of Tables

2.1 Cost coefficients and physical operating limits of generation units……...21

2.2 Ramp rate limits and POZ information of generation units……...21

2.3 Emission curve coefficients of generation units…….22

2.4 The transmission loss coefficients……..22

2.5 Comparison of the obtained results for Case 1……...25

2.6 The best obtained solutions of the proposed method (CA3) for case 1……..26

2.7 Comparison of the obtained results for Case 2……...29

2.8 The best obtained solutions of the proposed method (CA3) for case 2……..30

2.9 Comparison of the obtained results for Case 3……...33

2.10 The best obtained solutions of the proposed method (CA3) for case 3……34

3.1 Final optimized values for LSSVM-CA3 adjusting parameters (15 units system)……66

3.2 Comparison of the obtained results for MSE (15 units system)…….66

3.3 Comparison of the obtained results for MSE (40 units system)…….73

3.4 Final optimized values for LSSVM-CA3 adjusting parameters (40 units system)……73

3.5 Final optimized values for LSSVM-CA3 adjusting parameters (140 units system)……..78

3.6 Comparison of the obtained results for MSE (140 units system)……...78

3.7 hourly load data for 420 units system…….82

3.8 Final optimized values for LSSVM-CA3 adjusting parameters (420 units system)……..85

3.9 Comparison of the obtained results for MSE (420 units system)……...85

3.10 Comparison of the obtained results for the error analysis (420 units system)…….86

3.11 Results of random execution of the proposed algorithm (15 units system)…….86

3.12 Results of random execution of the proposed algorithm (40 units system)…….87

3.13 Results of random execution of the proposed algorithm (140 units system)……...87

3.14 Comparison of the proposed algorithm with the higher number of the population size of ANN-GAPSO (15 units system)……...87

3.15 Comparison of the proposed algorithm with the higher number of the population size of ANN-GAPSO (40 units system)……...88

3.16 Comparison of the proposed algorithm with the higher number of the population size of ANN-GAPSO (140 units system)…….88

3.17 Comparison of the proposed algorithm with LSSVM-GAPSO (15 units system)……...88

3.18 Comparison of the proposed algorithm with LSSVM-GAPSO (40 units system)……...89

3.19 Comparison of the proposed algorithm with LSSVM-GAPSO (140 units system)…….89

4.1 Example of unit combination based on priority listing order……...113

4.2 Solar radiation and corresponding power data…….121

4.3 Hourly wind speed and wind power data…….121

4.4 Load demand of 10-unit base problem…….122

4.5 Diesel unit characteristics of 10-unit base problem…….122

4.6 Comparison of hourly results of various DP-UC for 10-Diesel case……...122

4.7 10-Diesel system initial UC and ELD power [kW]…….……122

4.8 10-Diesel system UC and ELD power output [kW] incorporating renewable power plants……...123

4.9 Total production costs of various time resolutions with and without renewable power…..125

4.10 Comparison of available and required reserves' mean values with and without renewable power……..125

4.11 Comparison of hourly results of DP-BP and [13] for IEEE 118-bus case…….126

4.12 IEEE 118-bus test system initial UC and ELD power output [MW]…….126

4.13 IEEE 118-bus test system UC and ELD power output [MW] incorporating renewable power plants……...127

4.14 Total production costs of various time resolutions with and without renewable power…129

4.15 Comparison of available and required reserves' mean values with and without renewable power……..130

Nomenclature

Indexes

ANN	Artificial Neural Network
CA	Cultural Algorithm
CA3	Third version of the Cultural Algorithm
CEED	Combined environmental economic dispatch
ELD	Economic load dispatch
CF	Cost function
DRP	Demand response program
FC	Final production cost
KKT	Karush-Kuhn-Tucker
LSSVM	Least square support vector machine
MAE	Mean absolute error
MIQP	Mixed integer quadratic programming
MSE	Mean squared error
NRMSE	Normalized root mean squared error
OPF	Optimal power flow
RBF	Radial basis function
RMSE	Root mean squared error
PF	Penalization factor
PPFs	Price penalty factors
POZ	Prohibited operating zone
SVM	Support vector machine
UC	Unit commitment

Variables

a_i, b_i, c_i	Fuel cost coefficients of unit *i*
$\alpha_i, \beta_i, \gamma_i, \eta_i, \delta_i$	Emission cost coefficients of unit *i*

d_i, e_i	Fuel cost coefficients of unit *i* regarding valve-point effects
$B(t)$	Belief space of cultural algorithm
B_{ij}	ij^{th} element of the loss coefficient square matrix
B_{0i}	i^{th} element of the loss coefficient vector
B_{00}	Loss coefficient constant
cc_i	Cold start-up cost of the i^{th} diesel generator
csh_i	Cold start hour of the i^{th} diesel generator
$e_i(t)$	Vector which describes the status of the i^{th} diesel generator
$e_i^D(t)$	Denotes the availability of the i^{th} diesel generator
$e_j(t)$	Vector which describes the status of the j^{th} wind turbine
$e_j^W(t)$	Denotes the availability of the j^{th} wind turbine
$e_k(t)$	Vector which describes the status of the k^{th} PV generator
$e_k^{PV}(t)$	Denotes the availability of the k^{th} PV generator
$F_{ct}(P_i^t)$	Total CEED generation cost at time *t*
$f_{emc}(P_i^t)$	Emission cost function at time *t*
$f_{gc}(P_i^t)$	Generation cost function at time *t*
h_i	Coefficient of price penalty factor
$h_i^{max-max}$	Max-Max price penalty factor
$h_i^{max-min}$	Max-Min price penalty factor
$h_i^{min-max}$	Min-Max price penalty factor
$h_i^{min-min}$	Min-Min price penalty factor
hc_i	Hot start-up cost of the i^{th} diesel generator
$I_j(t)$	Closed interval of $N(t)$
l, u	The lower and upper bound which are initialized by the domain values
$L_j(t)$	Score of the lower bound at $N(t)$
N_G	Number of generation units
N_D	Number of diesel generator

N_{WT}	Number of wind turbine
N_{PV}	Number of PV generator
$N(t)$	Normative knowledge component of the cultural algorithm
N_{ij}	A normalized number for individual *i* and component *j*
n_s	Number of variables of the situational component
n_x	Number of variables of the normative component
nz_i	Number of prohibited zones for unit *i*
ψ	Sets of units with POZ
Ψ	Sets of units with S_R
P_i^t	Power output of unit *i* at time *t*
P_D^t	Load demand of the system at time *t*
P_i^0	Previous output power (*t-1*)
$P_{i,1}^L$	Lower bound of unit *i* at the first prohibited zone *i*
P_i^{min}, P_i^{max}	Minimum and maximum generation limits of the i^{th} generating unit
$P_{i,m}^L, P_{i,m-1}^U$	Lower and upper bound of the m^{th} prohibited zones of unit *i*
$P_{i,N_i^{PZ}}^U$	The last upper bound of the nz^{th} prohibited zones of unit *i*
$P_{i,l}^l, P_{i,l}^U$	Lower and upper bound of the l^{th} prohibited zones of unit *i*
$P_{i,k}^l, P_{i,k}^U$	Lower and upper bound of the k^{th} prohibited zones of unit *i*
$P_{i,nz}^l, P_{i,nz}^U$	Lower and upper bound of the nz^{th} prohibited zones of unit *i*
$P_{D_i}^{min}$	Minimum power output of i^{th} diesel generator
$P_{D_i}^{max}$	Maximum power output of i^{th} diesel generator
$P_D^*(t)$	Total available diesel generator
$P_W^*(t)$	Total available wind generation
$P_{PV}^*(t)$	Total available PV generation
$\underline{P_L}(t)$	Minimum diesel loading
$RD_i(t)$	Spinning down reserve
$S(t)$	Situational knowledge component of the cultural algorithm

S_i	Total required spinning reserve of the system
S_i^t	Spinning reserve from unit *i* at time *t*
S_R	Total system spinning reserve requirement
S_i^{max}	Maximum spinning reserve contribution of unit *i*
To	Number of time periods
$T_i^{on/off}$	Minimum up/down time of the i^{th} diesel generator
δ_j	Step size of the belief interval
${\delta_j}^2(t)$	The variance of normalized number N_{ij}
$U_j(t)$	Score of the upper bound of $N(t)$
UR_i, DR_i	Up and down ramp rate limits of unit *i*
$UR_i(t), DR_i(t)$	Up and down ramp capacity of the i^{th} diesel generator at each stage *t*
$X_j(t)$	Dimension of belief space at component *j*
$X_l(t)$	An accepted response
$X_i^{on/off}$	Time for which the i^{th} diesel unit has been on/off at stage *t*
$x_{ij}(t)$	The mean of normalized number N_{ij}
$x_{lj}(t)$	An accepted response of the component *j*
$\acute{x}_{ij}(t)$	Influence function
$x_j^{min}(t), x_j^{max}(t)$	Minimum and maximum boundary of the closed interval at generation *t*
$\hat{y}(t)$	Best individual of the solution vector

1. CHAPTER 1
Introduction

Introduction

1.1 Background of the study

A power system is a vast, complicated and interconnected power grid with the inclusion of generation, transmission lines, distribution, and loads. As the load points are generally located far away from the generation units, the generated electric power has to be transferred over long transmission lines which consequently leads to power loss. A main obligation of any power system operator is to ensure a reliable power supply delivery at a minimum cost for their customers. In order to accomplish this goal, it is necessary to monitor, analyse and control the operation of the power system at all times. Therefore, it is essential for the power system operators to have an efficient tool to optimally analyse the system behaviour. These useful and critical tools are commonly known as the optimization techniques such as unit commitment (UC) and economic load dispatch (ELD).

The UC problem is a process of selecting which generation units should be in service during a specified scheduling period and for how long. The committed generation units must meet the total system load demand as well as the required reserve levels at the lowest operating cost, subject to a number of system constraints. The operating cost of thermal generation units is comprised of variety costs such as fuel, start-up, transition, labour, and maintenance cost. The UC problem would become a considerably complex and challenging problem in the case of large interconnected power systems, where in some cases in the industry practices to avoid the increase in computation time, they terminate the optimization software and simply run the basic iterative methods to just have a fair estimation of the situation. Some of the well-known optimization techniques for solving UC are listed as follows:

- Priority list ordering
- Dynamic programming
- Lagrangian based methods
- Branch-and-bound methods
- Mixed integer programming methods

The economic load dispatch ELD as the main sub-problem of the UC only deals with the optimal allocation of the power generation between the running units while satisfying the power balance equations and maintaining the physical operational constraints of generation units. As the global awareness is increasing with respect to reducing the pollutant gasses, it would be more complex to find a solution for ELD problem with a multi-objective function which can simultaneously minimise generation fuel cost and regulate emission levels optimally. The resulting problem is called combined environmental economic dispatch (CEED), where the

CEED problem will be extremely non-convex and non-linear when considering the physical constraints of generation units such as valve-point effect, ramp-rate limits, and prohibited operating zones. In the past few years, a lot of optimization approaches have been applied to solve ELD and CEED problem, where some of these prominent approaches are listed as follows:

- Lambda iteration method
- Lagrangian multiplier method
- Gradient-based methods
- Linear programming
- Genetic algorithm
- Particle swarm optimisation
- Biography based method
- Ant colony optimisation
- Artificial bee colony optimisation

1.2 Aims of the study

The aims of the study are:

- To consider several physical and environmental constraints of generation units in solving CEED Problem.
- To presenting four new optimisation algorithms for solving the CEED problem based on cultural algorithm concept.
- To propose a hybrid mathematical method based on LSSVM-CA3 for solving the CEED problem.
- To propose a solution for real-time scheduling of generation units in electricity spot markets.
- To present a holistic optimization method for real-time prediction in a dynamic environment of the power grid.
- To present a robust solution for the sub-hourly UC problem based on the integration of dynamic programming and priority list ordering method.
- To consider a number of physical and operational constraints of thermal and distributed intermittent generators for the sub-hourly UC problem.
- To propose a practical solution for cost saving in the dispatch of a mixed-generation based system while satisfying the system's reliability.
- To apply and investigate the practicality of the methods and algorithms on standard benchmark models.

1.3 Contributions of the study

The contributions of the study are:

- Four different versions of the cultural algorithm have been introduced to solve CEED problem.
- The impact of four different types of penalty factor on the total generation cost has been examined.
- The proposed CA3 method has been tested and employed in the system with 50 generators with the consideration of all the constraints of the generation units as well as the environmental constraints.
- A hybrid mathematical method for the prediction of the behaviour of any dynamic system based on the least square support vector machine and the third version of the cultural algorithm (LSSVM-CA3) has been proposed.
- The proposed LSSVM-CA3 method has the ability to understand and predict the non-linear behaviour of the power grid considering several realistic physical constraints of generation units for solving the CEED problem.
- The proposed LSSVM-CA3 method has the capability to comprehend and predict the environmental aspects of generation units in the real-time analysis of a large-scale power system.
- The proposed LSSVM-CA3 method is capable of finding the optimum schedule of generation units for a large-scale power system in a real-time electricity market within an extremely fast calculation time.
- The proposed LSSVM-CA3 method is capable of maximization of social welfare while minimization of total cost of generation in the real-time electricity market.
- Introduced a mathematical method based on combination of dynamic programming and best per unit cost (DP-BP) for solving sub-hourly UC in presence of intermittent generators.
- The proposed DP-BP method introduced a new formulation of ramp rates limits for real-time scheduling of thermal units.
- Introduced a piecewise linear cost function for scheduling of generation units to reduce the computation time for sub-hourly UC.

1.4 Layout of the study

Chapter 1 represents the background and statement of the problem of the thesis. This chapter contains the aims of the study, key contributions of the study and organisation of the thesis.

Chapter 2 is based on the paper No.3, it describes the mathematical formulation of the CEED problem through to price penalty factors. The four versions of the cultural algorithm have been developed. The effectiveness of the proposed methods has been examined on different standard test systems.

Chapter 3 is established according to paper No. 5. This chapter describes a hybrid solution for the smart real-time scheduling generators based on least square support vector machine (LSSVM) and the third version of the cultural algorithm (CA3). The various scenarios and test cases have been considered to ensure the practicality of the proposed method.

Chapter 4 is structured on paper No. 4. This chapter formulated a unique solution for UC problem based on the combination of dynamic programming and priority list ordering method, where quadratic programming has been used to solve the ELD problem. Several operational constraints of thermal generators and uncertainty of renewable resources (the wind and solar) have been considered in process of optimization. The efficiency of the proposed method has been verified over two IEEE benchmarks, where results confirmed the applicability of the solutions.

Chapter 5 presents the conclusions of the study and some recommendations for the future work.

2. CHAPTER 2

Paper Number 3

Non-Convex optimisation of Combined Environmental Economic Dispatch through Cultural Algorithm with The consideration of the Physical Constraints of Generation units and Price Penalty Factors

Non-Convex optimisation of Combined Environmental Economic Dispatch through Cultural Algorithm with The consideration of the Physical Constraints of Generation units and Price Penalty Factors

Abstract- Four versions of cultural algorithm have been proposed to find an optimal solution of the combined environmental economic dispatch problem. The main objective of CEED is to simultaneously minimize two competitive objectives of fuel cost and emission, while satisfying various power system constraints such as the valve-point effect, emission costs, the prohibited operation zone, the ramp-rate limit, and the transmission losses. In order to solve this non-convex and non-continuous multi-objective optimization problem with cultural algorithm, the objective function has been converted to a single objective using a technique called price penalty factor. Four different types of penalty factors are examined in this paper. Three different test case systems with 5, 20, and 50 generation units have been implemented to investigate the performance and effectiveness of proposed algorithms. The cultural algorithm shows a superior performance in handling the combined environmental economic dispatch problem in comparison to other methods.

Keywords: Combined environmental economic dispatch, cultural algorithm, price penalty factors, prohibited operating zones, ramp-rate limits, valve-point effect.

2.1 Introduction

Economic dispatch (ED) is an optimization task in the power system that attempts to determine the optimal distribution of power demand among the committed generation units for the purpose of minimizing total operating cost while satisfying a set of equality and inequality system constraints. With increased environmental concerns and given that thermal power plants release significant amount of pollutants such as sulphur oxides (SO_x), nitrogen oxides (NO_X), carbon monoxide (CO), and carbon dioxide (CO_2) into the atmosphere, it has become essential to not only minimize the fuel cost but also the emission level of these harmful gases. In [1], several scenarios of emission reduction such as installation of pollution control devices, burning low-emission fuels, replacement of aged fuel burners and the use of renewable energy resources have been considered for combined environmental economic dispatch (CEED) problem. The latter solution has become an attractive short term strategy due to its economic advantages and ease of implementation [2], [3]. CEED is a multi-objective optimization problem that attempts to simultaneously minimize two competitive objectives of fuel cost and emission of gaseous pollutants which are both related to system constraints.

Various techniques have been proposed considering the CEED problem. The majority of the algorithms can be categorized as either mathematical or evolutionary optimization techniques. Mathematical techniques have fast computational time and they are able to find near exact solutions for convex problems through convex objective function, while sometimes they would fall in to local minima or maxima. Some researchers have tried to develop mathematical methods to handle the CEED problem. Nanda et al. aimed to solve the CEED problem concerning line power flow constraint by developing a classical technique based on coordination equations [4]. A single objective function using a linear combination of different objectives as a weighted sum was developed in [5]. Unfortunately, multiple runs are required for this method and it also fails to solve non-convex functions [6]. A nonlinear unconstrained/constrained multi-objective mathematical formulation based on a fast ε-constraint approach was introduced in [7] where fuel cost and environmental impact were treated as competing objectives.

The CEED problem becomes a nonlinear, non-convex and non-continuous optimization problem when the real-world power system constraints such as valve point effect, prohibited zone, ramp rate limits, and transmission losses are considered [8-10]. It is impractical to find a unique optimal solution using mathematical techniques with respect to all these constraints. To tackle this issue, researchers have been attracted to apply heuristic optimization algorithms to solve the CEED problem. These methods usually deal with non-smooth non-convex functions but, as a drawback, the computational time is long since they carry out a population of potential solutions simultaneously. Applications of different heuristic techniques pertaining to the CEED problem have been reported in literature. In [8], the price penalty approach has been presented, where the bi-objective CEED problem was converted to a single objective through to max-max price penalty factor, after which various heuristic techniques such as genetic algorithm (GA), evolutionary programming (EP), particle swarm optimization (PSO), and differential evolution (DE) were applied to obtain and compare the solutions for the IEEE 30-bus system and 15-unit system. The valve-point effect and transmission losses were not considered in this study [8]. In [11], the applicability of biogeography-based optimization technique to find the solution of CEED problem has been presented. The proposed algorithm was implemented in three, six and fourteen generation units test systems and results are compared to the solutions based on Newton–Raphson, Tabu search, GA, non-dominated sorting genetic algorithm (NSGA), fuzzy logic controlled genetic algorithm, PSO and DE. A game theory based model was developed in [3] to address the multi-objective dynamic economic emission dispatch problem taking into account transmission losses. Senthil proposed a lambda based approach using EP to solve the CEED problem considering powering limits [12]. The algorithm was tested on a power system consisting three and six generators. A gravitational search algorithm has been suggested for the solution of CEED problem in [13-16] and various test cases with and without the valve-point effect and

transmission losses were considered in these studies. Many other heuristic algorithms such as NSGA-II [17, 18], bacterial foraging [19-21], enhanced firefly algorithm [22], advanced parallelized PSO [23], fuzzified multi-objective PSO [24], multi-objective chaotic PSO [25], opposition-based harmony search algorithm [26], bee colony [2] and several others has been reported in the literature to obtain the solution of CEED problem.

Cultural Algorithm (CA) is an evolutionary optimization method which was first introduced by Reynolds in 1994 [27]. Cultural algorithm consists of an evolutionary population space (genetic component) and a belief space (cultural principals). CA was initially designed to handle single objective optimization problems. To cope with multi-objective problems, either a hybrid optimization algorithm should be developed or the multi-objective function should be converted to a single function. Few studies have successfully implemented CA for the solution of CEED problem. In [28], evolutionary programming was embedded into CA for this purpose and constraints such as ramp rate limits, forbidden zone of operation, valve point loading effects and transmission losses were considered. The method was tested on three generator, six generator and fourteen generator systems. Rui Zhang et al. [6] developed a hybrid PSO-CA technique to address the CEED problem considering prohibited operating zones and generators limit. Two test systems were implemented to verify efficiencies of proposed method. A hybrid multi-objective cultural algorithm method was presented in [29] to carry out the optimal short-term environmental/economic hydrothermal scheduling. The proposed hybrid method combined DE algorithm into the framework of CA.

In this study, an approach based on price penalty factor, i.e. ratio of fuel cost to emission value has been used to convert the multi-objective combined emission and economic dispatch problem into a single objective function. To replicate a real-world power system, the following constraints of generation units such as ramp-rate limits, prohibited operating zones, valve-point effect, and transmission losses have been considered. The effectiveness of CA in handling complex CEED problems has been verified on three test systems with 5, 20 and 50 generation units and non-smooth fuel cost functions. Simulation results have been compared with other heuristic optimization techniques such as biography based optimizer (BBO), restricted ant colony optimizer (ACOR), artificial bee colony (ABC), PSO, GA, hybrid GA and PSO (GAPSO), and firefly algorithm (FA). The main contributions of this paper are as follows:

i) Four different versions of cultural algorithm have been employed to solve CEED problem. To the best of authors' knowledge, a similar study has never been reported.
ii) The impact of four different types of penalty factor on the final price has been examined. No other study has investigated the effect of different penalty factors with the same system considerations and constraints.

iii) The test system with 50 generators and consideration of all the constraints of generation units imposes significant non-linearity to the system. The convergence to the optimal solution will become cumbersome as it is the largest reported test case for solving CEED problem.

The organization of this study is as follows. Sections 2.2 to 2.4 demonstrates the problem formulation and mathematical methods. Section 2.5 provides simulation results, where the effectiveness and superiority of the proposed method to solve the CEED problem has been comprehensively discussed. Subsequently, the conclusion is given in Section 2.6.

2.2 Problem Formulation

2.2.1 Combined environmental economic dispatch (CEED)

The main objective of classical economic load dispatch (ELD) is to minimize the total cost of generation by determining the optimum scheduling of generation units and ensuring the satisfaction of system constraints. This study has divided the operation constraints into two different categories. The first category is related to the particular characteristics of the generation units such as generation capacity, the valve-point effect and environmental emission levels, while the second one is associated to physical constraints such as ramp rate limits, prohibited operating zones and spinning reserve levels.

The cost objective function of CEED can be represented by means of a quadratic cost function [30]:

$$f_{gc}(P_i) = \sum_{i=1}^{N_G} \left(a_i + b_i P_i + c_i P_i^2\right) \quad (\$/h) \tag{1}$$

The effect of valve-point loading can be modelled by adding a recurring rectified term to the main cost function as given in [30], where the cost function curve with the effect of valve-point loading is shown in Fig 2.1:

$$f_{gc}(P_i) = \sum_{i=1}^{N_G} [\left(a_i + b_i P_i + c_i P_i^2\right) + \left|d_i \times \sin\{e_i \times \left(P_i^{min} - P_i\right)\}\right|] \quad (\$/h) \tag{2}$$

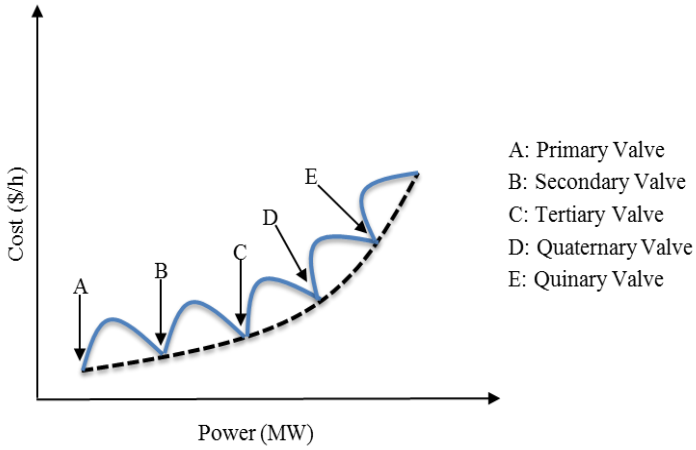

Fig. 2.1 Fuel cost function curve for CEED with valve-point loading effect

Most thermal and fossil-based generation units are major sources of nitrogen oxides (NO_x), and have been strictly advised by the environmental protection agency (EPA) to reduce their emissions. In this study, the emission of NO_x is considered to be optimally moderated from the environmental preservation point of view. The emission cost function, including consideration valve-point effect, can be expressed as follows [31]:

$$f_{emc}(P_i) = \sum_{i=1}^{N_G}[(\alpha_i + \beta_i P_i + \gamma_i P_i^2) + \eta_i \exp(\delta_i P_i)] \quad (lb/h) \tag{3}$$

The total generation cost of CEED as a multi-objective optimization can be converted into single objective function through the combination of generation cost and emission cost as well as the consideration of the price penalty factor h_i [32]:

$$F_{ct}(P_i) = f_{gc}(P_i) + h_i \times f_{emc}(P_i) \tag{4}$$

$$F_{ct}(P_i) = \left[\sum_{i=1}^{N_G}[(a_i + b_i P_i + c_i P_i^2) + |d_i \times \sin\{e_i \times (P_i^{min} - P_i)\}|] + h_i \times \sum_{i=1}^{N_G}[(\alpha_i + \beta_i P_i + \gamma_i P_i^2) + \eta_i \exp(\delta_i P_i)]\right] \quad (\$/h) \tag{5}$$

The proposed CEED objective function is subject to the following constraints:

2.2.1.1 Equality constraint

The total power output of the system should be capable to meeting the total load demand and power losses (I), and in case of lossless systems it should be able to satisfy the total load demand (II):

$$(I) \qquad \sum_{i=1}^{N_G} P_i = P_D + P_L \tag{6}$$

$$(II) \qquad \sum_{i=1}^{N_G} P_i = P_D \tag{7}$$

The power losses of the system can be determined by Korn's loss formula given in [33]:

$$P_L = \sum_{i=1}^{N}\sum_{j=1}^{N} P_i B_{ij} P_j + \sum_{i=1}^{N} B_{0i} P_i + B_{00} \tag{8}$$

Or re-written in matrix notation as:

$$P_L = P^T[B]P + B_0 P + B_{00} \tag{9}$$

2.2.1.2 Inequality constraint

For stable operation, all generation units are strictly constrained to operate at their minimum and maximum generation limits; consequently the inequality constraint is:

$$P_i^{min} \leq P_i \leq P_i^{max} \quad for\ i = 1,2,3 \ldots N_G \tag{10}$$

2.2.1.3 Ramp rate limits

Conforming to [34], the inequality constraints due to ramp rate constraints for changes in generation levels are modified; (I) as generation increases and (II) as generation decreases.

$$(I) \qquad P_i - P_i^0 \leq UR_i \tag{11}$$

$$(II) \qquad P_i^0 - P_i \leq DR_i \tag{12}$$

By considering the inequality constraints, equations (11) and (12) can be rewritten:

$$max\left(P_i^{min}, P_i^0 - DR_i\right) \leq P_i \leq min(P_i^{max}, P_i^0 + UR_i) \tag{13}$$

The Fig 2.2 shows the mechanism of the generation units when considering ramp rate limits.

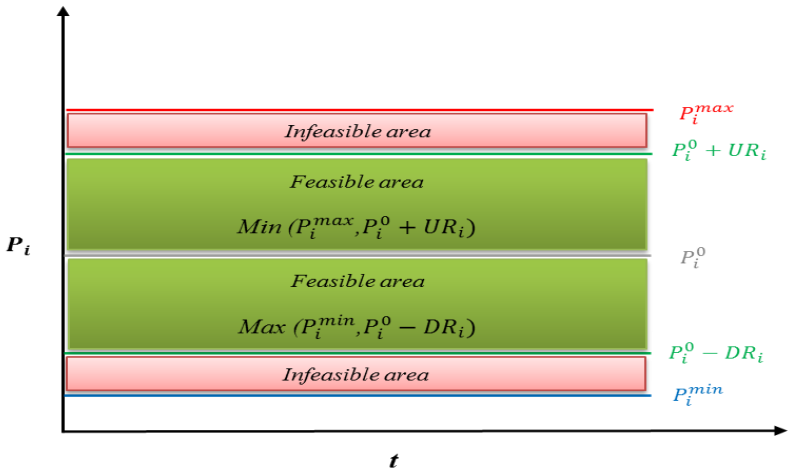

Fig. 2.2 Operation of generation units with considering ramp rate limits

2.2.1.4 Prohibited operating zone (POZ)

The POZ is an interval in which generation units are not able to operate due to the inherent nature of thermal units that may have steam valve operation or vibration in the shaft bearings. The principal of POZ has been depicted in Fig 2.3. The feasible operating zones of unit *i* are described as [35]:

$$\begin{cases} P_i^{min} \le P_i \le P_{i,l}^{l} \\ P_{i,l}^{u} \le P_i \le P_{i,k}^{l} \\ P_{i,k}^{u} \le P_i \le P_{i,nz_i}^{l} \\ P_{i,nz_i}^{u} \le P_i \le P_i^{max} \end{cases} \quad \forall i \in \Omega \qquad (14)$$

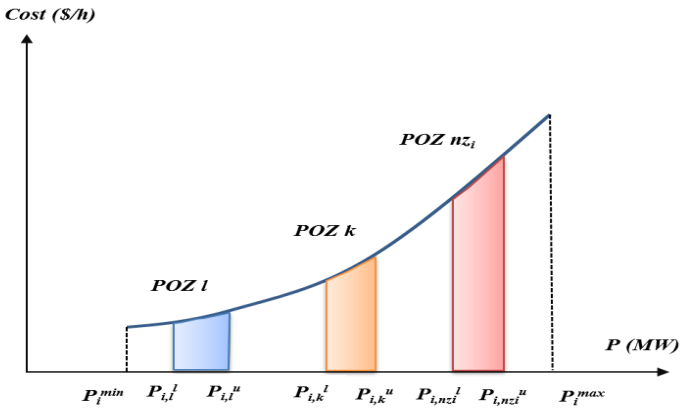

Fig. 2.3 Fuel cost function curve with prohibited operating zones

2.2.1.5 Spinning reserve

To have a reliable operation a minimum spinning reserve should be considered to meet the load fluctuation and unforeseen outages of the generation units and grid components [35]:

$$\sum_{i=1}^{N_G} S_i \geq S_R \tag{15}$$

where

$$S_i = \min\{P_i^{max} - P_i,\ S_i^{max}\};\qquad S_i = 0;\ \forall i \in \Omega \tag{16}$$

Ω is related to sets of units with having POZ. It is significant to mention that spinning reserve will be carried out from units without POZs. Those units with having no POZs are responsible for maintaining the system spinning reserve requirements which it can be set as a fraction of the load demand or equal to the capacity of largest unit [36].

2.2.1.6 Price penalty factors

Four different types of price penalty factors (PPFs) are proposed. PPFs describe the proportion between fuel cost and emission cost curves without considering the valve point effect. The PPFs are as follows (the PPFs are valid in condition of non-zero denominator):

1) Max-Max PPF:

$$h_i^{max-max} = \frac{a_i + b_i P_i^{max} + c_i (P_i^{max})^2}{\alpha_i + \beta_i P_i^{max} + \gamma_i (P_i^{max})^2} \qquad (\$/lb) \tag{17}$$

2) Max-Min PPF:

$$h_i^{max-min} = \frac{a_i + b_i P_i^{max} + c_i (P_i^{max})^2}{\alpha_i + \beta_i P_i^{min} + \gamma_i (P_i^{min})^2} \qquad (\$/lb) \tag{18}$$

3) Min-Max PPF:

$$h_i^{min-max} = \frac{a_i + b_i P_i^{min} + c_i (P_i^{min})^2}{\alpha_i + \beta_i P_i^{max} + \gamma_i (P_i^{max})^2} \qquad (\$/lb) \tag{19}$$

4) Min-Min PPF:

$$h_i^{min-min} = \frac{a_i + b_i P_i^{min} + c_i (P_i^{min})^2}{\alpha_i + \beta_i P_i^{min} + \gamma_i (P_i^{min})^2} \qquad (\$/lb) \tag{20}$$

The main purpose of PPFs is to convert the physical implication of emission standard from emission weight to the fuel cost of the emission.

2.3 Evaluation of generation levels

To ensure that the equality constraint of system is always maintained, this study proposes a power balance violation (PBV) formulation to continuously satisfy the equality constraint. Equation (6) is rewritten as:

$$\sum_{i=1}^{N_G} P_i \geq P_D + P_L \tag{21}$$

by modification on equation (21), the PBV is formulated as:

$$PBV = max(1 - \frac{\sum_{i=1}^{N_G} P_i - P_L}{P_D}, 0) \tag{22}$$

As long as the equation (21) is satisfied then the PBV is equal to zero. To maintain the equality constraint and find the most optimal solutions in the search space, the algorithm accepts the solutions which are able to hold the following relation:

$$P_D + P_L - \sum_{i=1}^{N_G} P_i = 0 \tag{23}$$

To accelerate the process of convergence to achieve of the optimal solutions, this study has used an evaluation function to push the answers of optimization algorithm towards the most possible optimum solution by means of penalization factor. The proposed method evaluation function which would be evaluated for each iteration is formulated as:

$$F_{eval} = F_{ct}(P_i) \times (1 + PF \times PBV) \tag{24}$$

In this study PF is considered to be equal to 1000, in many practical problems, the selection of the parameters is subject to the characteristics of the problem.

2.4 Cultural algorithms

The principals behind the cultural algorithm (CA) were proposed by Reynolds in 1994 [27]. CA is a type of computational intelligence algorithm which is inspired by the cultural inheritance process of several generations. The idea of this innovative optimization technique is that culture has the potential to be emblematically encoded and shared among populations of a society [37].

The mechanism of CA is based on the discovery of an elite individual in a population, and setting the aim of population to reach the same level as the elite's knowledge. The culture evolution of the population would improve the adaptability of the individuals towards the targeted aims and the speed of this process would be increased through guidance by the elite's knowledge.

2.4.1 The basic concepts of cultural algorithm

Culture is accumulated experience and learned behaviour of a group of people which can be called tradition of that group of people and which is maintained through generations.

CA is composed of two basic spaces: population space (to illustrate a genetic component according to Darwinian Theory) and belief space (to illustrate cultural principals) which differentiates the CAs from other evolutionary algorithms [37]. The population space represents and categorizes the individuals based on their specifications in each set, while the belief space collects the knowledge obtained by individuals.

At each iteration of CA, individuals in their population space can be substituted and updated by some of their generations via a communication protocol. This process can be handled by implementing any population-based operators or any other evolutionary algorithms such as ABC, BBO, FA and etc. [6]. The frame work of CA is depicted in Fig 2.4.

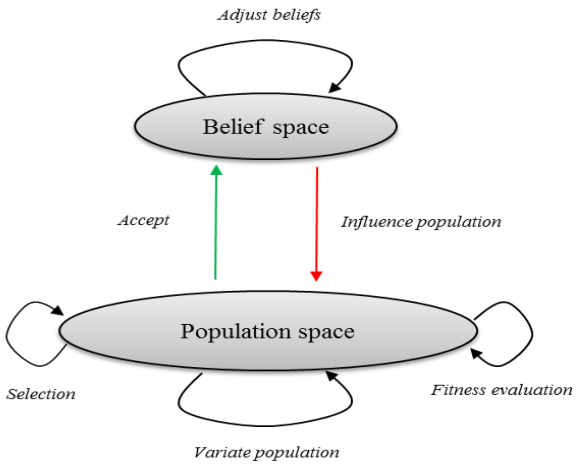

Fig. 2.4 Illustration of conceptual framework of cultural algorithm based on the two spaces

In each generation, individuals would be evaluated by the fitness function that is determined for evolutionary algorithm in the population space. Thereafter, an acceptance function is utilized to specify which individuals in the current population have a major influence on the current beliefs.

The experienced that has been acquired by accepted individuals would be applied to adjust the beliefs. Once the beliefs have been adjusted then they will be used to influence the improvement of the population. In order to vary the population space, the variation operators are responsible for using the beliefs to regulate the changes in individuals, where it is possible to use crossover and mutation function or a self-adapting control parameters as the variation operators [38].

2.4.2 Belief space

The belief space comprises a set of experience and knowledge structure of the individuals. Based on Engelbrecht [38], CA is composed of four sections, such as: knowledge components, acceptance functions, belief space adjustment and influence functions. The sections of belief space are introduced as follows:

2.4.2.1 Knowledge component

The belief space stores a set of knowledge components in order to demonstrate the behavioural patterns of accepted individuals from the population space. The forms of knowledge components and representation of data structure depends on the characteristics of the problem. The study has used the vector representations to describe this component [39]. The belief space can be categorized in two knowledge components [39]:

- *Situational knowledge component*: this component is responsible for finding the best solution in a particular period of time or a generation.
- *Normative knowledge component*: this component provides a criterion for each individual behaviour which would be considered as a guideline for the mutational adjustment of individuals. In the process of optimization these norms or intervals specify the suitable range that can be searched in each dimension.

The belief space can be mathematically expressed based on the definition of its components [38-39]:

$$B(t) = (S(t), N(t)) \tag{25}$$

where

$$S(t) = \{\hat{y}_l(t): l = 1, 2, 3, \dots, n_s\} \quad (26)$$

$$N(t) = (X_1(t), X_2(t), X_3(t), \dots, X_{n_x}(t)) \quad (27)$$

For each dimension of belief space the following information is required to be saved:

$$X_j(t) = (I_j(t), L_j(t), U_j(t)) \quad (28)$$

subject to

$$I_j(t) = \left[x_j^{min}, x_j^{max}\right] = [l, u] \quad (29)$$

2.4.2.2 Acceptance functions

To shape the beliefs in a particular population, this function decides which individuals of population will be utilized for this purpose. Acceptance functions can be arithmetically designed in two ways [38]:

- *Static*: *n%* individuals of a population will be selected.
- *Dynamic*: by using any selection methods of evolutionary algorithms like as elitism or roulette-wheel selection.

In this study, number of the selected individuals is determined by the following method according to [38]:

$$n_B(t) = \left[\frac{n_{pop}\gamma}{t}\right], \quad \gamma \in [0,1] \quad (30)$$

where

$n_B(t)$ is the number of selected individuals for forming the beliefs in a population

t is the number of iterations (generation)

n_{pop} is the number of population

2.4.2.3 Belief space adjustment

After selecting the number of individuals to form the beliefs, the interval of knowledge components can be updated though the following formulation [38-39]:

- Situational knowledge

$$S(t+1) = \{\hat{y}(t+1)\} \tag{31}$$

where

$$\hat{y}(t+1) = \begin{cases} min_{l=1,\dots,n_B(t)}\{X_l(t)\} & if\ f\left(min_{l=1,\dots,n_B(t)}\{X_l(t)\}\right) < f(\hat{y}(t)) \\ \hat{y}(t) & otherwise \end{cases} \tag{32}$$

- Normative knowledge

$$x_j^{min}(t+1) = \begin{cases} x_{lj}(t) & if x_{lj}(t) \le x_j^{min}(t)\ \ or\ \ f\left(X_l(t)\right) < L_j(t) \\ x_j^{min}(t) & otherwise \end{cases} \tag{33}$$

For updating the $L_j(t)$

$$L_j(t+1) = \begin{cases} f\left(X_l(t)\right) & if x_{lj}(t) \le x_j^{min}(t)\ \ or\ \ f\left(X_l(t)\right) < L_j(t) \\ L_j(t) & otherwise \end{cases} \tag{34}$$

$$x_j^{max}(t+1) = \begin{cases} x_{lj}(t) & if x_{lj}(t) \ge x_j^{max}(t)\ \ or\ \ f\left(X_l(t)\right) < U_j(t) \\ x_j^{max}(t) & otherwise \end{cases} \tag{35}$$

For updating the $U_j(t)$

$$U_j(t+1) = \begin{cases} f\left(X_l(t)\right) & if x_{lj}(t) \ge x_j^{max}(t)\ \ or\ \ f\left(X_l(t)\right) < U_j(t) \\ U_j(t) & otherwise \end{cases} \tag{36}$$

Where

$X_l(t), l = 1,2,3 \dots, n_B(t)$

2.4.2.4 Influence functions

The responsibility of these functions is to influence the population space based on the adjusted beliefs in order to define the mutational step size, and the direction of changes. All the CAs have the same procedure until this point, the study proposed different versions of CAs according to their influence function specifications. As it mentioned in [38-39], the CAs can be categorized in four different versions:

- *Cultural algorithm version 1 (CA1)*: only the normative knowledge component is utilized to specify step sizes:

$$\acute{x}_{ij}(t) = x_{ij}(t) + \delta_j \times N_{ij}(0,1) \tag{37}$$

The equation (37) can be rewritten as follows:

$$\acute{x}_{ij}(t) \sim N_{ij}(x_{ij}(t), {\delta_j}^2(t)) \tag{38}$$

where

$$\delta_j(t) = [x_j^{max}(t) - x_j^{min}(t)] \tag{39}$$

- *Cultural algorithm version 2 (CA2)*: only the situational knowledge component is used to specify the direction changes. In this version of CA, we assumed the strategy parameter is greater than zero ($\sigma_{ij} > 0$):

$$\acute{x}_{ij}(t) = \begin{cases} x_{ij}(t) + \left|\sigma_{ij}(t)N_{ij}(0,1)\right| & if\ x_{ij}(t) < \hat{y}_j(t) \\ x_{ij}(t) - \left|\sigma_{ij}(t)N_{ij}(0,1)\right| & if\ x_{ij}(t) > \hat{y}_j(t) \\ x_{ij}(t) + \sigma_{ij}(t)N_{ij}(0,1) & otherwise \end{cases} \tag{40}$$

- *Cultural algorithm version 3 (CA3)*: this version is combination of both knowledge components. The situational knowledge component is used to specify the step sizes, while the normative knowledge component is used for direction changes. The definition of $\acute{x}_{ij}(t)$ will remain as same as CA2, just the strategy parameter would be redefined as follows:

$$\sigma_{ij}(t) = \alpha\left[x_j^{max}(t) - x_j^{min}(t)\right], \quad 0 < \alpha < 1 \tag{41}$$

where α denotes the ratio of the strategy parameter.

- *Cultural algorithm version 4 (CA4)*: in the fourth version of CA, the normative knowledge component is assigned to handle the step sizes and direction changes.

$$x_{ij}(t) = \begin{cases} x_{ij}(t) + \left|\sigma_{ij}(t)N_{ij}(0,1)\right| & if\ x_{ij}(t) < x_j^{min}(t) \\ x_{ij}(t) - \left|\sigma_{ij}(t)N_{ij}(0,1)\right| & if\ x_{ij}(t) > x_j^{max}(t) \\ x_{ij}(t) + \beta \times \sigma_{ij}(t)N_{ij}(0,1) & otherwise \end{cases} \tag{42}$$

In CA4, the scaling factor is applicable for all the positive values ($\beta > 0$), and strategy parameter can be defined as in described in CA3. In all versions of CA influence functions, subscript *i* denotes the individual and subscript *j* describes the type of the knowledge component.

2.5 Results and discussion

The proposed algorithms were tested on different scenarios of CEED that consider the several physical constraints of generation units and system, including:

- with and without transmission loss
- with and without spinning reserve constraint
- with and without prohibited operating zones
- valve-point effect
- ramp rate limits
- fuel emission constraint
- price penalty factors

To investigate and verify the robustness of the proposed methods, they were tested on three different test systems 5, 20 and 50 generation units respectively. All the methods were implemented and compared in this study to show the capability of the methodology. The codes and algorithms have been developed on MATLAB 2013a to perform the case studies and executed on a personal computer with the following specifications, Intel® Core™ i7-3770 (3.40 GHz), 8.00 GB RAM (DDR5) and windows 8.1 operating system.

As all the evolutionary algorithms are highly sensitive to the tuning of their decision parameters and variables, the study selected the suitable settings for all versions of CA. These parameters are population size n_{pop}, acceptance ratio P_{accept}, ratio of strategy parameter α, scaling coefficient β set to 50, 0.15, 0.25, and 0.5 respectively. To have a uniform comparison among all the compared evolutionary algorithms, the spinning reserve requirement was set to 5% of total load demand as it mentioned as in [1], and the maximum iterations for all the trials were fixed on 300.

To validate the effectiveness of the proposed method of the study, the following case studies have been analysed and compared:

Case 1: 5 generation units; without considering POZ.

Case 2: 20 generation units (by four times replication of the test system of case 1); without considering power transmission losses and maintaining spinning reserve.

Case 3: 50 generation units (by ten times replication of the test system of case 1); without considering power transmission losses and maintaining spinning reserve.

2.5.1 Case 1

A small test system comprising of 5 generation units was considered based on [40-42] with a minor modification on the test system. The system specifications are given in Table 2.1, 2.2 and 2.3. The loss coefficients (B-coefficients) of the transmission network are given in Table 2.4, where the values are expressed in p.u. on a 100 MVA base. Table 2.1 lists the physical operating limits and cost coefficients of generation units. Table 2.2 lists the ramping limits as well as quantitative information of prohibited zones for the generation units. Table 2.3 lists a detailed associated emission cost for NO_x through its respective cost coefficients. The valve-point effect, ramp rate limits, spinning reserve requirement, emission constraints and the effect of price penalty factors (PPFs) on the total generation cost were considered on this case study. The total load demand of the test system was 730 MW. In this case, 100 trials have been carried out for the purpose of producing the results.

Table 2.1 Cost coefficients and physical operating limits of generation units

Unit	a_i *($/h)*	b_i *($/MWh)*	c_i *$/(MW)^2h*	d_i *($/h)*	e_i *(1/MW)*	P_i^{min} *(MW)*	P_i^{max} *(MW)*
1	25	2	0.008	100	0.042	10	75
2	60	1.8	0.003	140	0.04	20	125
3	100	2.1	0.0012	160	0.038	30	175
4	120	2	0.001	180	0.037	40	250
5	40	1.8	0.0015	200	0.035	50	300

Table 2.2 Ramp rate limits and POZ information of generation units

Unit	P^0 *(MW)*	*UR (MW)*	*DR (MW)*	*POZ (MW)*
1	70	30	30	[60 65]
2	100	30	30	[70 75]
3	150	40	40	[120 125]
4	110	50	50	[80 90]
5	270	50	50	[230 240]

Table 2.3 Emission curve coefficients of generation units

Unit	α_i *(lb/h)*	β_i *(lb/MWh)*	γ_i *lb/(MWh)^{2}h*	η_i *(lb/h)*	δ_i *(1/MW)*
1	80	-0.8050	0.0018	0.6550	0.0284
2	50	-0.5550	0.0150	0.5773	0.0244
3	60	-1.3550	0.0105	0.4968	0.0227
4	45	-0.6000	0.0080	0.4860	0.0194
5	30	-0.5550	0.0120	0.5053	0.0207

Table 2.4 The transmission loss coefficients

B				
0.000049	0.000014	0.000015	0.000015	0.000020
0.000014	0.000045	0.000016	0.00002	0.000018
0.000015	0.000016	0.000039	0.000010	0.000012
0.000015	0.000020	0.000010	0.000040	0.000014
0.000020	0.000018	0.000012	0.000014	0.000035

The best solution in the search space is shown in Fig 2.5, where the best solution is the solution that has the lowest total cost and lowest emission cost without violating any physical constraint. The convergence processes of the proposed algorithm with different PPFs are shown in Fig 2.6 (a, b, c and d) where the total cost is plotted against the number of iterations. The obtained results are compared with BBO, ACOR, ABC, PSO, GA, GAPSO, and FA. The Fig 2.6.a shows the convergence process with Max-Max PPF. As shown, CA3 has the second highest initial guess, however it reaches its optimum level less than 50 iterations with the last step of reduction occurring at 50th iteration with the best minimum cost of 2039.46 ($/h). In terms of the convergence process, most of the algorithms have reached to their optimum level after 50th iteration, where the BBO only succeeding in reach to the final iteration at close to the 250th iteration.

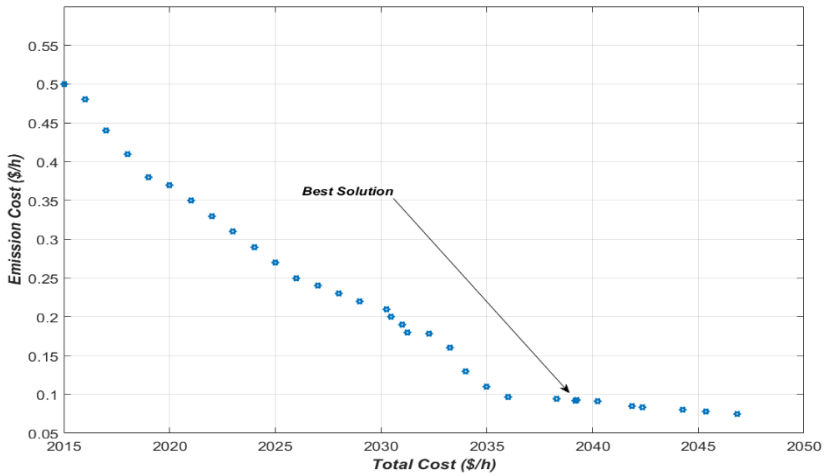

Fig. 2.5 Best obtained solution in the search space for case 1

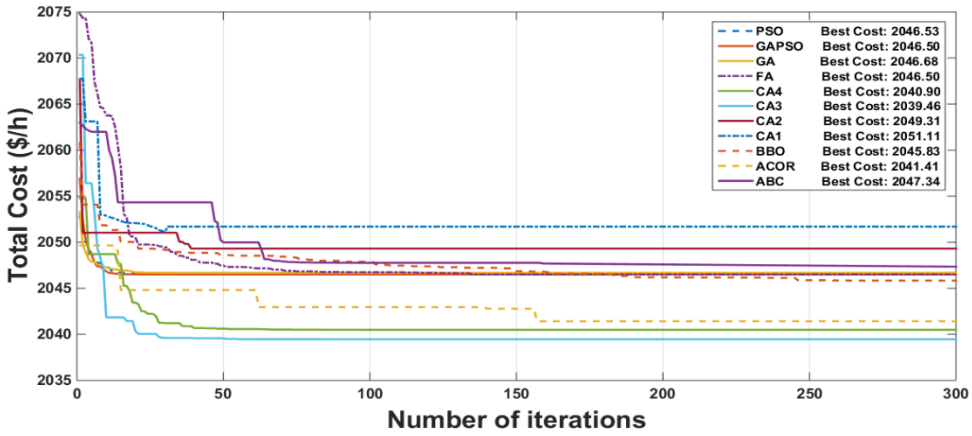

Fig. 2.6.a Convergence process of CEED cost through the Max-Max PPF (5 generation units)

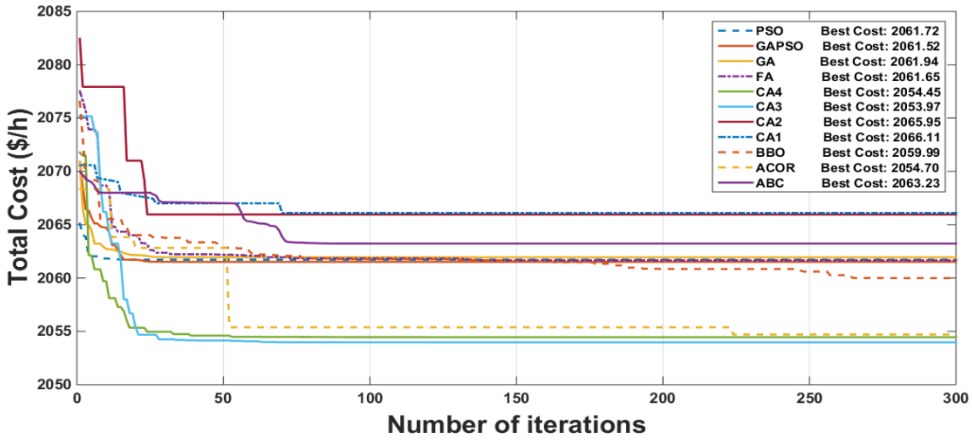

Fig. 2.6.b Convergence process of CEED cost through the Max-Min PPF (5 generation units)

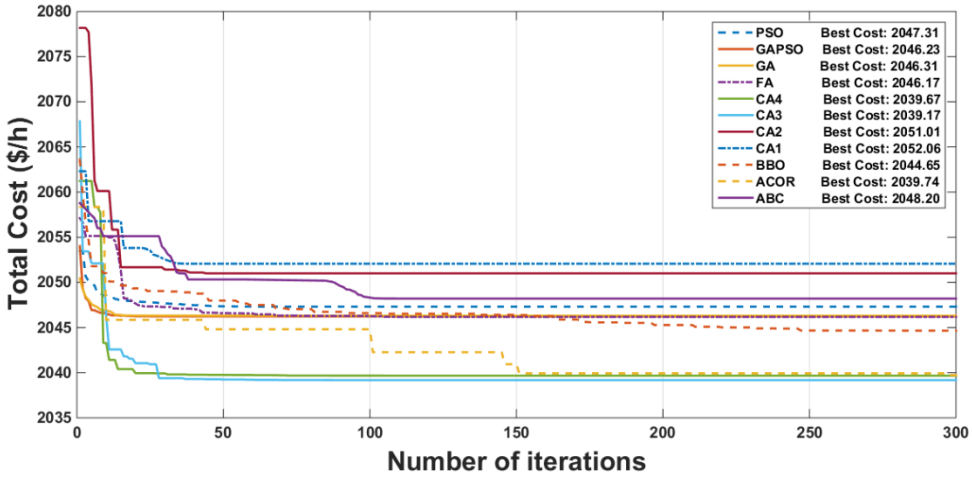

Fig. 2.6.c Convergence process of CEED cost through the Min-Max PPF (5 generation units)

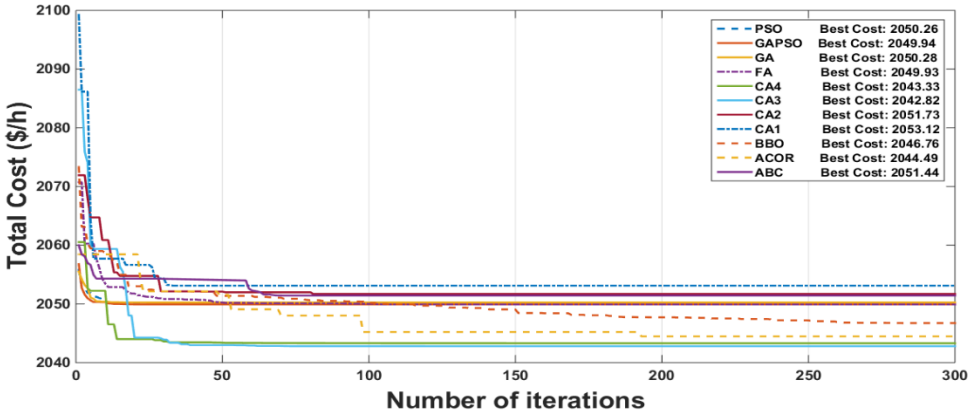

Fig. 2.6.d Convergence process of CEED cost through the Min-Min PPF (5 generation units)

By analysing Fig 2.6 (a, b, c and d), it can be seen that the proposed method is the most capable technique to find the best solution where its best obtained cost is at Min-Max PPF at 2039.17 ($/h). It is noticeable for all PPFs cases, the proposed method has achieved to the final optimization stage in less than 70 iterations, which indicates the convergence speed of proposed method. The maximum cost, average cost, minimum cost and average elapsed time for the proposed method and other methods are shown in Table 2.5. For ease of comparison, the elapsed time of each method has evaluated as an average. From Table 2.5, it is evident that the proposed method has achieved the lowest average and minimum total generation cost with respect to all PPFs cases among all the other methods. The most optimum average cost was achieved by CA3 through Min-Max PPF at 2042.5414 ($/h), where the average elapsed time was 2.4571 seconds. The breakdown of generator schedules is given in Table 2.6.

Table 2.5 Comparison of the obtained results for Case 1

5 Units System		Max Cost ($/h)	Avg Cost ($/h)	Min Cost ($/h)	Avg Elapsed Time (s)
BBO	Max Max	2054.5656	2047.5029	2045.8321	8.4732
	Max Min	2065.2573	2061.2359	2059.9912	
	Min Max	2050.3511	2046.0231	2044.6514	
	Min Min	2052.2072	2049.5228	2046.7632	
ACOR	Max Max	2305.1833	2067.3245	2041.4102	6.2199
	Max Min	2167.204	2057.1314	2054.7065	
	Min Max	2187.797	2049.3181	2039.7443	
	Min Min	2144.6517	2049.8958	2044.4932	
FA	Max Max	2047.8929	2046.2479	2046.5098	2.8594
	Max Min	2062.8454	2061.1854	2061.6578	
	Min Max	2047.8448	2045.8421	2046.1733	
	Min Min	2051.3145	2049.3753	2049.9321	
GAPSO	Max Max	2049.5923	2047.374	2046.5013	23.2906
	Max Min	2063.0634	2062.4204	2061.5215	
	Min Max	2049.798	2047.1124	2046.2341	
	Min Min	2051.9561	2050.6466	2049.9444	
PSO	Max Max	2049.7785	2047.5568	2046.5321	4.2648
	Max Min	2063.3545	2062.5546	2061.7235	
	Min Max	2049.8845	2047.3345	2047.3121	
	Min Min	2051.9623	2050.7465	2050.2632	
GA	Max Max	2049.8701	2048.0021	2046.6845	5.4049
	Max Min	2063.4025	2062.6801	2061.9432	
	Min Max	2050.1478	2047.7468	2046.3145	
	Min Min	2051.8845	2050.8865	2050.2842	
ABC	Max Max	2049.9904	2049.9879	2047.3458	6.3695
	Max Min	2064.6541	2062.8788	2063.23	
	Min Max	2050.7456	2048.4563	2048.2032	
	Min Min	2052.3545	2051.0002	2051.4433	
CA1	Max Max	2061.4022	2053.9172	2051.1125	1.2386
	Max Min	2081.2015	2068.8055	2066.1124	
	Min Max	2061.2573	2053.1706	2052.0645	
	Min Min	2065.9603	2056.1002	2053.1237	
CA2	Max Max	2061.8546	2053.9832	2049.3154	1.2594
	Max Min	2081.5487	2069.0458	2065.9541	
	Min Max	2061.7568	2054.0001	2051.0123	
	Min Min	2066.1254	2056.7453	2051.7311	
CA3	Max Max	2053.7469	2042.1457	2039.4621	1.3578
	Max Min	2063.6157	2056.2873	2053.9714	
	Min Max	2055.5814	2042.5414	2039.1724	
	Min Min	2056.2588	2045.6611	2042.8214	
CA4	Max Max	2053.8546	2042.5436	2040.9012	1.3281
	Max Min	2063.7654	2057.021	2054.4532	
	Min Max	2056.3254	2042.8547	2039.6714	
	Min Min	2056.5487	2045.8745	2043.3302	

Table 2.6 The best obtained solutions of the proposed method (CA3) for case 1

No. of units	1	2	3	4	5
Schedule (MW)	32.2494	108.7979	161.0268	226.8128	212.3711
Generation Cost ($/h)	97.8191	291.3472	469.2718	625.0697	489.9202
Valve-point Cost ($/h)	1.6309	8.6734	13.8865	21.6623	19.8049
Emission Cost ($/h)	0.0076	0.0218	0.0119	0.026	0.0247
Total Cost ($/h)			2039.178		
Ploss (MW)			11.258		

2.5.2 Case 2

In order to demonstrate the robustness of the proposed method on a larger test system, the proposed method was applied on a 20 units system. All the physical constraints of generation units as it described in case 1 (aside from spinning reserve requirement) as well as effect of POZs were considered in this case. The total load demand was 2920 MW. In this case, transmission line losses were neglected. To have the refinement process 100 runs have been performed for each method. Fig 2.7 illustrates the best obtained solution in the search space where the best solution is the solution that has the lowest total cost and lowest emission cost without violating any physical constraint. The comparison between the proposed method and the other evolutionary algorithms during the convergence process with consideration of their PPFs are depicted in Fig 2.8 (a, b, c and d).

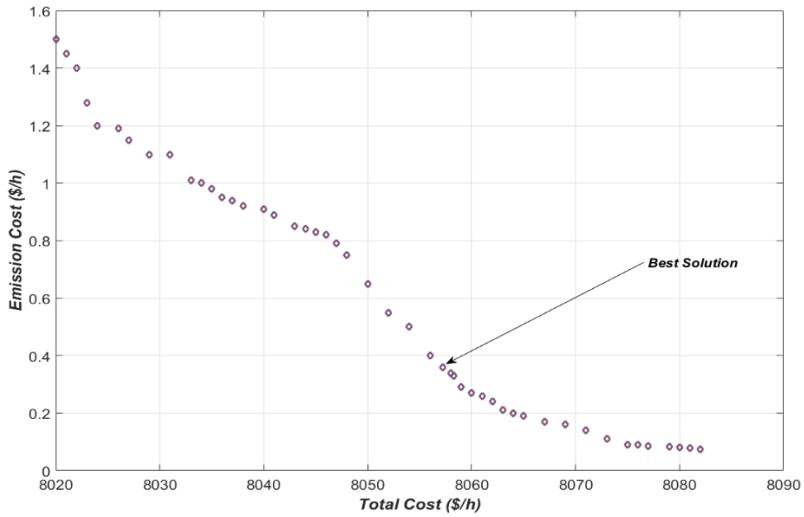

Fig. 2.7 Best obtained solution in the search space for case 2

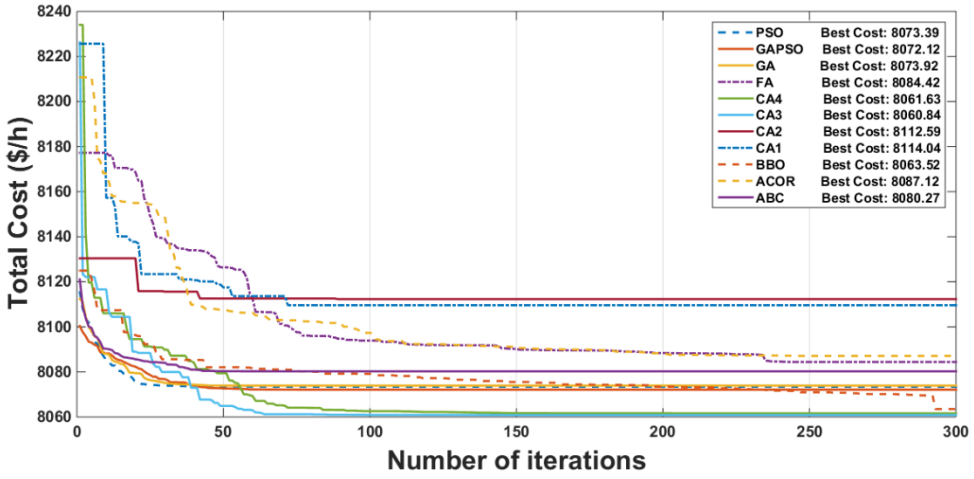

Fig. 2.8.a Convergence process of CEED cost through the Max-Max PPF (20 generation units)

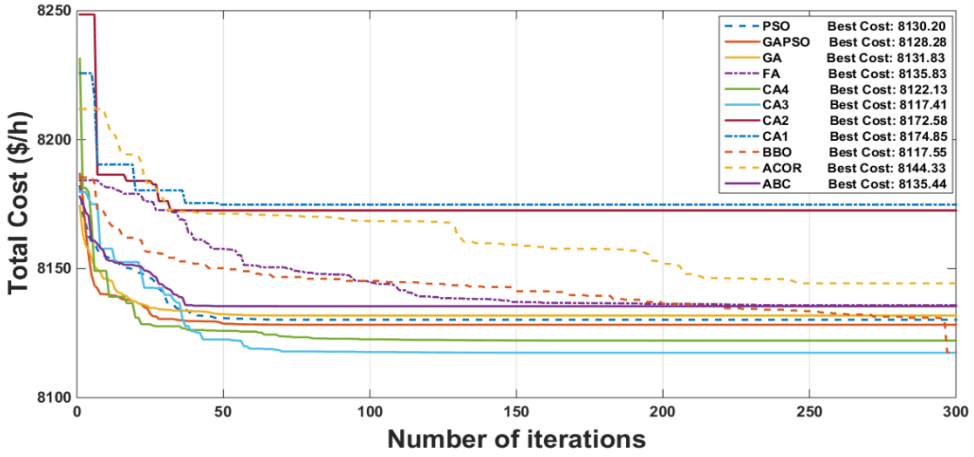

Fig. 2.8.b Convergence process of CEED cost through the Max-Min PPF (20 generation units)

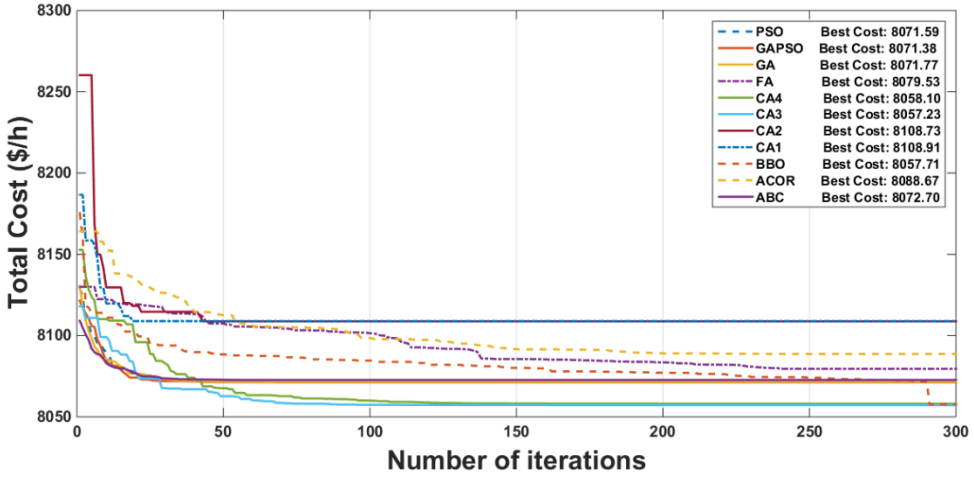

Fig. 2.8.c Convergence process of CEED cost through the Min-Max PPF (20 generation units)

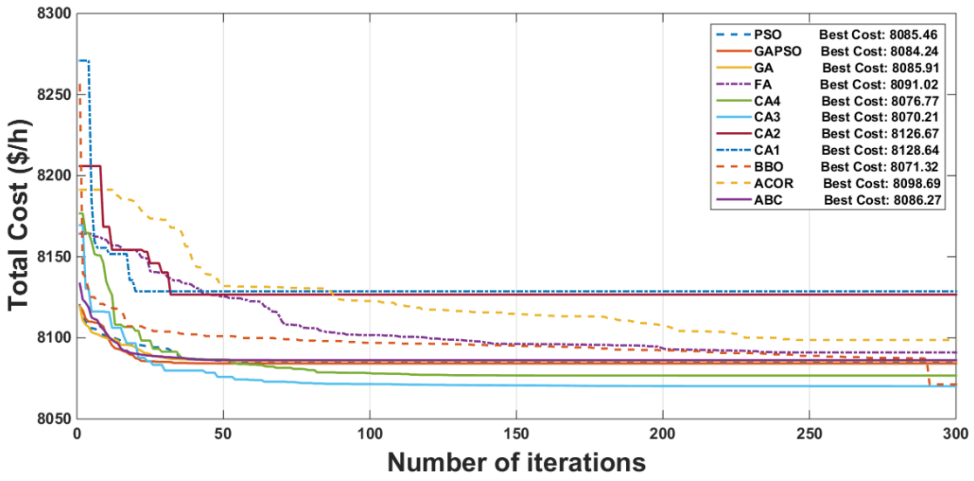

Fig. 2.8.d Convergence process of CEED cost through the Min-Min PPF (20 generation units)

It is clear from Fig 2.8 (a, b, c and d) that proposed method provides the lowest cost among the other methods in all cases. The convergence process has been extended in all methods due to enlargement of the test system; nevertheless the proposed method has converged in less than 100 iterations which indicates its effectiveness. It is noticeable that the Min-Max and Max-Min PPFs provide the lowest and highest total generation cost for the proposed method with costs of 8057.23 and 8117.41 ($/h) respectively. The detailed results of 20 units system with respect to all PPFs are shown in Table 2.7. It is clear that the proposed method obtained the lowest generation cost when compared to other techniques, where the minimum average cost is computed by its Min-Max PPF at 8062.79 ($/h). It is significant to mention that, even by enlarging the test system where degrees of non-convexity and non-linearity of the problem were significantly increased, still the proposed method managed to maintain a fast run time and its efficiency where the difference by the previous case is only 1.0993 (s). The proposed method in comparison to the other versions of cultural algorithm has a slightly longer time to converge as it is using both the knowledge components (situational and normative) for its influence function. Table 2.8 lists the best solution detailed information for generator schedules and their associated costs.

Table 2.7 Comparison of the obtained results for Case 2

20 Units System		Max Cost ($/h)	Avg Cost ($/h)	Min Cost ($/h)	Avg Elapsed time (s)
BBO	Max Max	8098.153	8074.88	8063.5204	24.3705
	Max Min	8144.5893	8132.983	8117.5522	
	Min Max	8090.8475	8073.56	8057.7132	
	Min Min	8103.9127	8089.66	8071.3245	
ACOR	Max Max	8111.0125	8095.4521	8087.1253	15.2124
	Max Min	8201.5435	8185.4565	8144.3356	
	Min Max	8225.5423	8100.0204	8088.6745	
	Min Min	8254.8457	8116.1024	8098.6974	
FA	Max Max	8104.181	8083.8803	8084.4253	2.8965
	Max Min	8171.9771	8142.0902	8135.8323	
	Min Max	8100.926	80820.7155	8079.5345	
	Min Min	8129.6365	8098.029	8091.0254	
GAPSO	Max Max	8083.9209	8073.9642	8072.1245	29.0153
	Max Min	8141.7844	8131.5726	8128.2845	
	Min Max	8083.1013	8072.2043	8071.3847	
	Min Min	8093.1127	8085.701	8084.2456	
PSO	Max Max	8101.2544	8088.4521	8073.5412	8.4742
	Max Min	8145.5478	8134.8542	8130.2045	
	Min Max	8090.6545	8086.7546	8071.5942	
	Min Min	8125.6587	8097.5687	8085.4675	
GA	Max Max	8107.8542	8089.4574	8073.9245	9.5049
	Max Min	8187.5687	8135.8765	8131.8345	
	Min Max	8100.2548	8088.5544	8071.7745	
	Min Min	8145.6578	8101.2587	8085.9175	
ABC	Max Max	8212.45	8100.4525	8080.2745	13.4197
	Max Min	8275.3587	8175.6547	8135.4457	
	Min Max	8212.5435	8111.5478	8072.7065	
	Min Min	8346.5435	8101.4587	8086.2745	
CA1	Max Max	8188.5478	8135.4578	8114.0423	2.1535
	Max Min	8254.5478	8178.7723	8174.8545	
	Min Max	8145.8528	8122.7744	8108.9147	
	Min Min	8185.9874	8150.5547	8128.6475	
CA2	Max Max	8133.5874	8117.5153	8112.5954	2.3326
	Max Min	8194.3054	8175.8547	8172.5874	
	Min Max	8134.3103	8109.3466	8108.7387	
	Min Min	8150.7771	8128.0509	8126.6787	
CA3	Max Max	8104.6353	8067.5709	8060.8475	2.4571
	Max Min	8158.7169	8118.3626	8117.4178	
	Min Max	8102.5586	8062.7931	8057.2354	
	Min Min	8113.2448	8074.6219	8070.2145	
CA4	Max Max	8104.7854	8079.8745	8061.6354	2.4003
	Max Min	8167.5841	8137.8745	8122.7854	
	Min Max	8103.0124	8078.4658	8058.1088	
	Min Min	8113.4521	8095.5478	8076.7754	

Table 2.8 The best obtained solutions of the proposed method (CA3) for case 2

No. of units	Generation Cost ($/h)	Valve-point Cost ($/h)	Emission Cost ($/h)
1	194.7436	4.1731	111.1813
2	303.2718	9.1448	189.9149
3	494.4372	14.951	159.6987
4	525.0536	16.8705	226.6024
5	364.8159	13.3442	259.8991
6	173.8	3.6644	100.1128
7	304.3839	9.1885	191.2985
8	538.1718	16.7753	213.0985
9	494.7868	15.3844	193.5774
10	487.7093	19.6945	489.8998
11	252.1073	5.4799	148.477
12	353.5921	11.0752	258.1048
13	509.845	15.5974	177.3859
14	564.3889	18.7764	274.5581
15	375.5084	13.9146	276.861
16	267.9472	5.8215	160.3977
17	274.3523	7.9916	155.9378
18	492.5598	14.872	157.6237
19	551.3042	18.1456	257.9524
20	361.8258	13.184	255.2554
Total Cost ($/h)		12390.491	

2.5.3 Case 3

To verify the ability of the proposed method with greater complexity and non-convexity, the method has been tested on 50 units system, which is the largest test system that considers all the physical constraints of the generation units found in literature. The total demand for the system is equal to 7300 MW. Fig 2.9 illustrates the best solution in the search space. Fig 2.10 (a, b, c and d) represent the convergence process of optimization, where the methodology has successfully employed and the obtained results show the effectiveness of CA3 in finding the most optimum solution in all the considered PFFs cases. By increasing the complexity of the solution, the CA3 has been able to acquire the least cost solution as well as reaching to the final value of the convergence process in almost 100 iterations in the most cases. The minimum total cost obtained by CA3 through Min-Max PPF is 20181.96 ($/h).

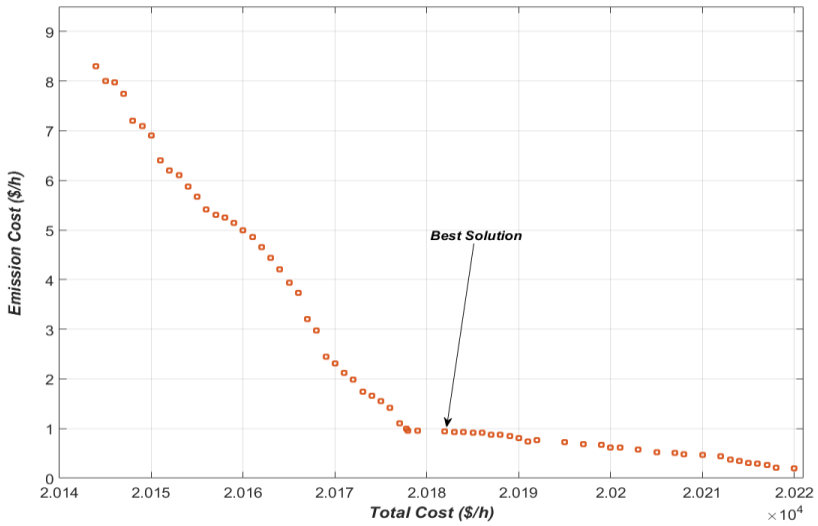

Fig. 2.9 Best obtained solution in the search space for case 3

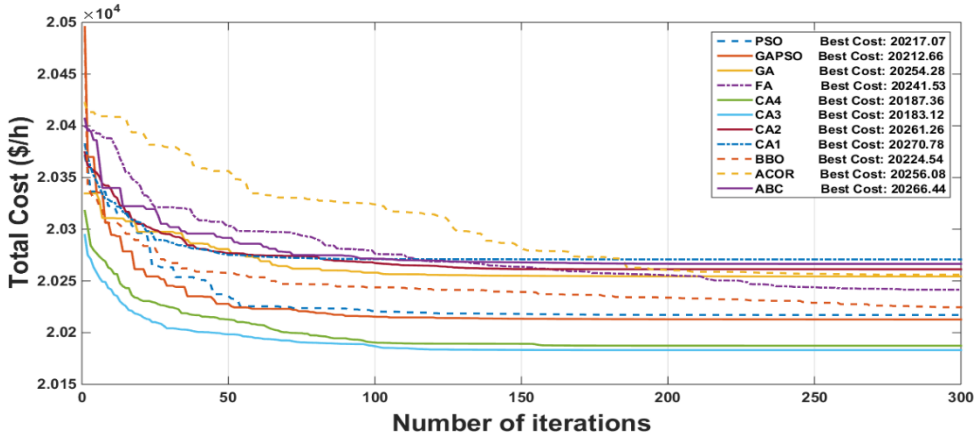

Fig. 2.10.a Convergence process of CEED cost through the Max-Max PPF (50 generation units)

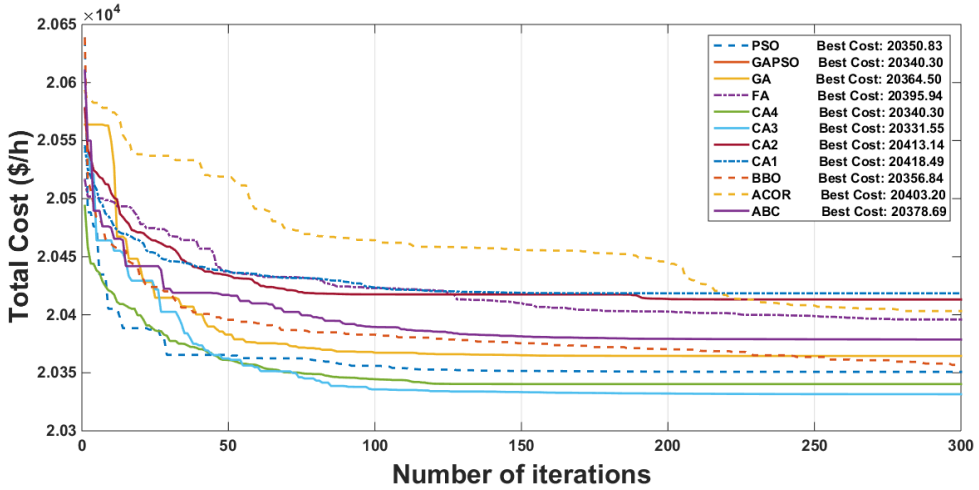

Fig. 2.10.b Convergence process of CEED cost through the Max-Min PPF (50 generation units

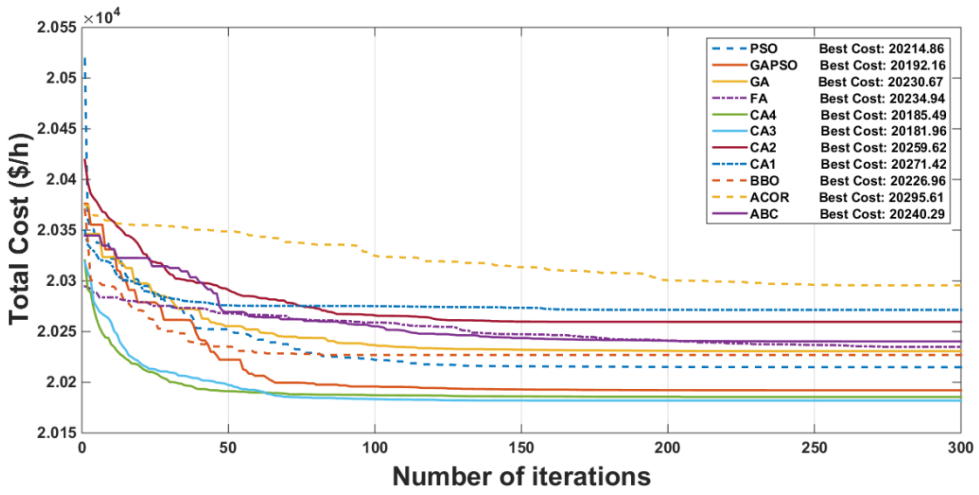

Fig. 2.10.c Convergence process of CEED cost through the Min-Max PPF (50 generation units)

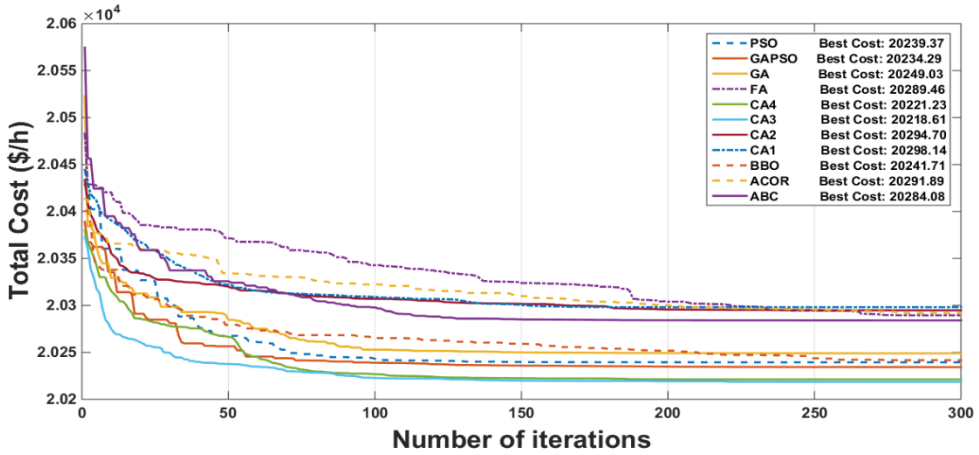

Fig. 2.10.d Convergence process of CEED cost through the Min-Min PPF (50 generation units)

The details of the solutions are found in the Table 2.9, where the CA3 has acquired the lowest total generation costs in comparison to the other methods. As is seen, all the versions of CA are fairly fast in terms of convergence while the CA3 is the most robust and fastest algorithm in finding the most optimal solution. The second algorithm which has almost the same time to convergence is FA, however from the results it is obvious that FA is not as capable as CA3 in terms of computation efficiency and convergence. In this case the best average cost has been obtained by the proposed method of the study (CA3) at 20190.24 ($/h) within 3.7235 seconds. Detailed information regarding the best solution generator schedules and their associated costs is listed in Table 2.10.

Table 2.9 Comparison of the obtained results for Case 3

50 Units System		Max Cost ($/h)	Avg Cost ($/h)	Min Cost ($/h)	Avg Elapsed time (s)
BBO	Max Max	20486.2304	20245.0990	20224.5400	49.4478
	Max Min	20637.9955	20383.5605	20356.8399	
	Min Max	20370.6733	20233.6180	20226.9600	
	Min Min	20400.5471	20264.9528	20241.7100	
ACOR	Max Max	20422.1366	20301.0561	20256.0804	23.4582
	Max Min	20592.5007	20459.5694	20403.2000	
	Min Max	20374.6079	20319.3026	20295.6132	
	Min Min	20413.5235	20316.6638	20291.8900	
FA	Max Max	20399.4607	20274.9511	20241.5302	3.2163
	Max Min	20516.1290	20420.7332	20395.9400	
	Min Max	20294.6761	20251.9225	20234.9412	
	Min Min	20482.8795	20332.3212	20289.4600	
GAPSO	Max Max	20495.4164	20223.9754	20212.6601	48.1425
	Max Min	20493.7161	20351.2567	20340.2991	
	Min Max	20376.1368	20209.1629	20192.1619	
	Min Min	20388.8804	20246.6771	20234.2913	
PSO	Max Max	20370.6965	20229.7232	20217.0722	14.2585
	Max Min	20637.1721	20360.1736	20350.8318	
	Min Max	20519.0375	20231.8353	20214.8612	
	Min Min	20428.6969	20255.4949	20239.3713	
GA	Max Max	20334.6094	20263.9854	20254.2839	16.1012
	Max Min	20563.8023	20380.1259	20364.5017	
	Min Max	20346.2926	20244.1745	20230.6732	
	Min Min	20384.2346	20263.2494	20249.0332	
ABC	Max Max	20406.7888	20277.9392	20266.4438	20.3574
	Max Min	20610.1221	20395.0305	20378.6912	
	Min Max	20344.7634	20257.7363	20240.2925	
	Min Min	20574.4659	20303.0045	20284.0838	
CA1	Max Max	20382.1294	20276.4824	20270.7821	3.0765
	Max Min	20545.0166	20428.1621	20418.4901	
	Min Max	20349.7902	20276.4795	20271.4176	
	Min Min	20444.1817	20312.4488	20298.1400	
CA2	Max Max	20374.2832	20271.1612	20261.2616	3.5132
	Max Min	20577.7849	20425.5726	20413.1428	
	Min Max	20419.3395	20274.1327	20259.6235	
	Min Min	20433.4961	20307.4231	20294.6977	
CA3	Max Max	20294.3789	20190.7251	20183.1180	3.7235
	Max Min	20540.3924	20349.5904	20331.5500	
	Min Max	20318.4603	20190.2474	20181.9615	
	Min Min	20373.0573	20228.6551	20218.6160	
CA4	Max Max	20317.6973	20198.0954	20187.3556	3.5257
	Max Min	20493.7161	20351.2567	20340.2991	
	Min Max	20320.1584	20191.5621	20185.4861	
	Min Min	20379.9107	20236.2923	20221.2304	

Table 2.10 The best obtained solutions of the proposed method (CA3) for case 3

No. of units	Schedule (MW)	Generation Cost ($/h)	Valve-point Cost ($/h)	Emission Cost ($/h)
1	40	117.8	2.1989	0.008
2	116.6705	310.8429	9.4413	0.0248
3	160.6625	468.3663	13.848	0.0118
4	158.3568	461.7905	13.7443	0.0116
5	252.9479	591.2801	24.7313	0.0373
6	40	117.8	2.1989	0.008
7	109.7629	293.7169	8.7675	0.0222
8	162.3045	472.4507	14.0216	0.0122
9	159.8847	465.3326	13.9214	0.0118
10	251.3998	587.3225	24.5436	0.0367
11	40.0138	117.8364	2.1999	0.008
12	120.2852	319.9189	9.7937	0.0263
13	170.6043	493.1961	14.8988	0.0141
14	160	465.6	13.9347	0.0118
15	252.774	590.8353	24.7102	0.0372
16	43.5479	127.2671	2.4589	0.0083
17	121.2372	322.3225	9.8865	0.0267
18	160.9754	469.1442	13.8811	0.0119
19	159.0099	463.304	13.82	0.0117
20	245.9009	573.3225	23.8767	0.0348
21	40.1514	118.1998	2.21	0.008
22	112.1372	299.5711	8.9991	0.0231
23	162.0619	471.847	13.996	0.0121
24	159.883	465.3285	13.9212	0.0118
25	265.3076	623.1359	26.229	0.0422
26	40.222	118.3864	2.2152	0.008
27	114.4183	305.2277	9.2216	0.0239
28	135.2949	406.0849	11.1644	0.0071
29	160	465.6	13.9347	0.0118
30	271.1008	638.2249	26.9305	0.0446
31	40.2503	118.4613	2.2173	0.008
32	119.811	318.7238	9.7475	0.0261
33	164.7089	478.4434	14.2758	0.0127
34	159.9998	465.5995	13.9347	0.0118
35	266.2775	625.655	26.3465	0.0426
36	40.4806	119.0706	2.2342	0.008
37	122.9967	326.7787	10.0581	0.0274
38	147.5973	436.0962	12.4663	0.0092
39	156.0101	456.3594	13.4723	0.0112
40	240	558.4	23.1608	0.0327
41	42.303	123.9223	2.3677	0.0082
42	108.4978	290.6113	8.6441	0.0217
43	154.0886	452.0781	13.1529	0.0104

44	159.9994	465.5986	13.9346	0.0118
45	240	558.4	23.1608	0.0327
46	40	117.8	2.1989	0.008
47	118.785	316.1426	9.6474	0.0257
48	164.2809	477.3758	14.2305	0.0126
49	160	465.6	13.9347	0.0118
50	266.9978	627.5278	26.4337	0.0429
Total Cost ($/h)			20181.9612	

2.6 Conclusions

Four different versions of CA have been proposed to solve the CEED problem while the main emphasis of emission reduction is focused on the NO_x gases. The proposed method employed the two knowledge components of the belief space to characterize the versions of the CA. To enhance the performance of the proposed algorithms, various sophisticated and highly efficient influence functions based on the mixture of situational and normative knowledge component were applied to our CA versions to find the optimal solution in the complex non-linear problem of CEED. In order to validate the effectiveness of the proposed method, different test cases (5, 20 and 50 units system) with inclusion of network and physical constraints of generation units such as valve-point effect, emission constraints, ramp rate limits and prohibited zones have been studied. To maintain the equality and inequality constraints of CEED, an effective and simple function handle was introduced to find the feasible space and escape local optima. The multi-objective CEED problem has been converted to a single objective problem through the four types of price penalty factors (PPFs) to investigate the precise effects of emission levels on the total generation costs. The simulation results demonstrate the superiority of the CA3 in achieving the best possible solution in a fast computation time in comparison with the other methods in all the test cases. The results conclude that Min-Max price penalty factor yields a noticeable lower total generation cost for CEED among all the studied cases of PPFs.

2.7 References

[1] J. Talaq, F. El-Hawary and M. El-Hawary, "A summary of environmental/economic dispatch algorithms," *IEEE Transactions on Power Systems*, vol. 9, no. 3, pp. 1508 - 1516, 1994.

[2] D. Aydina, S. Özyönb, C. Yasarb and T. Liao, "Artificial bee colony algorithm with dynamic population size to combined economic and emission dispatch problem," *International Journal of Electrical Power & Energy Systems*, vol. 54, pp. 144-153, 2014.

[3] N. I. Nwulu and X. Xia, "Multi-objective dynamic economic emission dispatch of electric power generation integrated with game theory based demand response programs," *Energy Conversion and Management*, vol. 88, p. 963–974, 2015.

[4] J. Nanda, L. Hari and M. Kothari, "Economic emission load dispatch with line flow constraints using a classical technique," *IEE Proceeding - Generation, Transmission and Distribution*, vol. 141, no. 1, pp. 1-10, 1994.

[5] J. Dhillon, S. Parti and D. Kothari, "Stochastic economic emission load dispatch," *Electric Power Systems Research*, vol. 26, no. 3, p. 179–186, 1993.

[6] R. Zhang, J. Zhou, L. Mo, S. Ouyang and X. Liao, "Economic environmental dispatch using an enhanced multi-objective cultural algorithm," *Electric Power Systems Research*, vol. 99, p. 18–29, 2013.

[7] V. Vahidinasab and S. Jadid, "Joint economic and emission dispatch in energy markets: A multiobjective mathematical programming approach," *Energy*, vol. 35, no. 3, p. 1497–1504, 2010.

[8] I. J. Raglend, S. Veeravalli, K. Sailaja, B. Sudheera and D. Kothari, "Comparison of AI techniques to solve combined economic emission dispatch problem with line flow constraints," *International Journal of Electrical Power & Energy Systems*, vol. 32, no. 6, p. 592–598, 2010.

[9] B. Gjorgieva and M. Cepin, "A multi-objective optimization based solution for the combined economic-environmental power dispatch problem," *Engineering Applications of Artificial Intelligence*, vol. 26, no. 1, p. 417–429, 2013.

[10] C. Palanichamy and N. S. Babu, "Analytical solution for combined economic and emissions dispatch," *Electric Power Systems Research*, vol. 78, no. 7, p. 1129–1137, 2008.

[11] P. K. Roy, S. P. Ghoshal and S. S. Thakur, "Combined economic and emission dispatch problems using biogeography-based optimization," *Electrical Engineering*, vol. 92, no. 4-5, pp. 173-184, 2010.

[12] M. Senthil, "Combined economic emission dispatch using evolutionary," *IJCA Special Issue on Evolutionary Computation*, pp. 62-66, 2010.

[13] U. Güvenç, Y. Sönmez, S. Duman and N. Yörükeren, "Combined economic and emission dispatch solution using gravitational search algorithm," *Scientia Iranica*, vol. 19, no. 6, p. 1754–1762, 2012.

[14] B. Shaw, V. Mukherjee and S. Ghoshal, "A novel opposition-based gravitational search algorithm for combined economic and emission dispatch problems of power systems," *International Journal of Electrical Power & Energy Systems*, vol. 35, no. 1, p. 21–33, 2012.

[15] S. Mondal, A. Bhattacharya and S. H. n. Dey, "Multi-objective economic emission load dispatch solution using gravitational search algorithm and considering wind power penetration," *International Journal of Electrical Power & Energy Systems*, vol. 44, no. 1, p. 282–292, 2013.

[16] S. Jiang, Z. Ji and Y. Shen, "A novel hybrid particle swarm optimization and gravitational search algorithm for solving economic emission load dispatch problems with various practical constraints," *International Journal of Electrical Power & Energy Systems*, vol. 55, p. 628–644, 2014.

[17] M. Basu, "Dynamic economic emission dispatch using nondominated sorting genetic algorithm-II," *International Journal of Electrical Power & Energy Systems*, vol. 30, no. 2, p. 140–149, 2008.

[18] R. T. F. A. King, H. C. S. Rughooputh and K. Deb, "Evolutionary Multi-objective Environmental/Economic Dispatch: Stochastic Versus Deterministic Approaches," *Evolutionary Multi-Criterion Optimization*, vol. 34, no. 10, pp. 677-691, 2005.

[19] B. Panigrahi, V. R. Pandi, S. Das and S. Das, "Multiobjective fuzzy dominance based bacterial foraging algorithm to solve economic emission dispatch problem," *Energy*, vol. 35, no. 12, p. 4761–4770, 2010.

[20] P. Hota, A. Barisal and R. Chakrabarti, "Economic emission load dispatch through fuzzy based bacterial foraging algorithm," *International Journal of Electrical Power & Energy Systems*, vol. 32, no. 7, p. 794–803, 2010.

[21] R. Azizipanah-Abarghooee, "A new hybrid bacterial foraging and simplified swarm optimization algorithm for practical optimal dynamic load dispatch," *International Journal of Electrical Power & Energy Systems*, vol. 49, p. 414–429, 2013.

[22] T. Niknam, R. Azizipanah-Abarghooee, A. Roosta and B. Amiri, "A new multi-objective reserve constrained combined heat and power dynamic economic emission dispatch," *Energy*, vol. 42, no. 1, p. 530–545, 2012.

[23] H. Hamedi, "Solving the combined economic load and emission dispatch problems using new heuristic algorithm," *International Journal of Electrical Power & Energy Systems*, vol. 46, pp. 10-16, 2013.

[24] L. Wang and C. Singh, "Environmental/economic power dispatch using a fuzzified multi-objective particle swarm optimization algorithm," *Electric Power Systems Research*, vol. 77, no. 12, p. 1654–1664, 2007.

[25] J. Cai, X. Ma, Q. Li, L. Li and H. Peng, "A multi-objective chaotic particle swarm optimization for environmental/economic dispatch," *Energy Conversion and Management*, vol. 50, no. 5, p. 1318–1325, 2009.

[26] A. Chatterjee, S. Ghoshal and V. Mukherjee, "Solution of combined economic and emission dispatch problems of power systems by an opposition-based harmony search algorithm," *International Journal of Electrical Power & Energy Systems*, vol. 39, no. 1, p. 9–20, 2012.

[27] R. G. Reynolds, "An Introduction to Cultural Algorithms," in: *Evolutionary Programming --- Proceedings of the Third*, San Diego, USA, 1994, pp. 131-136.

[28] B. Bhattacharya, K. Mandal and N. Chakraborty, "A multiobjective optimization based on cultural algorithm for economic dispatch with environmental constraints," *International Journal of Scientific & Engineering Research*, vol. 3, no. 6, pp. 1-8, 2012.

[29] Y. Lu, J. Zhou, H. Qin, Y. Wang and Y. Zhang, "A hybrid multi-objective cultural algorithm for short-term environmental/economic hydrothermal scheduling," *Energy Conversion and Management*, vol. 52, no. 5, p. 2121–2134, 2011.

[30] X. Xia and A. M. Elaiw, "Optimal dynamic economic dispatch of generation: A review," *Electr. Power Syst. Res*., vol. 80, no. 8, pp.975–986, Aug. 2010.

[31] M. Basu, "An interactive fuzzy satisfying-based simulated annealing technique for economic emission load dispatch with nonsmooth fuel cost and emission level functions" *Electric Power components and Systems*., vol. 32, no. 2, pp.163–173, 2004.

[32] S. Krishnamurthy and R. Tzoneva, "Comparative analyses of min-max and max-max price penalty factor approaches for multi criteria power system dispatch problem with valve point effect loading using lagrange's method" *International Conference on Power and Energy Systems*, pp. 1–7, Chennai, 2011.

[33] H. Saadat, Power System Analysis, McGrawHill, 1999.

[34] S. Chakraborty, T. Senjyu, A. Yona, A. Y. Saber and T. Funabashi, "Solving economic load dispatch problem with valve-point effects using a hybrid quantum mechanics inspired particle

swarm optimisation" *Generation, Transmission and Distribution, IET*., vol. 5, no. 10, pp. 1042–1052, 2011.

[35] D. N. Vo, P. Schegner, and W. Ongsakul, "Cuckoo search algorithm for non-convex economic dispatch" *Generation, Transmission and Distribution, IET*., vol. 6, no. 7, pp. 645–654, 2013.

[36] M. Q. Wang, H. B. Gooi, S. X. Chen and S. Lu, "A mixed integer quadratic programming for dynamic economic dispatch with valve point effect" *Power Systems, IEEE Transactions on*., vol. 29, no. 5, pp. 2097–2106, 2014.

[37] W. Durham. Co-Evolution: Genes, Culture and Human Diversity. Stanford University Press, 1994.

[38] Andries P. Engelbrecht. Computational intelligence, an introduction. John Wiley & Sons, Second edition, 2007.

[39] R.G. Reynolds and C. Chung. Knowledge-based Self-Adaptation in Evolutionary Programming using Cultural Algorithms. Evolutionary Computation, *IEEE International Conference on.*, pp. 71–76, Indianapolis, 1997.

[40] T. Niknam, R. Azizipanah-Abarghooee, and J. Aghaei, "A new modified teaching-learning algorithm for reserve constrained dynamic economic dispatch," *IEEE Trans. Power Syst*., vol. 28, no. 2, pp. 749–763, May 2013.

[41] C. K. Panigrahi, P. K. Chattopadhyay, R. N. Chakrabarti and M. Baso "Simulated annealing technique for dynamic economic dispatch" *Electric Power components and Systems*., vol. 34, no. 5, pp. 577–586, 2006.

S. Krishnamurthy and R. Tzoneva, "Comparative analyses of min-max and max-max price penalty factor approaches for multi criteria power system dispatch problem using lagrange's method" *Recent Advancements in Electrical, Electronics and Control Engineering (ICONRAEeCE), 2011 International Conference on*, pp. 36–43, Sivakasi, 2011.

3. CHAPTER 3

Paper Number 5

Smart Real-Time Scheduling of Generation units in an Electricity Market Considering Environmental Aspects and Physical Constraints of Generators

Smart Real-Time Scheduling of Generation units in an Electricity Market Considering Environmental Aspects and Physical Constraints of Generators

Abstract- Optimal scheduling of generating resources plays a significant role as a decision-making tool for power system operators in the liberalized and real-time electricity spot markets. The real-time scheduling of generation units will become a very complex task with respect to the instantaneous fluctuation of the load demand due to several demand response scenarios in the smart grid context. In this study, a hybrid mathematical method for the online scheduling of units based on the least square support vector machine (LSSVM) and the third version of cultural algorithm (CA3) has been presented, where the CA3 has been specifically employed to tune the adjusting parameters of LSSVM. For the training purpose of the proposed method, the optimal scheduling of the daily load curve for three different test systems and various physical and environmental constraints of generation units have been prepared by using a modified mixed integer quadratic programming (MIQP) to deal with non-convex behaviours of the test systems. A mean squared error (MSE) objective function has been used to reduce the prediction errors during the training process to enhance the precision and reliability of the results. A radial basis function (RBF) and the proposed LSSVM-CA3 were used to check the convergence process. A high accuracy of generator schedule predictions are demonstrated by comparing the results of the proposed method with those of artificial neural networks. From the results, it can be inferred that the method is highly compatible for real-time dispatching of generation resources in deregulated electricity markets.

Keywords: Combined environmental economic dispatch, the third version of the Cultural Algorithm (CA3), least square support vector machine (LSSVM), Real-time scheduling, physical constraints of generators.

3.1 Introduction

Due to deregulation of power systems, it is vital to operate the power grid with the highest possible degree of reliability and economy to enhance the competition of power plants in liberalized electricity markets. This problem can be solved by the economic load dispatch (ELD) problem through a set of sophisticated computational skills which tackle different power grid constraints [1]. The aim of the ELD problem is to define the optimal scheduling of generation units which minimizes the total generation cost while all the operational constraints and the load demand are satisfied. This task can be very challenging when considering the environmental aspects of conventional generators, such as coal, oil and natural gas units. The reduction of fossil-fuel based generation resources and the improvement of their energy efficiency is a foremost priority of the energy roadmaps in many countries worldwide [2]. In addition, conventional

generators may have physical constraints, such as prohibited operating zones (POZs) which is associated with their steam valve operation or any vibration in their shaft bearings. The operating area of generation units that have POZs can be divided into a number of feasible sub-regions. This issue converts the classical ELD problem into a non-convex and nonlinear problem with discontinuous operating zones, where the problem simultaneously requires the minimization of the total generation cost and the emission level while maintaining the equality and inequality constraints of the system [3]. The new resulting problem is called combined environmental economic dispatch (CEED). Classical approaches, such as the gradient method, linear programming, the lambda iteration method, quadratic programming, the base point and participation factors method, the Lagrange relaxation algorithm and etc., have substantial difficulty in dealing with the CEED problem [4]. New types of deterministic optimization algorithms with the inclusion of modification techniques such as mixed integer programming, nonlinear programming algorithm and dynamic programming for solving the CEED problem have been presented [5].

As the CEED problem is the main subroutine of a bigger problem, the so-called unit commitment (UC), and lots of valuable contributions with respect to deterministic optimization algorithms have been made in this area. Therefore, it would be appreciated to tackle some of the recent innovative solutions for the UC and its applications. Koltsaklis et al. [6] presented a generic mixed-integer linear programming (MILP) which incorporates a unit commitment solution for daily energy planning with a long-term generation expansion framework with several system considerations including ramping limits, system reserve requirements, renewable penetration limits as well as the CO2 emission effects of conventional generation resources. The same authors developed a mid-term energy planning (MEP) model through a unit commitment model for generation and transmission system planning with an ability to perform a day-ahead electricity market calculation for yearly basis. Their proposed method is capable of quantifying the effects of different costs on the day-ahead electricity market and the energy mixture of the system [7].

Niknam et al. [8] proposed a new mathematical solution for the UC problem based on benders decomposition where the solution divides the UC into a master problem and a sub-problem. They have tried to solve the master problem with help of the mixed integer optimization where a non-linear optimization has been assigned to take care of the sub-problem. Simoglou et al. [9] presented a new 0/1 MILP formulation for the self-scheduling of thermal generation resources in the co-optimized energy and reserve day-ahead markets where the generation units start-up cost has been divided into three subcategories as hot, warm and cold through to each predefined power output trajectories. Delarue et al. [10] investigated the effect of uncertainty of the load and wind generation on the multi-day ahead UC where they have assumed the perfect prediction of the load demand for initial hours as the starting point. Thereafter, the consecutive

UCs have been performed to find the optimal scheduling of the generation units where the new load forecasts have been achieved through different percentages of the load deviation and a number of test system scenarios. A novel UC-MILP based on branch and bound method is modelled in [11], where they have proposed three sets of symmetry breaking constraints for UC according to different considered time horizons.

Some of the recent studies in the area of the UC have attempted to model the intermittent behaviour of wind energy in order to investigate the influence of wind power output on the scheduling of the other thermal units. Wang et al. [12] analysed the impacts of the high level of wind penetration on thermal generation with a stochastic UC model while they have used a point forecast method to capture the uncertainty of the wind power output. In [13] a new model of UC based on a modified bender decomposition has been presented, where the developed model has the ability to capture the sub-hourly variability of the wind power. Most of the deterministic optimization algorithms have difficulty in finding the optimal solution for large-scale power systems with mixed generation resources, where these methods fall into local minima due to the oscillation of their decision parameters resulting in an increase in the computation time.

In the past few decades, many evolutionary computational algorithms such as genetic algorithm (GA) [14], particle swarm optimization (PSO) [15], artificial bee colony (ABC) [16], harmony search (HS) [17] and tabu search algorithm (TSA) [18] have been used to solve power system problems. Most of the probabilistic or metaheuristic algorithms are inspired by nature through global search space properties. Secui aimed at solving dynamic economic dispatch through a modified ant colony optimization algorithm by considering the valve-point effect on the generation cost [19]. A combination of a chaotic self-adaptive and a differential harmony search algorithm has been proposed to find the optimal scheduling of generation units in [20]. Xiong et al. [21] proposed a multi-strategy ensemble biography-based optimization (MsEBBO) for solving the ELD problem, where they have added three extensions to the main components of the BBO (migration model, migration operator and mutation operator). Their proposed method simultaneously makes a balance between exploration and exploitation in the search space in order to enhance the efficiency of the optimization process. Alsumait et al. [22] presented a new hybrid intelligent approach based on GA, pattern search (PS) and sequential quadratic programming (SQP) to solve the ELD problem while considering the valve-point effect, where each one of the optimizers has been assigned a separate task. In the same study, GA has been assigned as the main optimizer, whereas PS and SQP are utilized to adjust different tuning parameters of GA to increase the accuracy of the solution. Tsai et al. [23] developed a new PSO algorithm with a constriction factor (PSO-CF) for the trading of CO2 emission cost embedded into traditional ELD. They have introduced two operators, called random particles, and fine-tuning to improve the drawbacks of the classical PSO in searching for the global optimum. In [24], the authors proposed

an environmental-economic dispatch model which simultaneously considers carbon capture plant scheme and uncertainty of wind generation in the framework of a two-stage robust optimization. Since both objectives are convex functions, they have utilized the Pareto front in combination with the ε-constraint method to find the optimal scheduling of generation units. The Nash bargaining criterion has been used to determine the fair trade-off between the generation cost and the carbon emission. In [25], a hybrid evolutionary algorithm for solving the ELD problem with the consideration of the valve-point effect has been formulated. The presented method combines a fuzzy adaptive PSO with the Nelder-Mean (NM) search method called (FAPSO-NM). In order to enhance the effectiveness of their algorithm, the NM algorithm has been assigned as a local search algorithm in surrounding of the global solution found by FAPSO. In [26], a hybrid method for solving dynamic economic emission dispatch based on chemical reduction optimization (CRO) has been presented, while for the reduction of the computational time a differential evolution algorithm has been incorporated with CRO. In [27], the CEED problem has been solved through the PSO method, while two important factors of the power market such as transmission congestion distribution (TCD) and reactive TCD have been taken into account.

The usage of metaheuristic optimization algorithms to solve real world problems has gained the interest of numerous researchers around the globe due to their efficiency. However, most of these methods require to be executed several times to find the best solution, therefore they are not time efficient for real-time electricity market operation with the large-scale of generation units connected to the power grid.

In the last few years, another type of metaheuristic algorithm and artificial intelligence which is based on the concept of the human brain process has been employed to solve the CEED problem. The artificial neural networks (ANNs) have the ability to learn the behaviour of the power grid through the online observation of the system or through historical data. The ANNs are then able to predict the possible solutions for the objective function. An enhanced augmented Lagrange Hopfield neural network (ALHN) is presented in [28] and used to solve the economic dispatch while the cost function has been considered as a piecewise quadratic cost. Their proposed method investigated the problem in two phases; in the first phase, a heuristic optimization method was used to select the type of fuel for each generating unit of the system and in the second phase the ALHN was used to find the optimal solution of the economic dispatch with respect to the chosen fuel type. Canizes and his colleagues proposed a method to determine the required reserve level for the electricity market dispatching system [29]. Their proposed method was based on submitting bids from the generators to the spot market where the market clearing prices were calculated by a mixed integer non-linear programming algorithm. After the collection of the market prices and generator schedules, an ANN was used to predict the required level of spinning and non-spinning reserve for a day-ahead market. In [30], a robust radial basis kernel function

(RBFK) based on an ANN was developed to solve the CEED problem, where the max-max price penalty factor was used to convert the emission volume into its respective price. In [31], a methodology using a combination of orthogonal least-squares (OLS) and enhanced particle swarm optimization (EPSO) algorithms to build a three layers RBF network for real-time CEED has been proposed. Kar et al used a hybrid ANN based on the back-propagation algorithm (BP-ANN) to find the optimum solution of the CEED problem where the volume of NOx was optimally regulated [32]. The adjusting parameters of the BP algorithm were optimally tuned during the convergence process, while the influence of other types of normalization rules and adjusting parameters, such as the number of hidden layers, the number of nodes in the hidden layers have been considered in [32].

Almost all the different types of neural networks based methods have some deficiencies in defining the network structure, and this problem would specifically increase the running time for real-time applications of ANN methods in a dynamic environment [33]. In addition, ANNs have a large number of adjusting parameters including the number of hidden layers, the number of neurons, input weight matrices, layer weight matrices and bias vectors, etc., and it requires the human interferences during the optimization process. In contrast to ANNs, support vector machines (SVMs) have an uncomplicated structure with only two adjusting parameters (which significantly reduces the running time of prediction process) as well as having the capability to be applied to any function within a dynamic environment. The basic concept of SVMs is based on the machine learning pattern, which was initially developed to solve classification problems [34]. SVMs present a promising performance in linear and non-linear identification applications through the use of linear constrained quadratic programming (QP) and Vapnik's ε-insensitive loss function, respectively. In [35], a hybrid method based on GA and SVM was proposed for the identification of electricity fraud through the daily load profile, where the SVM detected abnormalities due to a fraud incident. In order to enhance the capability of SVM, Mustaffa et al, coupled the classic SVM with the least-square method as well as a variant model of artificial bee colony to forecast the crude oil prices based on the time series data [36]. In [37], a method based on LSSVM and independent component analysis (ICA) optimizer has been presented for short term load forecasting. In order to enhance the prediction accuracy of LSSVM, the ICA transformed the dimensions of the input data from a higher level into a lower level, which also decreased the complexity of the model structure for the LSSVM.

The main idea of this study is to propose a methodology to calculate the optimal dispatch of generation units in the real-time electricity market, where the generator schedules must be evaluated in less than 15 minutes. The proposed method has the capability to predict the optimal dispatches of generation units with the high level of accuracy in less than 10 seconds for a large-scale power system, where it is approximately 100 times faster than the other widely industrial

used methods such as MIQP considering the physical and environmental constraints of generators. In order to understand the behaviour of any system in a suitable manner, the proposed method (LSSVM-CA3) requires historical data based on the hourly load curve of the system for at least one day. Thereafter, it has the ability to predict any unknown load point within the daily load curve with a high level of precision. In this regard, the following sophisticated mathematical formulation has been proposed.

The third version of cultural algorithm (CA3) has recently been proposed by Goudarzi et al [46]. CA3 has demonstrated a high capability of solving non-convex problems with a high degree of non-linearity. In this study, CA3 was used to optimally tune the two adjusting parameters of the LSSVM (γ and σ^2) in order to decrease the estimated error of the objective function. In order to prepare the training data set, a modified mixed integer quadratic programming (MIQP) has been used to obtain the optimum scheduling of the generation units according to the daily load curve of the selected test systems. To investigate the practicality of the proposed method (LSSVM-CA3), it has been compared with other hybrid methods of ANNs. The main innovative contributions of the proposed method are as follows:

i) A hybrid mathematical method for the prediction of the behaviour of any dynamic system based on the least square support vector machine and the third version of the cultural algorithm (LSSVM-CA3) has been proposed.

ii) The proposed method has the ability to understand and predict the non-linear behaviour of the power gird considering several realistic physical constraints of generation units for solving the CEED problem.

iii) The proposed method has the capability to comprehend and predict the environmental aspects of generation units in the real-time analysis of a large-scale power system.

iv) The proposed method is capable of finding the optimum schedule of generation units for a large-scale power system in a real-time electricity market within an extremely fast calculation time.

v) The proposed method is capable of maximization of social welfare while minimization of total cost of generation in the real-time electricity market.

The organization of the paper is as follows. Section 3.1 describes the background of the study through a comprehensive introduction. Sections 3.2 to 3.5 demonstrates the problem formulation and mathematical concepts of the proposed method. Section 3.6 provides the discussion of the obtained results. The conclusion is given in Section 3.7.

3.2 Problem formulation

3.2.1 Time window for the wholesale electricity market operation

As the main focus of study is the real-time scheduling of generation units in the electricity market, the time frame for the market operation is depicted in Fig 3.1. All the given terminologies in Fig 3.1 are defined as follows:

3.2.1.1 Capacity Market

This is designed to guarantee an adequate and reliable generating capacity and is always available by providing payments to encourage investment in new capacity or for existing capacity to remain open. In other words, it is the primary policy of any market operation to ensure the security of electricity supply, while it has a time span from 1 to 5 years [39].

3.2.1.2 Multi Day-ahead Unit Commitment

The unit commitment schedule of the dispatchable generation units should be prepared by the system operator in less than 24 hours while the physical constraints of the generation units should be considered. In this context, hydro and nuclear units would be treated as must-run units (to be responsible for the base-load) in the day-ahead market.

3.2.1.3 Day-ahead Market

Market participants are required to submit their bids or offer within a pre-specified submission time. The contracts will be settled between seller and buyer for the delivery of power in the following day, where the price is set and the trade is agreed. It is vital to indicate that the offers or bids are the financial key performances of any business process [38]. The detailed operations for day-ahead market can be listed as follows [59]:

- 24 hours ahead scheduling considering the load forecast of the next day
- Determining the commitment of the slow thermal units

3.2.1.4 Intraday Scheduling

The intraday scheduling supplements the day-ahead market and provides any necessary changes to balance between supply and demand. The detailed operations for intraday scheduling can be listed as follows [59]:

- 4 hours ahead scheduling of generators (until cover the entire day)
- Determining the commitment of the fast operating units

3.2.1.5 Real-time Market

The system operator is required to provide the generating unit dispatches, reserve margins, real-time locational marginal prices (LMPs) and market clearing prices (MCPs) every 5 to 15 minutes.

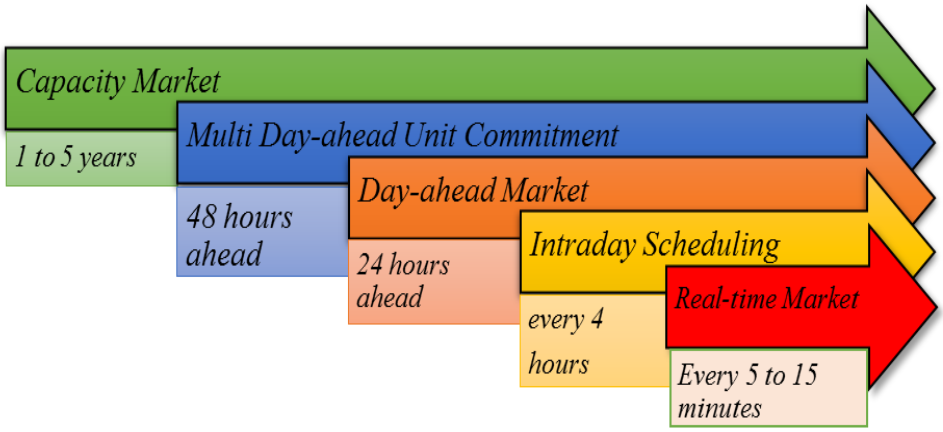

Fig. 3.1 Time frame of the electricity market operation

3.2.2 Combined environmental economic dispatch (CEED)

The main elements of the electrical power grid which have a significant influence to deliver the power generation at the least cost are optimum scheduling of generation units, fuel cost, and transmission line losses. The most effective generating unit in the power grid is not able to guarantee to decrease or minimize the total generation cost as it may be located far away from the load demand which would effectively lead to greater transmission losses or a variation in the fuel cost according to the geographical location of generation units. The main aim of the combined environmental economic dispatch (CEED) method is to minimize the total generation cost by satisfying the power grid operation constraints and considering the environmental aspects of generation [40].

The generation cost function of the CEED method can be defined as follows:

$$f_{gc}(P_i^t) = \sum_{i=1}^{N_G} \left(a_i + b_i P_i^t + c_i (P_i^t)^2\right) \quad (1)$$

In the conventional approach, economic load dispatch (ELD) makes a simplification by assuming that the efficiency of the electrical power generators increases cubically, quadratically, piece-wise linearly or sometimes can be formulated linearly with respect to the power output. In real life practice, the volume of the steam entering the turbines would be controlled by sets of separate nozzles. Each one of the nozzle sets accomplishes the best efficiency when the generating unit is operating at full capacity. By increasing the power output of the generation units, their respective valves will be opened in series to obtain the highest possible efficiency for the considered power output. The valve-point effect introduces a ripple in the heat rate function which leads to non-linearity and discontinuity of the fuel cost function [41]. A rectified sinusoidal term can be added to the previous equation for precise modelling of the generator cost function with the consideration of the valve-point effect:

$$f_{gc}(P_i^t) = \sum_{i=1}^{N_G} [\left(a_i + b_i P_i^t + c_i (P_i^t)^2\right) + \left|d_i \times \sin\{e_i \times (P_i^{min} - P_i^t)\}\right|] \tag{2}$$

As most of the fossil fuel based generation units are the main sources of SO_x and NO_x, they have been firmly instructed by the environmental protection agency (EPA) to decrease their production emission levels. This study considered NO_x to be optimally regulated for the environmental aspects. The emission objective function with the inclusion of the valve-point effect can be represented as [26]:

$$f_{emc}(P_i^t) = \sum_{i=1}^{N_G} [\left(\alpha_i + \beta_i P_i^t + \gamma_i (P_i^t)^2\right) + \eta_i \exp(\delta_i P_i^t)] \tag{3}$$

In order to evaluate the total cost of generation for the CEED problem the two independent cost functions can be combined by means of a price penalty factor which converts the multi-objective function into a single-objective term as follows [42]:

$$F_{ct}(P_i^t) = f_{gc}(P_i^t) + h_i^{max-max} \times f_{emc}(P_i^t) \tag{4}$$

$$\begin{aligned} F_{ct}(P_i^t) = \sum_{i=1}^{N_G} & \left(a_i + b_i P_i^t + c_i (P_i^t)^2\right) + \left|d_i \times \sin\{e_i \times (P_i^{min} - P_i^t)\}\right| \\ & + h_i^{max-max} \\ & \times \sum_{i=1}^{N_G} \left(\alpha_i + \beta_i P_i^t + \gamma_i (P_i^t)^2\right) + \eta_i \exp(\delta_i P_i^t) \end{aligned} \tag{5}$$

where $h_i^{max-max}$ denotes the price penalty factor (PPF) in dollar per hour. The PPF is the ratio between the maximum generation cost function and the maximum emission objective function, where it can be written as [43]:

$$h_i^{max-max} = \frac{(a_i + b_i P_i^{max} + c_i (P_i^{max})^2) + \left| d_i \times \sin\{e_i \times (P_i^{min} - P_i^{max})\} \right|}{\left(\alpha_i + \beta_i P_i^{max} + \gamma_i \left(P_i^{max}\right)^2\right) + \eta_i \exp(\delta_i P_i^{max})} \quad (6)$$

In a general form the proposed CEED objective function can be rewritten as follows:

$$F_{ct}(P_i^t) = \omega_1 \times f_{gc}(P_i^t) + \omega_2 \times h_i^{max-max} \times f_{emc}(P_i^t) \quad (7)$$

where the ω_1 and ω_2 are the weighting factors of the proposed formulation, in such a way that:

$\omega_2 = 0$ for the pure economic dispatch without the consideration of emission cost

$\omega_1 = 0$ for the pure emission dispatch without the consideration of generation cost

ω_1 and $\omega_2 = 1$ for the combined environmental economic dispatch

Subject to the following constraints:

The first set of constraints is related to the systematic constraints which are required to be maintained.

3.2.2.1 Power Balance Equality constraint

$$\sum_{i=1}^{N_G} P_i^t = P_D^t \quad (8)$$

The total generation should be able to satisfy the given load demand at any interval, where P_D^t represents the total system load demand at interval *t*.

3.2.2.2 Inequality constraints of the generators

For the safety purposes of the generation units as well as the stable operation of the system, all the generation units are firmly limited to operate within their minimum and maximum generation capacity; accordingly, the inequality constraint can be stated as follows:

$$P_i^{min} \leq P_i^t \leq P_i^{max} \quad for\ i = 1,2,3 \ldots N_G \quad (9)$$

The second set of constraints is associated with the physical constraints of the generation units which are required to be strictly upheld.

3.2.2.3 Ramp rate limits

In CEED formulation, the power output is commonly presumed to be regulated efficiently and instantly. In the real practices, ramp rate limit confines the operating range of all the generation units within two independent intervals [44]; (1) as generation increases and (2) as generation decreases:

$$max\left(P_i^{min}, P_i^0 - DR_i\right) \leq P_i^t \leq min(P_i^{max}, P_i^0 + UR_i) \tag{10}$$

subject to

$$(1) \qquad P_i^t - P_i^0 \leq UR_i \tag{11}$$

$$(2) \qquad P_i^0 - P_i^t \leq DR_i \tag{12}$$

3.2.2.4 Prohibited operating zone (POZ)

Modern generation units with the inclusion of the valve-point effect have several prohibited operating zones (POZs) which impose a number of discontinuities in their power generation output [44]. Consequently, in practical operation, POZs splits the operating range among minimum and maximum generation limits into fragmented convex sub-sections. The practical operating zones can be expressed as:

$$\begin{cases} P_i^{min} \leq P_i^t \leq P_{i,1}^L \\ P_{i,m-1}^U \leq P_i^t \leq P_{i,m}^L \\ P_{i,N_i^{PZ}}^U \leq P_i^t \leq P_i^{max} \end{cases} \qquad m = 2, \dots, N_i^{PZ}; \forall i \in \psi \tag{13}$$

3.2.2.5 Spinning reserve

A minimum system spinning reserve is required to be considered to satisfy the system load demand and be responsible for any frequency changes due to load fluctuations in real-time systems [45]:

$$\sum_{i \in \Psi} S_i^t \geq S_R \tag{14}$$

where

$$S_i^t = \min\left\{\left(P_i^{max} - P_i^t\right), S_i^{max}\right\}, \qquad \forall i \in (\Psi - \psi) \tag{15}$$

$$S_i^t = 0, \quad \forall i \in \psi \tag{16}$$

The spinning reserve requirement should be carried out by the units without POZs, where they have no restriction to regulate their power generation smoothly within the boundaries.

3.2.2.6 Power balance handling

In order to guarantee that the power balance generation and equality constraint are continuously sustained, the study considered a power balance violation (PBV) method. The PBV can be described as [46]:

$$\sum_{i=1}^{N_G} P_i^t \geq P_D^t \tag{17}$$

subject to

$$PBV = max(1 - \frac{\sum_{i=1}^{N_G} P_i^t}{P_D}, 0) \tag{18}$$

As long as PBV is set to zero, the equality constraint has been maintained where the algorithm should only accept the solutions which are capable of holding the following relationship:

$$P_D^t - \sum_{i=1}^{N_G} P_i^t = 0 \tag{19}$$

The study has utilized an evaluation function to speed up the convergence process and obtain the optimum solutions. This approach uses a penalization factor (PF) method to push the answers towards the best possible solution. The proposed method can be expressed as follows:

$$F_{eval} = F_{ct}\left(P_i^t\right) \times (1 + PF \times PBV) \tag{20}$$

In this study, the initial value of PF has been considered equal to 1,000. Nevertheless, this value could vary up to 1,000,000 based on many factors such as the topology and nature of the problem.

3.3 The third version of Cultural Algorithm (CA3)

Many decades ago, a number of scientists who were working on the social behaviour of people suggested an idea that culture has the ability to be transferred to a population through an inheritance mechanism. In 1994 Reynolds proposed an algorithm based on the cultural model [47]. The cultural algorithm (CA) was established according to the behaviour of elite individuals

in a certain population, where their behaviour is transmitted inherently from generation to generation through motivated operators. The elite group of the population characterizes and regulates the norms [48]. The selection basis of this elite group is based on many factors such as physical appearance, wealth, and knowledge. The knowledge and ideas of those individuals become the most effective leading factor of the society. Culture or tradition improves from a generation to the next generation in order to make them more conscious and capable of survival. The evolution of a population is a process where the knowledge that has been obtained by elite individuals through generations in the search space (belief space) would be kept to direct the behaviour of the other individuals. CA has been implemented based on the two basic components namely the population space and the belief space. The population space is responsible for the storage of an individual's information, and the responsibility of the belief space is to shape and maintain the cultural knowledge during the evolution process. The general framework of CA is depicted in Fig 3.2.

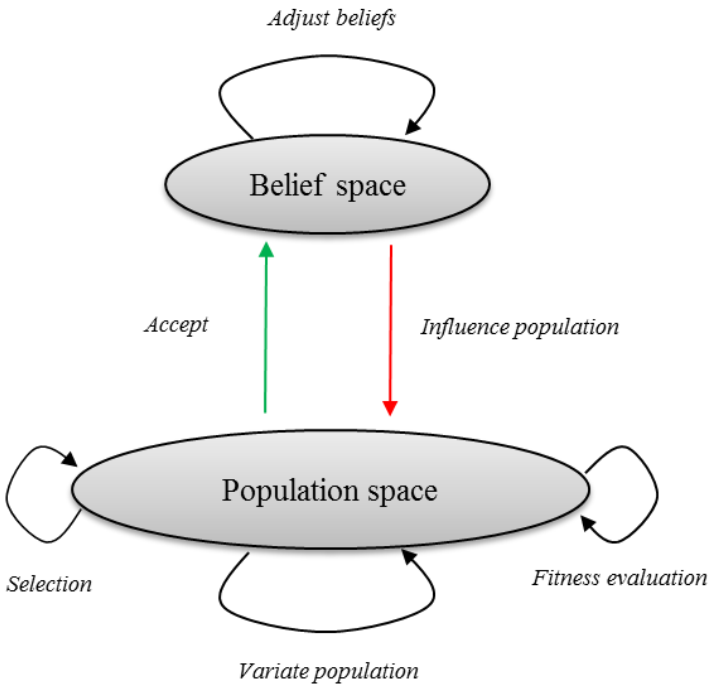

Fig. 3.2 Conceptual framework of cultural algorithm based on the two spaces

CA can be categorized into different versions based on their influence functions. The responsibility of the influence function is to affect the population according to the regulation of beliefs to determine the mutational step size and the direction of changes. Goudarzi, et al [46]. proposed four versions for CA, where the third version (CA3) was found as the most efficient version for the CEED optimization. CA3 is based on two knowledge components; the situational

knowledge component and the normative knowledge component. The situational knowledge component is in charge of finding the best possible solution in a generation, and is formulated as [46]:

$$S(t+1) = \{\hat{y}(t+1)\} \tag{21}$$

where

$$\hat{y}(t+1) = \begin{cases} min_{l=1,\dots,n_B(t)}\{X_l(t)\}, & if\ f\left(min_{l=1,\dots,n_B(t)}\{X_l(t)\}\right) < f(\hat{y}(t)) \\ \hat{y}(t) & otherwise \end{cases} \tag{22}$$

subject to

$$X_l(t), l = 1,2,3 \dots, n_B(t) \tag{23}$$

$$n_B(t) = \left[\frac{n_{pop}\gamma}{t}\right], \quad \gamma \in [0,1] \tag{24}$$

where

$n_B(t)$ is the number of selected individuals for forming the beliefs in a population

t is the number of iterations (generation)

n_{pop} is the size of population

The normative knowledge is the component which prepares different scales for each individual behaviour in order to direct them towards their mutational adjustments. The normative knowledge can be mathematically expressed as:

$$x_j^{min}(t+1) = \begin{cases} x_{lj}(t), & if\, x_{lj}(t) \le x_j^{min}(t)\ \ or\ \ f\left(X_l(t)\right) < L_j(t) \\ x_j^{min}(t) & otherwise \end{cases} \tag{25}$$

For updating the $L_j(t)$

$$L_j(t+1) = \begin{cases} f\left(X_l(t)\right), & if\, x_{lj}(t) \le x_j^{min}(t)\ \ or\ \ f\left(X_l(t)\right) < L_j(t) \\ L_j(t) & otherwise \end{cases} \tag{26}$$

$$x_j^{max}(t+1) = \begin{cases} x_{lj}(t), & if\, x_{lj}(t) \ge x_j^{max}(t)\ \ or\ \ f\left(X_l(t)\right) < U_j(t) \\ x_j^{max}(t) & otherwise \end{cases} \tag{27}$$

For updating the $U_j(t)$

$$U_j(t+1) = \begin{cases} f\big(X_l(t)\big), & if\, x_{lj}(t) \geq x_j^{max}(t) \;\; or \;\; f\big(X_l(t)\big) < U_j(t) \\ U_j(t) & otherwise \end{cases} \tag{28}$$

As proposed in this version, the step size would be defined by means of situational knowledge where the changes in direction would be carried out by normative knowledge. CA3 can be described as:

$$\acute{x}_{ij}(t) = \begin{cases} x_{ij}(t) + \left|\sigma_{ij}(t) N_{ij}(0,1)\right| & if\; x_{ij}(t) < \hat{y}_j(t) \\ x_{ij}(t) - \left|\sigma_{ij}(t) N_{ij}(0,1)\right| & if\; x_{ij}(t) > \hat{y}_j(t) \\ x_{ij}(t) + \sigma_{ij}(t) N_{ij}(0,1) & otherwise \end{cases} \tag{29}$$

subject to

$$x_{ij}(t) \sim N_{ij}(x_{ij}(t), {\delta_j}^2(t)) \tag{30}$$

$$\delta_j(t) = [x_j^{max}(t) - x_j^{min}(t)] \tag{31}$$

$$\sigma_{ij}(t) = \alpha \times \delta_j(t), \quad 0 < \alpha < 1 \tag{32}$$

It is important to mention that, the CA3 is characteristically so fast because it uses two knowledge components (situational knowledge and normative knowledge) as two powerful search engines in the search space to find the optimal solution and it significantly speeds up the convergence process and reduces the running time. Any further details and illustration of the CA3 method can be found in [46].

3.4 Least square support vector machine (LSSVM)

The least square support vector machine (LSSVM) was introduced by Suykens and colleagues and is based on the principal of support vector machine (SVM) [49]. In LSSVM, equality constraints are used as a replacement for inequality constraints through a least square cost function to tackle the difficulty of calculations towards optimal solutions. The proposed cost function can be solved by means of linear Karush-Kuhn-Tucker (KKT) optimality conditions instead of a quadratic programming problem. Consequently, the classical SVM can be reformulated as the following LSSVM cost function [50]:

$$cost\; function = \frac{1}{2} w^T w + \frac{1}{2} \gamma \sum_{k=1}^{N} e_k^2 \tag{33}$$

subject to

$$y_k = w^T \varphi(x_k) + b + e_k, \quad k = 1, 2, 3 \dots, N \tag{34}$$

where

b is the bias

w^T is transposed vector of the output layer

$\varphi(x)$ is the feature map

γ is the adjustable parameter

e_k is the error variable

x_k k^{th} number of input data

y_k k^{th} number of output data

As the vector w can increase to infinite dimensions, making the optimization process cumbersome as in eq. (33). To overcome this problem, LSSVM has tried to calculate the model in the dual space instead of in the primal space. The Lagrangian solution can be applied as follows [51]:

$$L(w, b, e, a) = \frac{1}{2} w^T w + \frac{1}{2} \gamma \sum_{k=1}^{N} e_k^2 - \sum_{k=1}^{N} a_k (w^T \varphi(x_k) + b + e_k - y_k) \tag{35}$$

where a_k denotes the Lagrangian multiplier. The KKT optimality conditions can be expressed by [52]:

$$\begin{cases} \dfrac{\partial L}{\partial w} = 0 \ \rightarrow w = \displaystyle\sum_{k=1}^{N} a_k \varphi(x_k) \\ \dfrac{\partial L}{\partial b} = 0 \ \rightarrow \displaystyle\sum_{k=1}^{N} a_k = 0 \\ \dfrac{\partial L}{\partial e_k} = 0 \ \rightarrow a_k = \gamma e_k, \quad k = 1, 2, 3 \dots, N \\ \dfrac{\partial L}{\partial a_k} = 0 \ \rightarrow w^T \varphi(x_k) + b + e_k - y_k = 0, \quad k = 1, 2, 3 \dots, N \end{cases} \tag{36}$$

N is the number of data points in the training set $\{x_k, y_k\}_{k=1}^{N}$, where $x_k \in R^n$ and $y_k \in R$. Based on the KKT optimality condition the parameters a_k,e_k, w and b can be computed. These conditions are almost identical to the standard form of SVM as a classifier, apart from the condition $a_k = \gamma e_k$ [51].

To come up with the sparseness property of LSSVM, it is possible to go through the elimination process of w and e where the resultant solution can be expressed as follows:

$$\begin{bmatrix} 0 & 1_v^T \\ 1_v & \Omega + \frac{1}{\gamma} I \end{bmatrix} \begin{bmatrix} b \\ \alpha \end{bmatrix} = \begin{bmatrix} 0 \\ y \end{bmatrix} \tag{37}$$

where

$y = [y_1; \dots; y_N]$

$1_v = [1_1; \dots; 1_N]$

$\alpha = [a_1; \dots; a_N]$

$\Omega_{kl} = \varphi(x_k)^T \varphi(x_l)$ for $k, l = 1,2,3, \dots, N$

By means of Mercer's condition and the mapping feature the Kernel function can be written as follows [51]:

$$K(x, y) = \sum_{i=1}^{N} \varphi_i(x)\varphi_i(y), \quad x, y \in \mathbb{R}^n, \tag{38}$$

The aforementioned condition is held if and only if, for any function *g(x)* that $\int g(x)^2 dx$ is finite, there would be one solution:

$$\int K(x, y)g(x)g(y)dxdy \geq 0 \tag{39}$$

As consequence of the above condition the solution of the kernel can be represented as a bullet operator $\left(K(\cdot,\cdot)\right)$ such that:

$$K(x_k, x_l) = \varphi(x_k)^T \varphi(x_l), \quad k \; and \; l = 1, 2, 3 \dots, N \tag{40}$$

The LSSVM for the function estimation can be simplified as:

$$y(x) = \sum_{k=1}^{N} \alpha K(x, x_k) + b \tag{41}$$

where α and b are the key parameters to determine. γ is the first adjustable parameter of the LSSVM and as it is a Kernel-based technique, it is required to consider the parameters of kernel

functions as another (or second) adjustable parameter of the algorithm. Accordingly, the RBF Kernel function that has been used in this study can be given by [51, 52]:

$$K(x, x_k) = \exp(-\frac{\|x_k - x\|^2}{\sigma^2}) \tag{42}$$

The developed LSSVM model has two adjustable parameters (γ and σ^2). The accuracy of the algorithm is highly dependent on its own adjustable parameters. The study utilized CA3 to tune and find the most optimum values of the adjustable parameters to minimize the deviation of the predicted data points. Fig 3.3 and Fig 3.4 represent the network structure and flow chart process of the LSSVM-CA3, respectively.

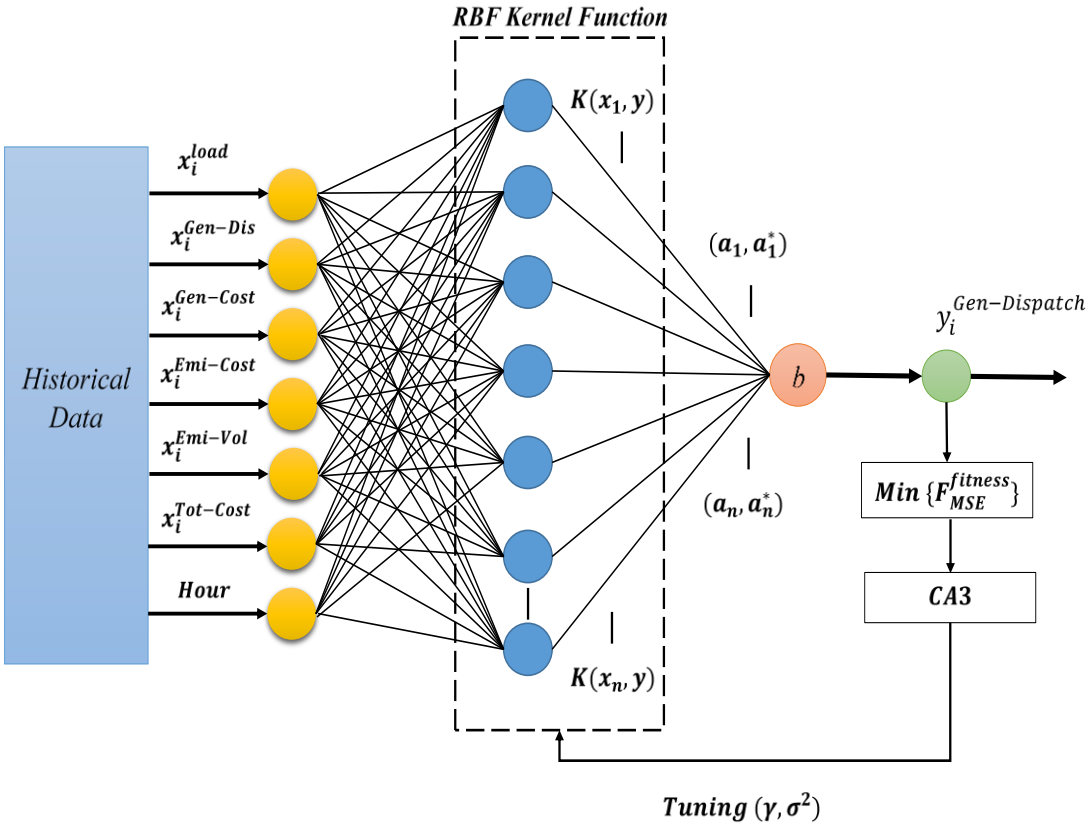

Fig. 3.3 General network structure of LSSVM-CA3

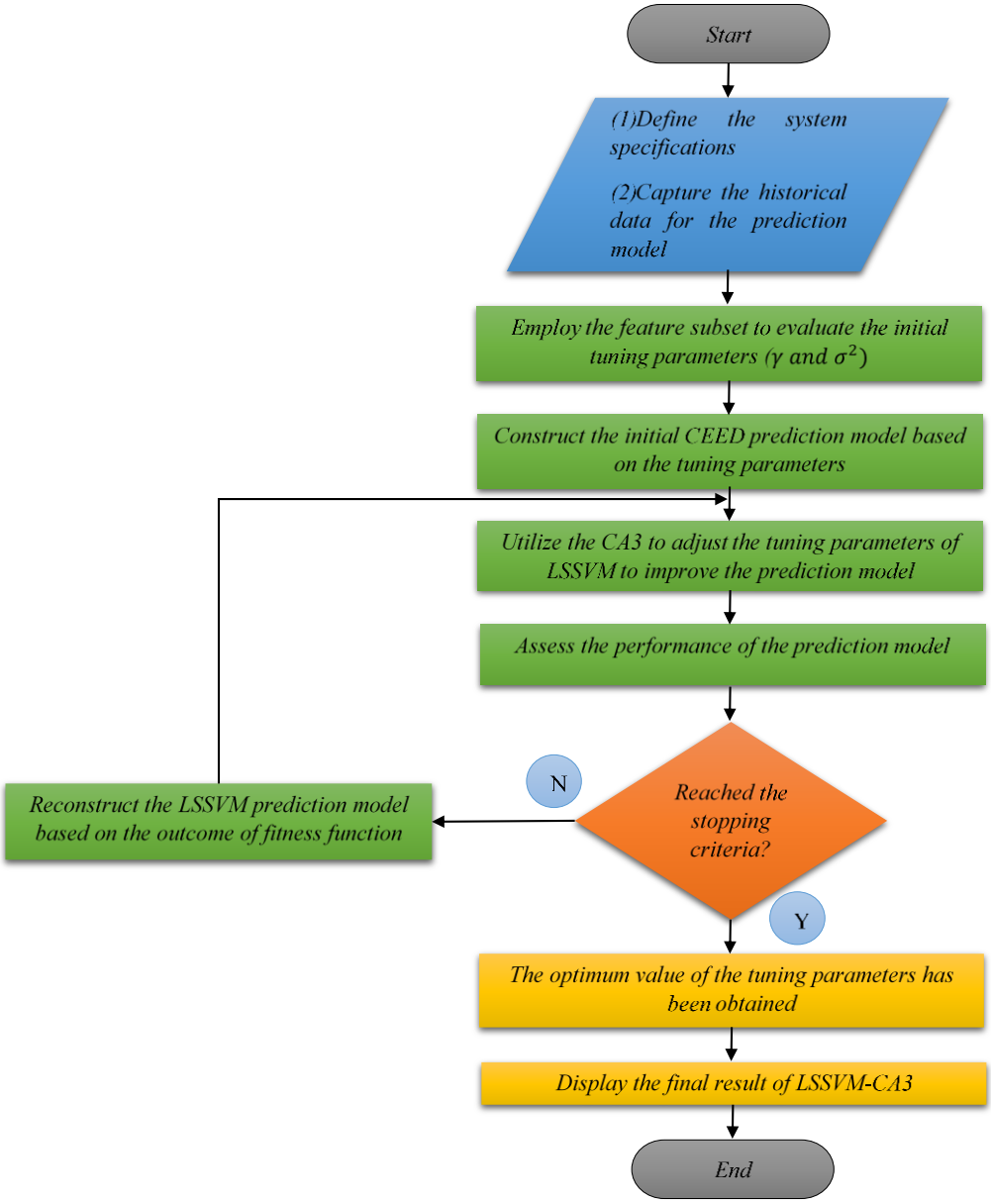

Fig. 3.4 flow chart process of LSSVM-CA3

3.5 Evaluation of prediction performance

The precision of the proposed method (LSSVM-CA3) was examined by means of mean squared error (MSE), root mean squared error (RMSE), normalized root mean squared error (NRMSE) and mean absolute error (MAE). These four performance measurement techniques are extensively used to examine how well a method performs in prediction or fitting of the actual values.

MSE is extensively used to measure the difference between predicted values by a method and actual values. This method compares the mean of squared residuals against the predicted values. RMSE can be assessed by taking a root of the calculated MSE. The evaluated RMSE has a wide range of units with respect to the different test cases. In order to have a uniform comparison capability of RMSE for different methods with diverse units, the non-dimensional form of RMSE known as NRMSE is used. NRMSE is achieved by normalizing the RMSE value to the range of the observed data [53]. Thus the NRMSE values that are closer zero are more desirable, and they represent the better performance of the applied method. The respective formulation for MSE, RMSE and NRMSE can be described as:

$$MSE = \frac{1}{N_G}\sum_{i=1}^{N_G}\left(P_i^{Actual} - P_i^{Predict}\right)^2 \tag{43}$$

$$RMSE = \sqrt{\frac{1}{N_G}\sum_{i=1}^{N_G}\left(P_i^{Actual} - P_i^{Predict}\right)^2} \tag{44}$$

$$NRMSE = \frac{RMSE}{P_i^{max} - P_i^{min}} \tag{45}$$

P_i^{Actual} is the actual generation schedule of the units

$P_i^{Predict}$ is the predicted generation schedule of the units

MAE has also been used to assess the performance of LSSVM- CA3. The evaluation range of MAE is the same as RMSE, however in MAE the values in this study are not expressed in percentage. The mathematical formulation of MAE is as follows [54]:

$$MAE = \frac{1}{N_G}\sum_{i=1}^{N_G}\left|P_i^{Actual} - P_i^{Predict}\right| \tag{46}$$

3.6 Results and discussion

In this study, the proposed LSSVM-CA3 method was used to predict and determine the most optimum scheduling of generation units in the real-time system for solving the CEED problem and has been tested on different scenarios. To examine the effectiveness of the proposed method for practical purposes, it has been tested on three different test systems through several considerations test system characteristics. All comparison cases were performed to demonstrate the applicability of the methodology of the study. All the algorithms have been implemented on MATLAB 2015a. They have been executed on a personal computer with the following specifications, Intel® Core™ i5-3210M (3.1 GHz), 6.00 GB RAM (DDR3) and win 8.1 operating system (OS). All the intelligent methods are very sensitive to their adjusting parameters; therefore the study has considered the following values for the compared methods:

GA:

- Population size: 50
- Maximum number of iterations: 50
- Crossover probability: 0.8
- Mutation probability: 0.1

PSO:

- Population size: 50
- Maximum number of iterations: 50
- C1 and C2: 2
- Inertia weight: Min= 0.4 and Max= 0.9

ICA:

- Population size: 50
- Maximum number of iterations: 50
- Number of empires: 10
- Selection pressure: 1
- Assimilation coefficient: 1.5
- Revolution probability: 0.05
- Revolution rate: 0.1
- Colonies mean cost coefficient: 0.2

CA3:

- Population size: 50
- Maximum number of iterations: 50
- Acceptance ratio: 0.15
- Strategy parameter: 0.25
- Scaling coefficient: 0.5

The study has considered a daily load curve (24 hour load points) according to the capability of each test system for handling of the load demand, while the daily load curves have been specified in each studied case. Daily load curves have been used for training purposes of all predictors. In real practice, by having the historical data of any system over a sufficient period of time and using the maximum likelihood method (MLE) the most probable load points of the system during a day can be determined. Due to the unavailability of data for the loss coefficients in different hours of the day in each test system, the calculation of power loss has not been taken into account. All the required data regarding the test system specifications are given in the appendix section. As the renewable energy resources (RESs) like wind and solar have an uncertain and intermittent behaviour, therefore, they require another mathematical approach to model and forecast their generation behaviour before any prediction process regarding the optimal scheduling of the available units, where in this study we assumed all the generation units are running and they are available to be scheduled at any time. Therefore, in the current study, we have not considered any RESs in the studied test cases.

The main focus of the study is to find a fast, intelligent and practical solution for the real-time scheduling of generation units through to CEED problem, not the unit commitment (UC) problem. Therefore, the proposed solution for the real-time CEED problem only deals with the optimal allocation of the load demand among the running units while satisfying the power balance equations and considering the physical operating limits and environmental constraints of generation units.

Almost all of the deterministic mathematical methods are incapable of solving the non-convex problem with discontinuous domains. This study used one of the most recent methods which is widely used in industries and wholesale electricity spot markets to solve the CEED problem with discontinuous operating zones. This method is based on mixed integer quadratic programming (MIQP) while the Branch-and-Bound method through a binary tree with the interior-point algorithm is coupled with MIQP to deal with discontinuous zones [55]. To simulate the same approach of solving the CEED as it is practiced in real-time electricity markets, the study applied MIQP to compute the optimal scheduling of generation units for each hour of the day

which was used for a realistic comparison between the proposed method and the current industrial approach in solving CEED as well as the preparation of a database for training purposes.

The calculated database has been divided into two subsets namely, training and testing. To enhance the applicability of the model, the entire database has been randomly divided into the following percentages; 80% used for the training set and 20% used for the testing set. The training set was applied to generate the model structure and the testing set was employed to examine the final performance and validity of the proposed model. As all the compared predictors were coupled with an optimization algorithm for tuning their adjusting parameters, therefore the validation set was not considered. The adjusting parameters of LSSVM (γ and σ^2) are optimized by CA3, while the adjusting parameters of ANN such as input weight matrix (IW), layer weight matrix (LW) and bias vectors (b) have been optimally tuned by GAPSO, PSO, GA and ICA respectively. To investigate the practicality and the robustness of the proposed method it has been compared to four most prominent prediction methods developed namely; ANN-GAPSO, ANN-PSO, ANN-GA and ANN-ICA. The objective function of all prediction methods is to minimize the errors in prediction according to mean squared error (MSE) technique.

In this study, a specific design has been used for the RBF-kernel function to approximate a very precise initial guess based on the input data. The basic kernels have been used as a predefined set of initial guess of the kernel matrices. The utilized kernel learning algorithm operates by inserting the data into a Euclidean space. Thereafter, it searches for a linear relationship between the inserted data points. The inserting is achieved implicitly, by identifying the internal products between each pair of data points in the embedding space. This information is stored in the kernel matrix, which is a symmetric and positive semidefinite matrix that encodes the relative positions of all data points. The determined Kernel matrix helps the SVM to predict a very accurate initial guess which effectively causes a reduction in the initial MSE in the prediction process.

To demonstrate the practicality of the proposed method in the prediction of the generating unit's schedules, two unknown load points were selected within the generation capacity range. Both of the load points for each test system were selected in a way that they can distinctly demonstrate the capability of LSSVM-CA3, where the first load point was located in the lower generation range and the second one was picked from a challenging operating area of the generation units, where they have the highest probability of occurrence during a day. For both load points, a number of the scheduling scenarios could be taken into account with regard to the flexibility of the generation units in the least cost operation.

In order to have a unified comparison for all studied cases, the spinning reserve requirement was set as 5% of total load demand as in [56]. The study executed 20 trials for each scenario to

produce fair results and consideration of any associated error in calculations, while the maximum number of iterations for all the trials was fixed at 50. Due to the large dimension of the test systems, it is not feasible to present the generators' dispatches, however, the final evaluations for each scenario have been tabulated as a means of comparison.

3.6.1 Test Case 1

This case attempted to demonstrate the efficiency of the proposed method of study to find the optimal scheduling of generation units without using the CEED method. For this purpose, the proposed method was applied to find the optimal scheduling of a 15 units test system, where the system specifications are available in Appendix A. The effect on the total generation cost of ramp rate limits, spinning reserve requirement and prohibited operating zones were considered. Fig 3.5 depicts the daily load curve for this test system, while the highest and lowest load of the day were equal to 1511 and 2815 MW, respectively. The hourly load, total generation cost of each hour and their respective generator schedules have been used as inputs for training and constructing the initial model. MIQP has been used to find the most optimum schedules for every given load point of the day. Two random load points (1600 and 2475 MW) among the given load points have been selected to be found by LSSVM-CA3 and the other methods, where for comparison purposes the schedules of these two load points have been found by MIQP. The process of convergence of the adjusting parameters of all predictor methods in order to minimize the MSE for both the selected load points are shown in Fig 3.6 (a and b).

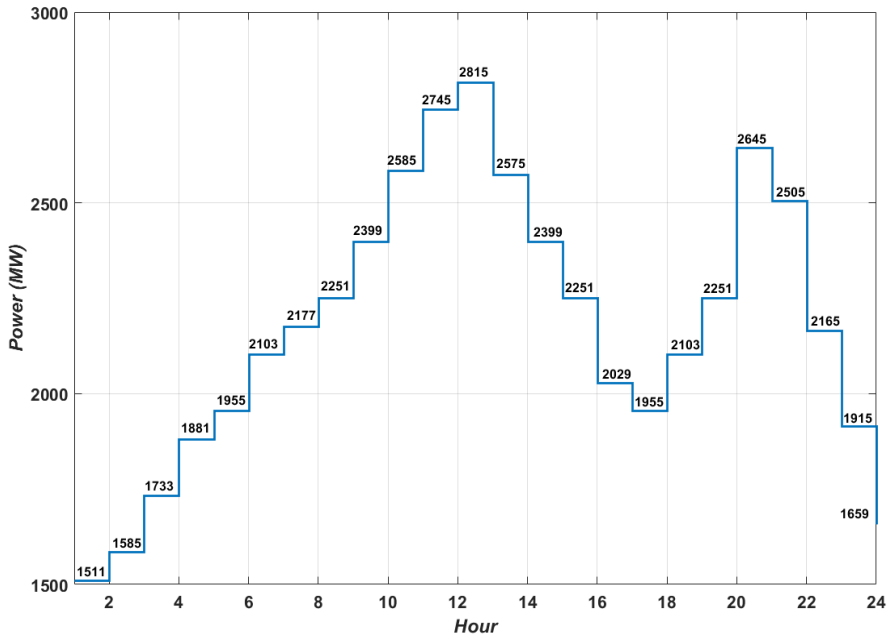

Fig. 3.5 Daily load curve for 15 units system

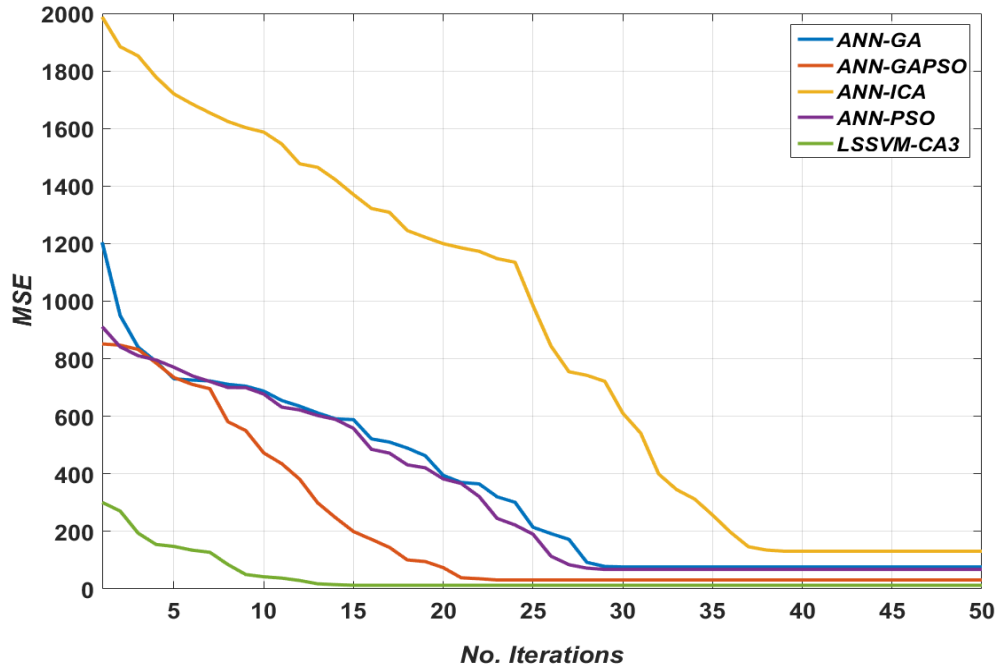

Fig. 3.6.a Convergence process of LSSVM-CA3 adjusting parameters (first predicted load point, 1600 MW)

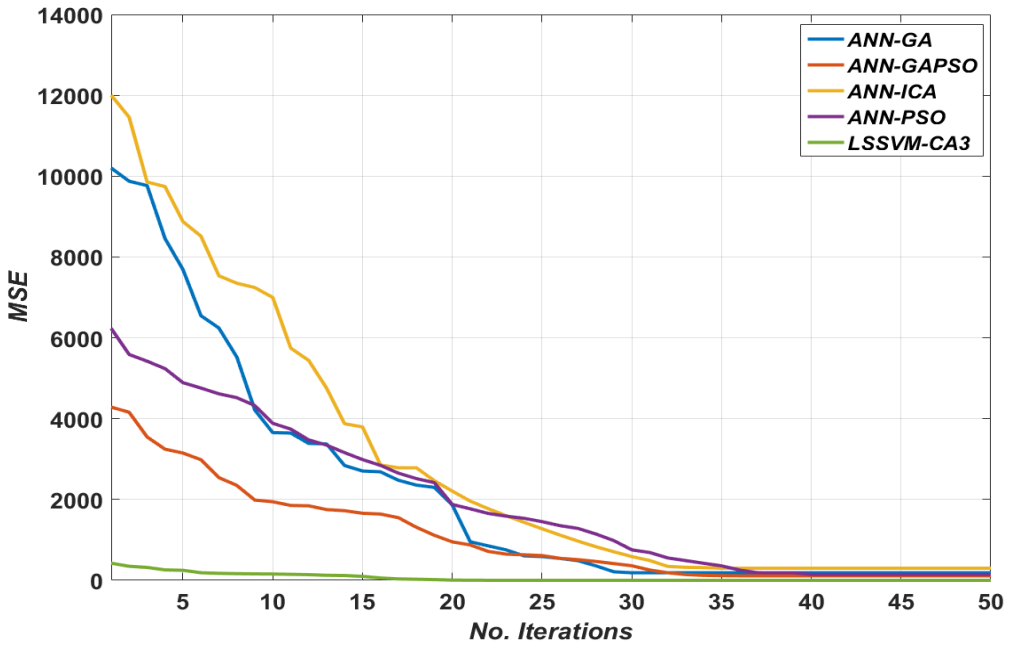

Fig. 3.6.b Convergence process of LSSVM-CA3 adjusting parameters (second predicted load point, 2475 MW)

As it can be seen from Fig 3.6.a and 3.6.b, the proposed algorithm (LSSVM-CA3) has reached to its optimum level in less than 17 iterations for the both load points, whereas the other

methods have reached in closer to 30th iterations. Table 3.1 tabulates the final values of the adjusting parameters for the LSSVM-CA3. Table 3.2 tabulates the maximum cost, average cost, minimum cost, and average elapsed time for all the compared methods. For simplicity of comparison, the elapsed time of each method was calculated for the average time of all 20 trials. From Table 3.2, it is clear that the LSSVM-CA3 has obtained the lowest average and minimum total generation cost in comparison to the other methods with the lowest processing time.

Table 3.1 Final optimized values for LSSVM-CA3 adjusting parameters (15 units system)

Load Point (MW)	γ	σ^2
1600	114.21	3.24
2475	743710.44	68.84

Table 3.2 Comparison of the obtained results for MSE (15 units system)

1600 MW	Min	Avg	Max	Avg Elapsed Time (s)
LSSVM-CA3	12.72	49.74	128.38	0.13
ANN-GAPSO	31.38	278.08	737.69	15.24
ANN-PSO	67.97	274.86	803.64	2.46
ANN-GA	76.76	280.31	911.17	2.15
ANN-ICA	131.20	402.16	1554.21	6.22
MIQP	…	…	…	35.36
2475 MW				
LSSVM-CA3	0.78	40.27	102.43	0.14
ANN-GAPSO	109.07	731.67	3338.70	17.57
ANN-PSO	144.07	290.35	774.21	2.85
ANN-GA	186.12	520.05	976.64	3.39
ANN-ICA	299.15	579.99	1255.03	5.86
MIQP	…	…	…	35.75

Fig 3.7.a and 3.7.b show the residuals representation of the methods for both the load points compared to the calculated actual values using MIQP. For accurate evaluation of the predictions, the residual set has been divided into two subsets; train and test. In order to have a precise

assessment of residual behaviours, the confidence bound has been set as 25% of the highest deviation from the actual generation units' schedules. Placement of more residual values within the confidence bound and closer to the actual data line (actual generator schedules calculated by MIQP) demonstrates the higher accuracy of the method. The LSSVM-CA3 represents the highest accuracy for both load points in comparison to the other methods. For the first load point, the placement of the residuals for the different subsets are 91.67% for the training phase, 66.67% for the testing phase with a total of 86.67%. In the case of the second selected load point, the performance of the proposed method is absolutely outstanding by having 100% accuracy of prediction placement within the confidence bound, where the second best method is ANN-GAPSO by having 66.67% placement inside the confidence bound in total.

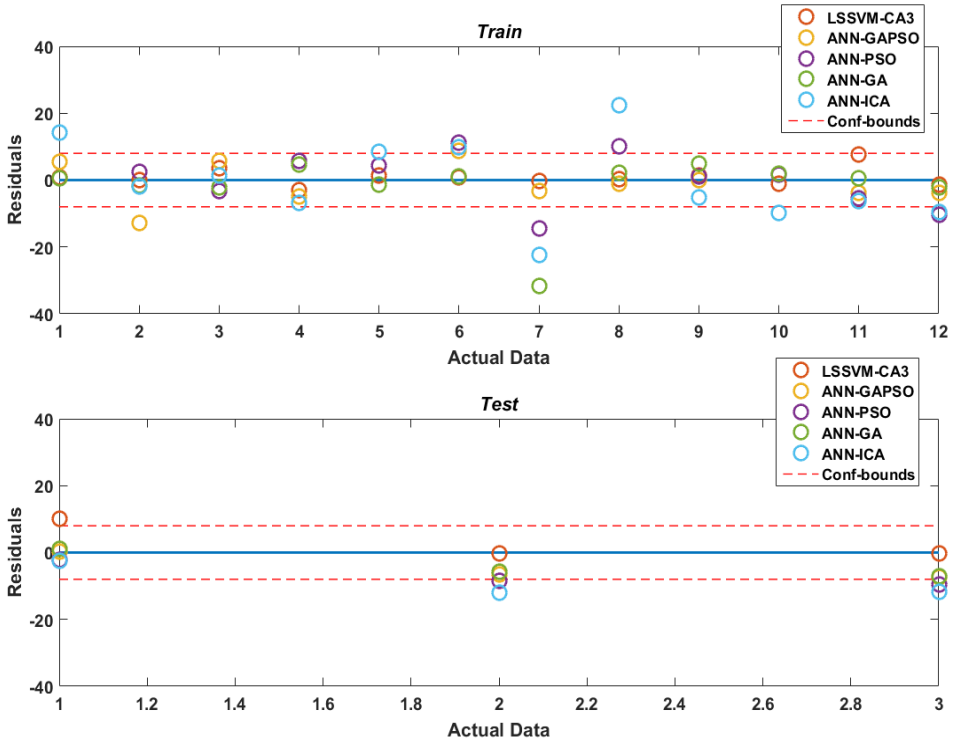

Fig. 3.7.a Residual representation for the first predicted load point (1600 MW)

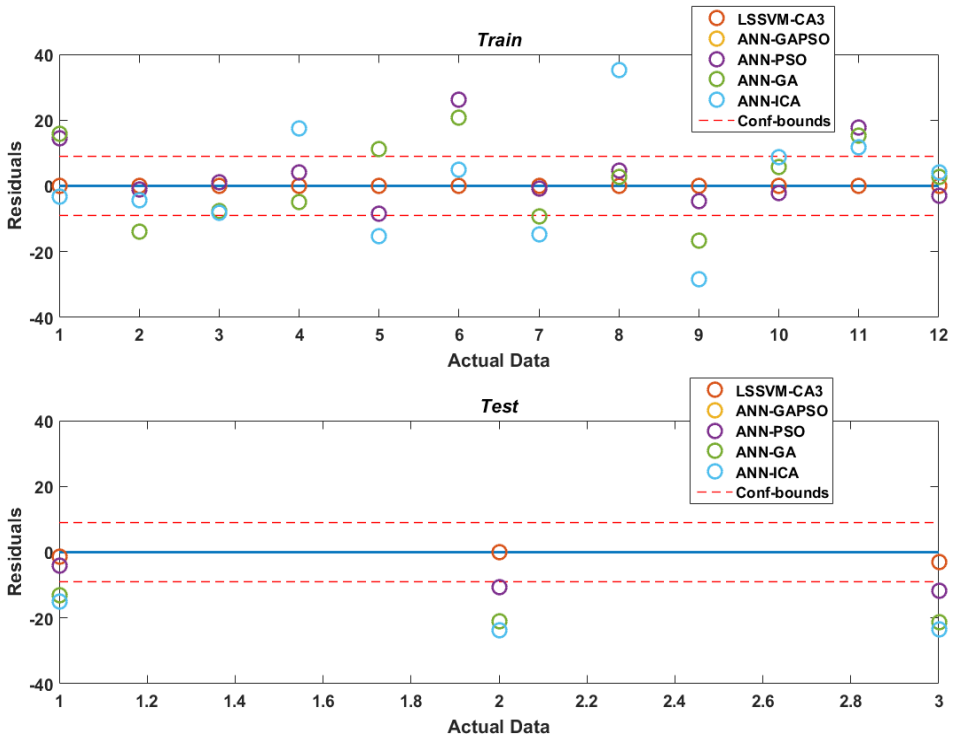

Fig. 3.7.b Residual representation for the second predicted load point (2475 MW)

The performance of all predictors are examined by two other statistical methods namely; root mean squared error (RMSE) and mean absolute error (MAE). From Fig 3.8.a and 3.8.b, it is evident that the LSSVM-CA3 has achieved considerably lower values for both predicted load points.

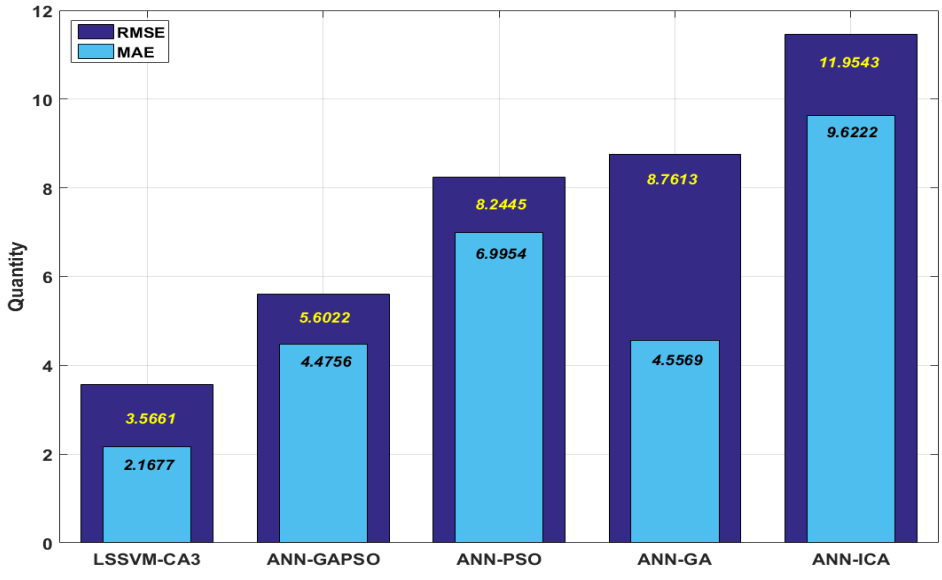

Fig. 3.8.a Evaluation of RMSE and MAE for the first predicted load point (1600 MW)

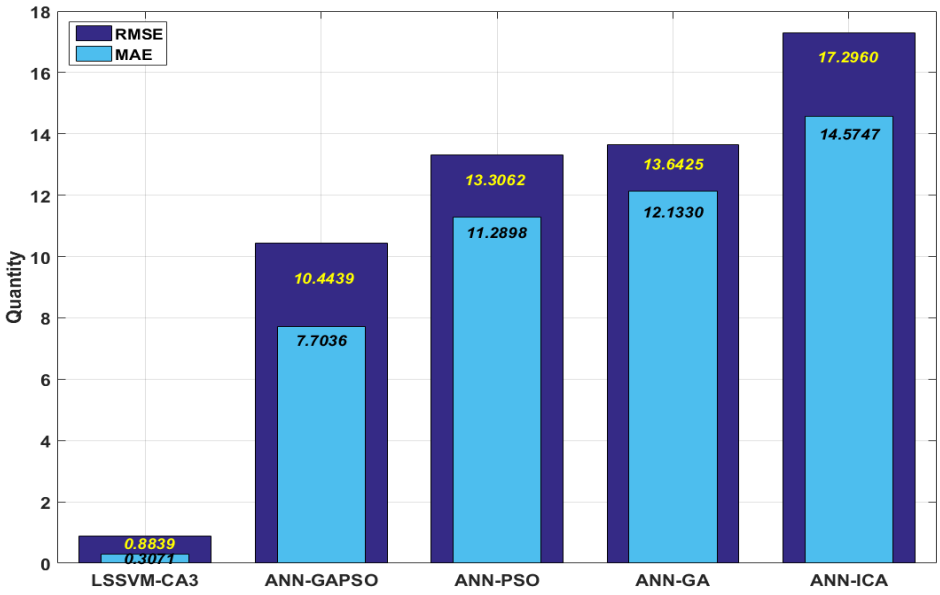

Fig. 3.8.b Evaluation of RMSE and MAE for the second predicted load point (2475 MW)

3.6.2 Test Case 2

In order to validate the efficiency of the proposed method of study on a larger test system, LSSVM-CA3 is applied to 40 units system. The system specification is available in Appendix B. In this case, the effect of ramp rate limits, spinning reserve requirement, valve-point loading and emission volume, as well as its associated costs, were considered. The daily load curve for the 40 units system is shown in Fig 3.9. Fig 3.10 shows the three-dimensional representation of total generation cost for the entire given load curve. The peak load of the day is equal to 10500 MW. The hourly load, total generation cost, emission volume, emission cost, generation cost of each unit and generator schedules have been used as the training inputs for the test case. The two random load points for the prediction purposes was 7550 and 8260 MW. The load point 8260 MW, presented a challenging load point due the characteristics of this test system because there are a number of generators which have the same generation capacity to be scheduled while they have a very different behaviour from their emission volume production. This situation created a considerable challenge for the convergence of the optimization algorithm. The comparison between the proposed method and the other predictors during the convergence process of adjusting parameters is depicted in Fig 3.11 (a and b).

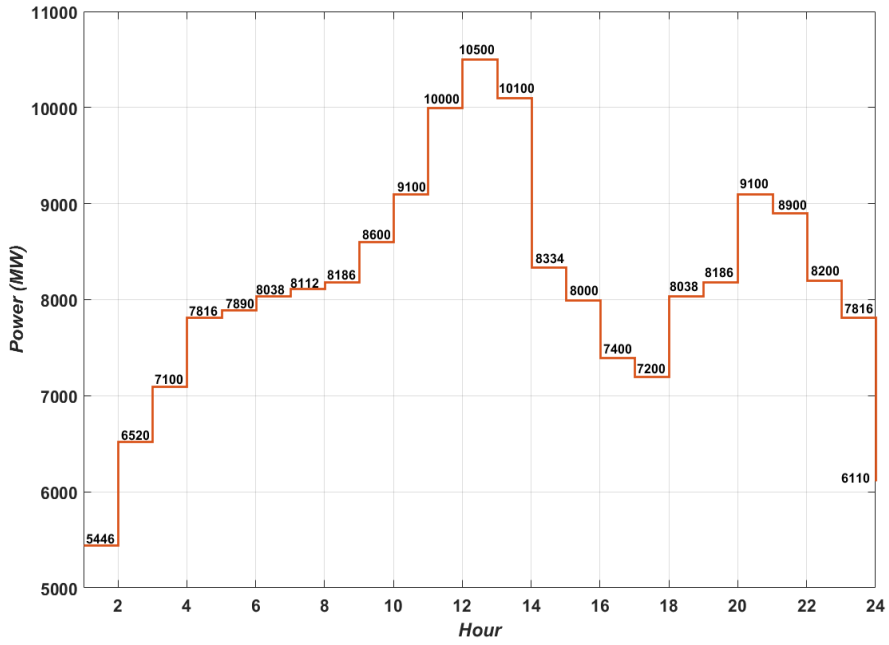

Fig. 3.9 Daily load curve for 40 units system

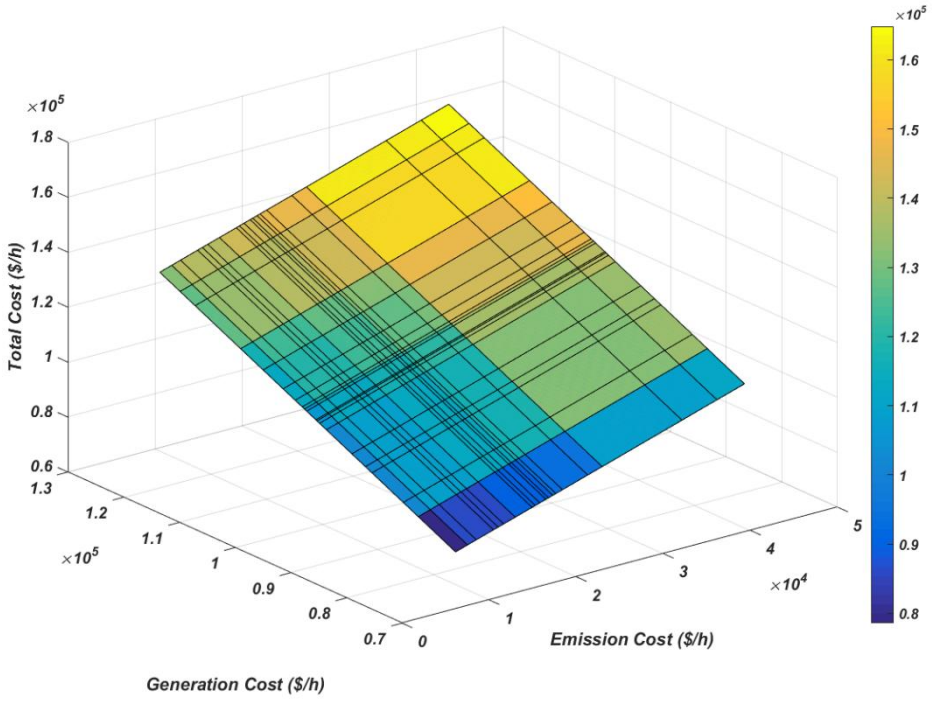

Fig. 3.10 Total generation cost of the day for the 40 units system

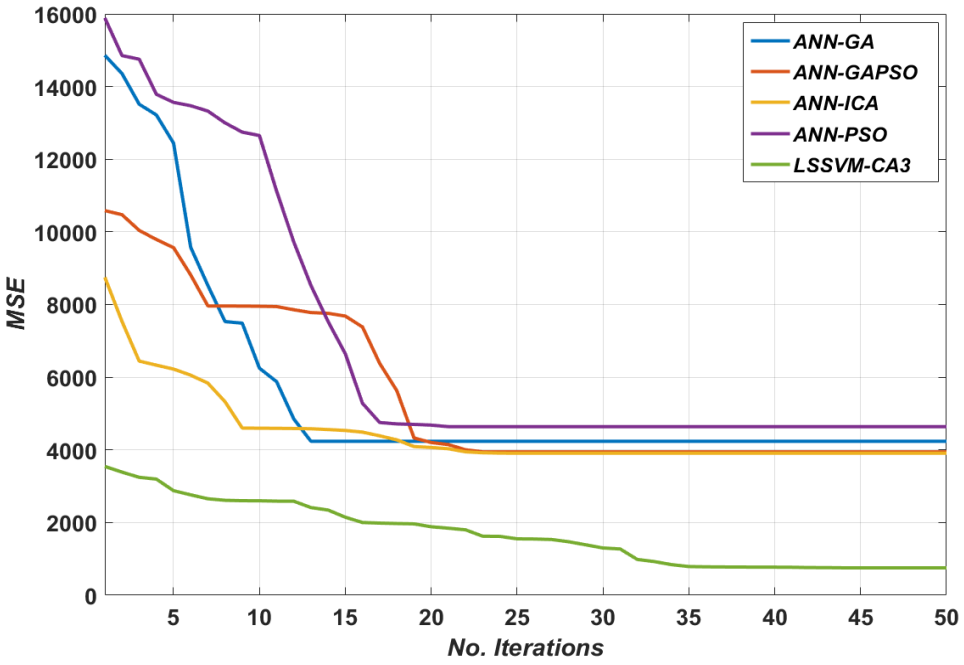

Fig. 3.11.a Convergence process of LSSVM-CA3 adjusting parameters (first predicted load point, 7550 MW)

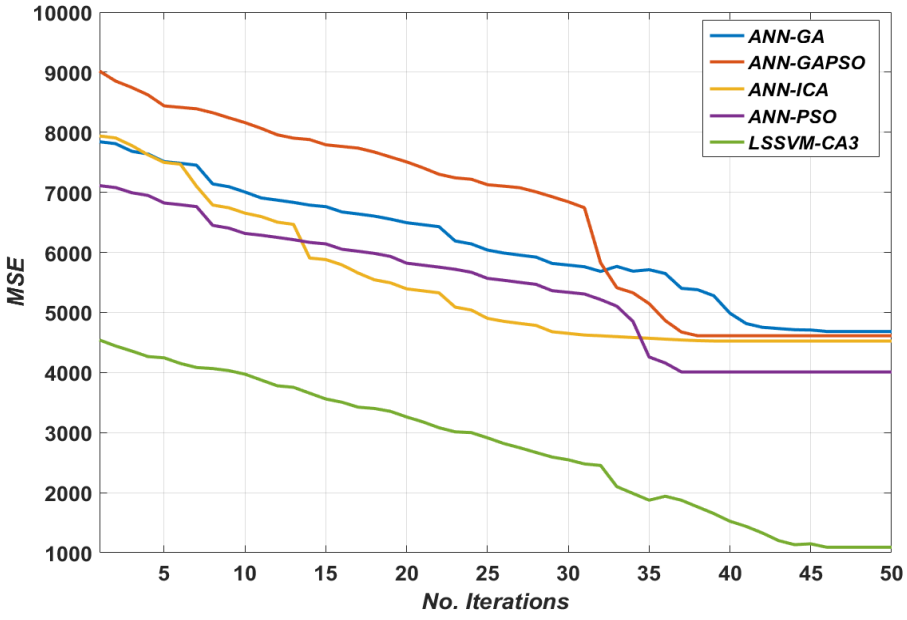

Fig. 3.11.b Convergence process of LSSVM-CA3 adjusting parameters (second predicted load point, 8260 MW)

It is evident that by the consideration of the effect of valve-point loading on the generation and emission objective function for all the generation units of this test system, all the prediction methods faced a considerable challenge in finding the optimum values of the adjusting parameters. As it can be seen, most of them have reached their final values towards 50 iterations, whereas for the second load point (8260 MW) most of them reached their final point marginally before the 40th iteration. ANN-ICA showed a better performance in comparison with the other methods of ANN, where it achieved the second rank in the first load point after LSSVM-CA3 and third rank after ANN-PSO in the second load point. Nonetheless, the LSSVM-CA3 achieved the lowest values of MSE in comparison to the other methods for both load points. It can be inferred that the performance of all other predictors are highly reliant on the nature of the problem, unlike LSSVM-CA3 which has shown superior performance in all studied cases. The detailed MSE results of the 40 unit system are shown in Table 3.3. Table 3.4 tabulates the final values of the adjusting parameters for the LSSVM-CA3. From Table 3.3, it is apparent that the proposed method achieved the lowest MSE in comparison to other techniques, where the minimum MSE for the first and the second load points are 753.9947 and 1090.6507, respectively. However, from the results of Table 3.3, it can be inferred that, by increasing the level of nonlinearity which has been imposed by the system because of the valve-point effect the MSE values for all the methods have been considerably increased.

By increasing the dimension of the test system it was expected that were would be a considerable increment in run-time of MIQP, however this was not the case. The reason was that the generation units did not have any POZs, therefore a simple MIQP has been used to find the optimal solutions. That is why, the MIQP run-time has been significantly reduced. The physical considerations for this test system are less realistic in comparison to real world practice due to the absence the POZs. The main aim of investigating this test system was to analyse the behaviour and the processing time of the prediction methods in absence of the POZs. The LSSVM-CA3 method maintained the very quick and efficient run-time when compared to the previous case.

Table 3.3 Comparison of the obtained results for MSE (40 units system)

7550 MW	Min	Avg	Max	Avg Elapsed Time (s)
LSSVM-CA3	753.99	1740.69	2252.17	1.55
ANN-GAPSO	3947.07	5742.35	9243.48	18.46
ANN-PSO	4638.41	5954.64	7907.23	4.66
ANN-GA	4236.25	6578.47	12339.93	4.88
ANN-ICA	3907.89	5244.00	7734.23	12.56
MIQP	…	…	…	3.25
8260 MW				
LSSVM-CA3	1090.65	1951.57	3088.06	1.29
ANN-GAPSO	4612.22	5971.63	8016.21	17.33
ANN-PSO	4009.55	5272.94	6155.87	5.15
ANN-GA	4683.69	5503.89	7366.83	5.23
ANN-ICA	4542.76	5792.29	7766.02	12.86
MIQP	…	…	…	3.83

Table 3.4 Final optimized values for LSSVM-CA3 adjusting parameters (40 units system)

Load Point (MW)	γ	σ^2
7550	26.88	7.40
8260	74390.99	5.99

Fig 3.12 (a and b) exhibits the residuals representation of the methods for both the load points. The LSSVM-CA3 obtained the highest accuracy for both the load points. For the first load point (7550 MW) the placement of the residuals within the confidence bound is illustrated as follows; 93.75% for training phase, 87.5% for the testing phase and with a total of 92.50%. In the case of the second load point, the residual placement results are listed as; 84.38% for training phase, 87.50% for the testing phase and in total 85.00%.

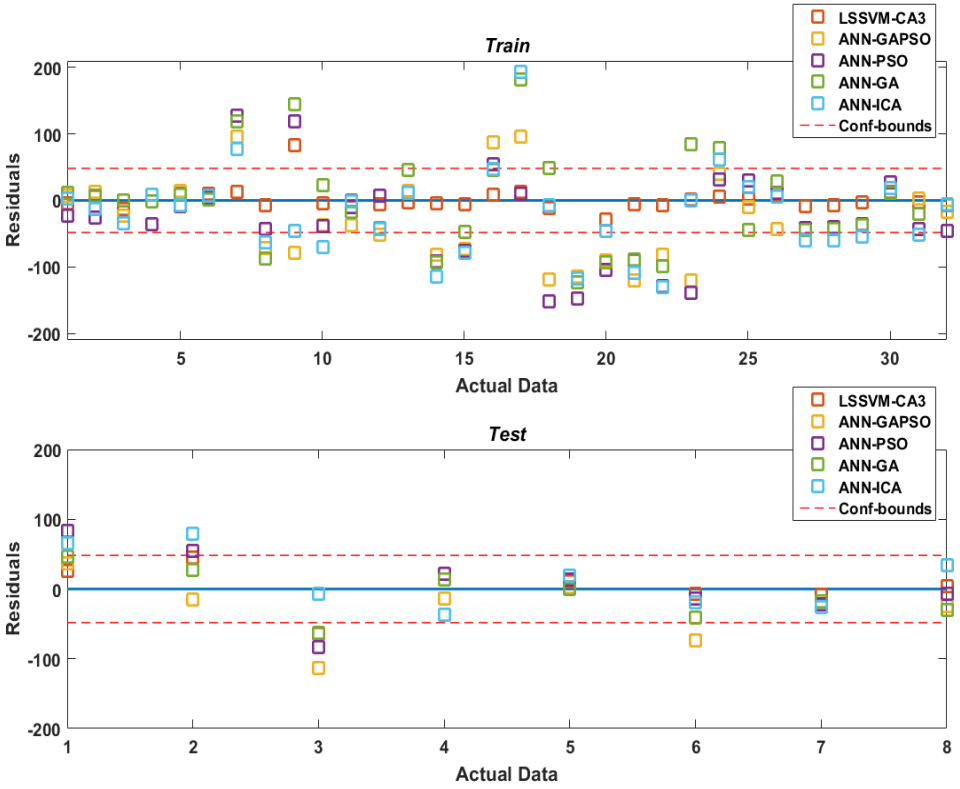

Fig. 3.12.a Residual representation for the first predicted load point (7500 MW)

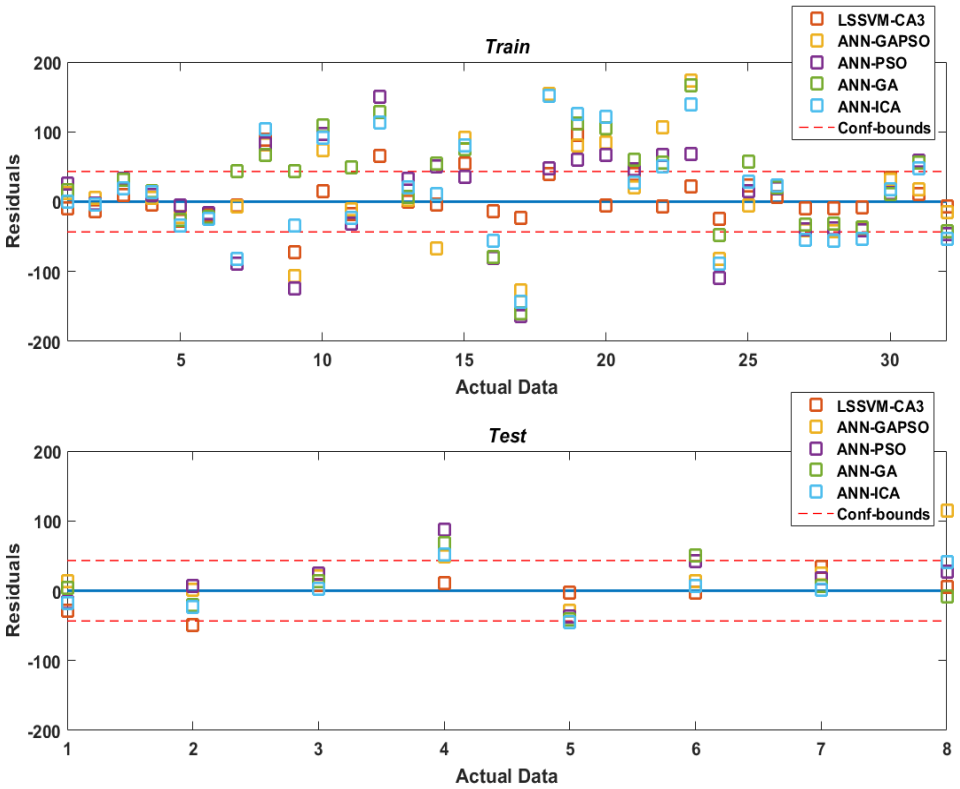

Fig. 3.12.b Residual representation for the second predicted load point (8260 MW)

Fig 3.13 (a and b) compares the performance of all predictors for RMSE and MAE error estimation. After LSSVM-CA3 which obtained the lowest errors for both load points, the ANN-ICA and ANN-PSO reached to the lowest errors in the first and second load points, respectively. This incident confirms that the performance of the methods depends on the topology of the problem; however, again the LSSVM-CA3 regardless of the system characteristics exhibited precise prediction of the generator's schedules.

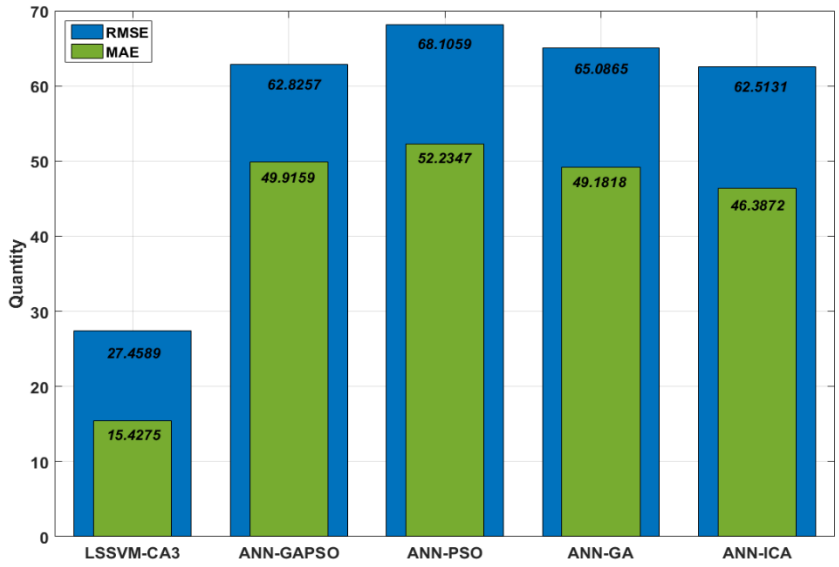

Fig. 3.13.a Evaluation of RMSE and MAE for the first predicted load point (7500 MW)

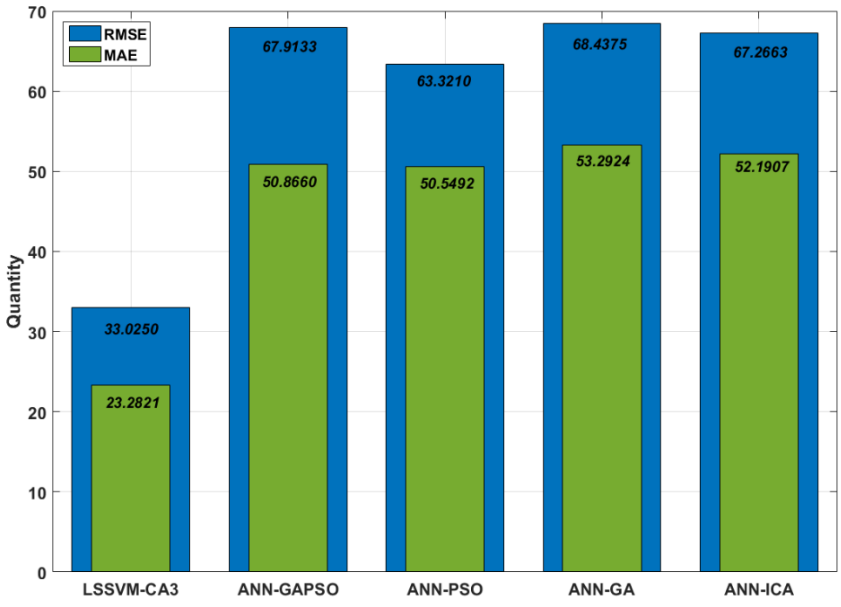

Fig. 3.13.b Evaluation of RMSE and MAE for the second predicted load point (8260 MW)

3.6.3 Test Case 3

This test case was performed to verify the robustness and practicality of the proposed method on a large-scale power system with the higher dimension of complexity. The LSSVM-CA3 was employed on a 140 unit system to predict the optimum scheduling of the generation units, where the system specification is available in Appendix C. This test system was based on a realistic Korean power system, which consists of 140 thermal units such as coal, LNG, LNG-CC, nuclear and oil. The effect of ramp rate limits, prohibited operating zones, spinning reserve requirement, and valve-point loading were taken into account as the physical constraints of the generation units. Fig 3.14 depicts the daily load curve of this test system. For this system, the maximum generation capacity to satisfy the load demand was equal to 50,000 MW and the minimum is set to 35,000 MW. The hourly load, total generation cost, generation cost of each unit with the consideration of the valve-point effect cost and the generator schedules have been utilized as the training inputs. In this case, 36,500 and 41,800 MW are selected as the random load points to be predicted by the methods. This test system had a substantial non-linearity and non-convexity in its operating zones due to its characteristics which made the optimization process cumbersome for any methods to evaluate the most optimum solution for any given load point.

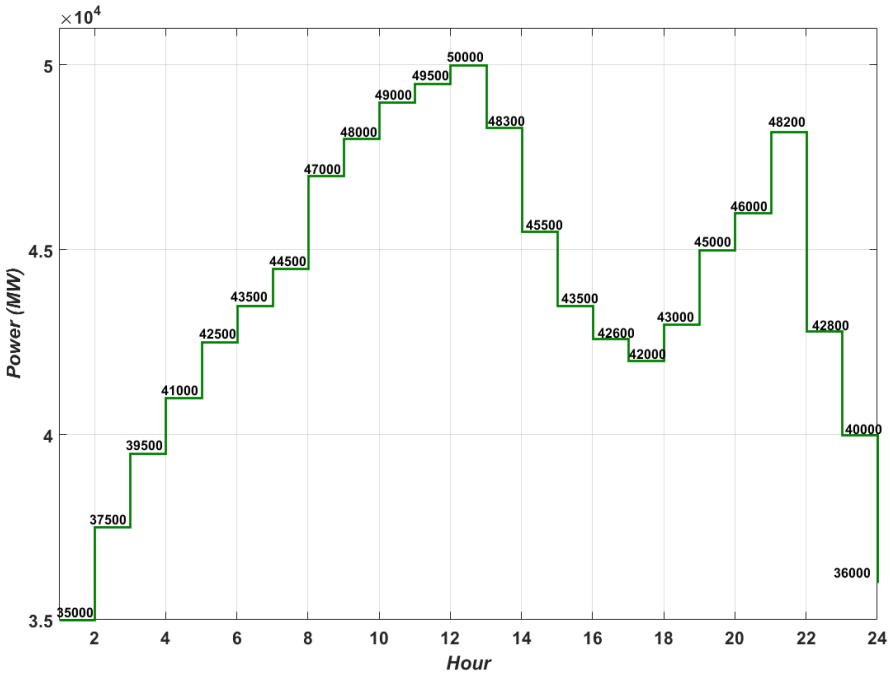

Fig. 3.14 Daily load curve for 140 units system

Fig 3.15 (a and b) illustrates the convergence process of adjusting parameters of the prediction methods to achieve the least possible errors. The methodology of the study successfully

acquired the lowest MSE for both load points in comparison to the other methods. For both load points, the LSSVM-CA3 reached its final optimum level in less than 17th iterations while the other methods took approximately 30 iterations to reach their final stage of optimization of their adjusting parameters. Table 3.5 shows the final values of adjusting parameters for the LSSVM-CA3 for both load points.

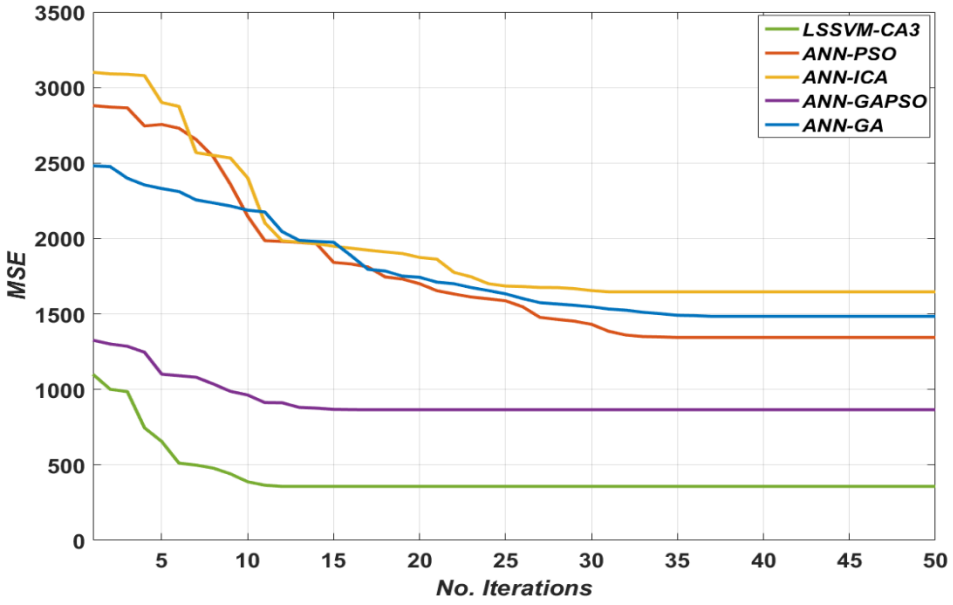

Fig. 3.15.a Convergence process of LSSVM-CA3 adjusting parameters (first predicted load point, 36500 MW)

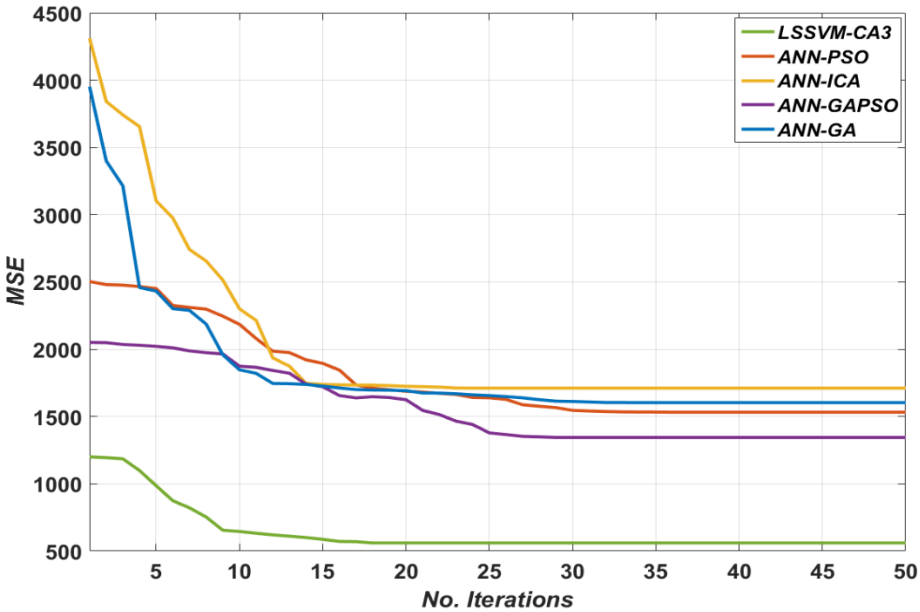

Fig. 3.15.b Convergence process of LSSVM-CA3 adjusting parameters (second predicted load point, 41800 MW)

Table 3.5 Final optimized values for LSSVM-CA3 adjusting parameters (140 units system)

Load Point (MW)	γ	σ^2
36500	63381.17	26822.02
41800	23.56	4.71

The comprehensive investigation of the methods for evaluating MSE are found in Table 3.6, where LSSVM-CA3 obtained the lowest minimum of MSE in comparison to the other methods with 353.1383 and 512.0360 for the first and second load point, respectively. It can be observed from Table 3.6, the proposed method has accomplished the prediction in less than 2 seconds with a noticeable accuracy for both selected load points while the other methods could not achieve even 50% of its precision within approximately 4 to 23 times higher processing time. Table 3.6 demonstrates the superior performance of the proposed method through to accurate prediction of generator schedules with a large-scale of complexity. ANN-GPSO, ANN-PSO, ANN-GA and ANN-ICA have a significant poor performance when compared to LSSVM-CA3. It is significant to mention that, even if considering a larger system, the proposed algorithm is able to determine the optimal allocation of power among the generation units in a very fast processing time, which indicates the applicability of the proposed method for real-time management and operation of the power grid where the system operator needs to run several scenarios with respect to the fluctuations of load demand and demand response programs.

Table 3.6 Comparison of the obtained results for MSE (140 units system)

36500 MW	Min	Avg	Max	Avg Elapsed Time (s)
LSSVM-CA3	353.14	370.99	398.54	1.87
ANN-GAPSO	865.48	1384.96	1697.52	46.85
ANN-PSO	1344.16	1604.88	2170.54	7.25
ANN-GA	1483.91	1723.95	1941.63	8.13
ANN-ICA	1646.36	1876.39	2850.12	39.24
MIQP	…	…	…	289.33
41800 MW				
LSSVM-CA3	512.04	870.79	1191.83	1.95
ANN-GAPSO	1349.40	1644.57	2043.18	47.82
ANN-PSO	1532.17	1866.91	2435.48	7.84
ANN-GA	1603.25	1933.66	3020.83	8.77
ANN-ICA	1711.14	2063.72	2701.94	41.36
MIQP	…	…	…	312.41

Most of the previous studies in this area discussed the outlier predictions through the leverage method to show the notable performance of their methods. In this study, a strong focus on the placement of the predictions within the confidence bound as well as their concentration around the horizontal actual data line have been considered, as it can indicate a good agreement between the predictions and the actual values. Fig 3.16 (a and b) describe the residual placement of the predictions. LSSVM-CA3 acquired the best results for both load points, where the placement of the residuals within the confidence bound for the first load point (36,500 MW) is as the following order; 90.18% for the training, 100% for the testing with a total of 92.14%. In the case of the second load point (41,800 MW), the detailed assessment of the residual placement was as follows; 83.93% for the training, 100% for the testing and in total 87.14%. It is evident that even by enlarging the test system and considering a number of constraints, the residuals have been located considerably close to the actual data line.

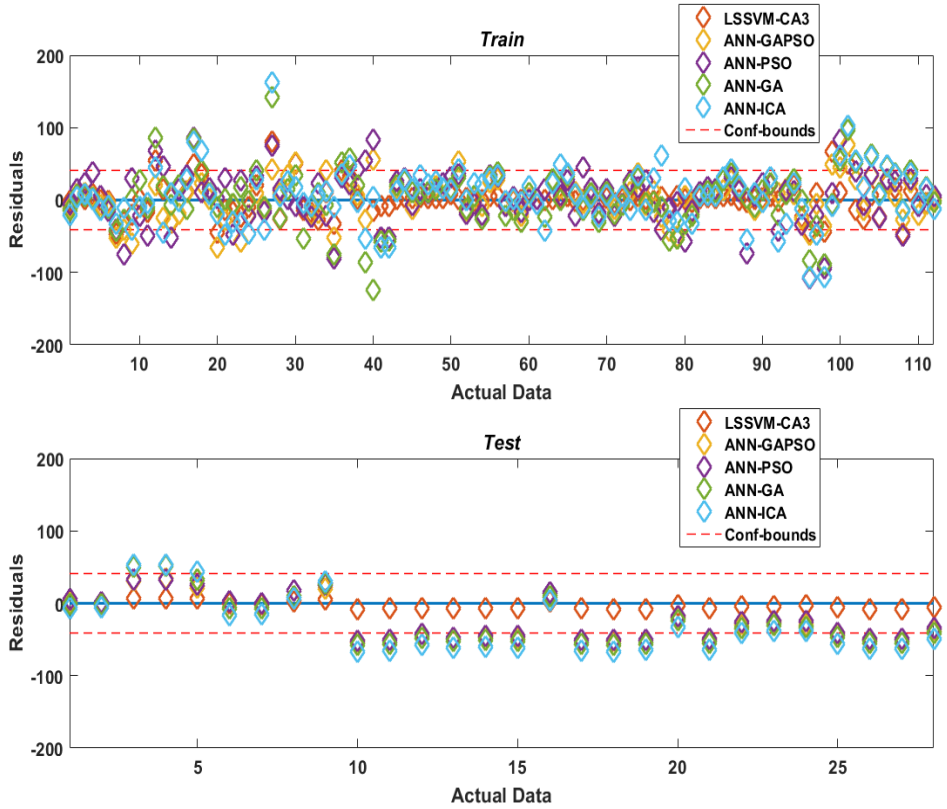

Fig. 3.16.a Residual representation for the first predicted load point (36500 MW)

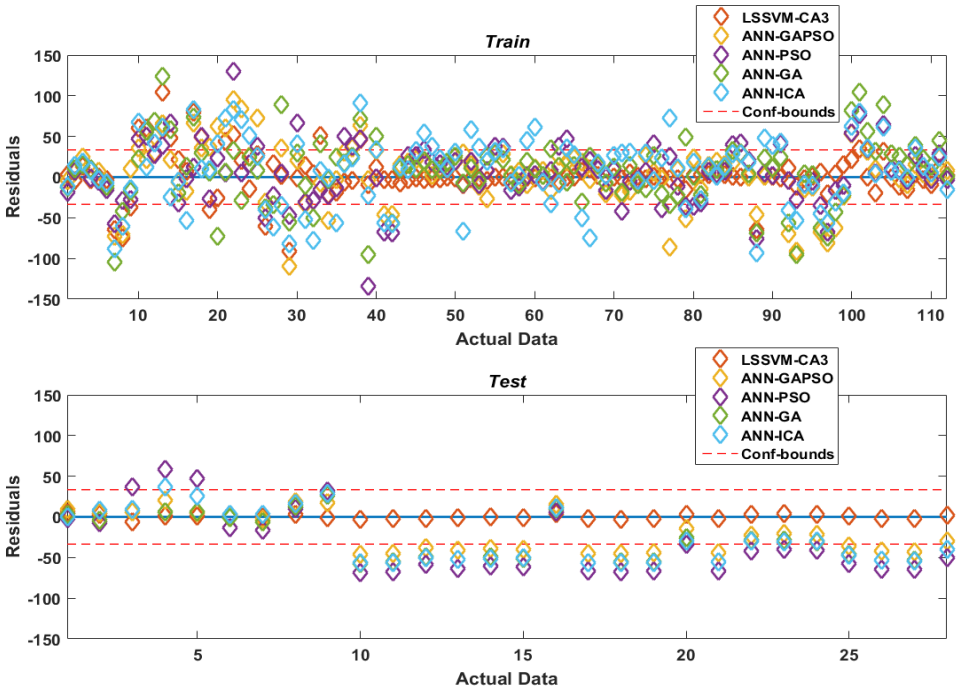

Fig. 3.16.b Residual representation for the second predicted load point (41800 MW)

The RMSE and MAE comparison for all prediction methods is shown in Fig 3.17 (a and b). The LSSVM-CA3 demonstrated excellent performance for load points, where the minimum values of MAE are respectively; 10.37 and 12.53for the first and second load points. In case of RMSE, the values are as follows for the first and second load point; 18.79 and 22.63.

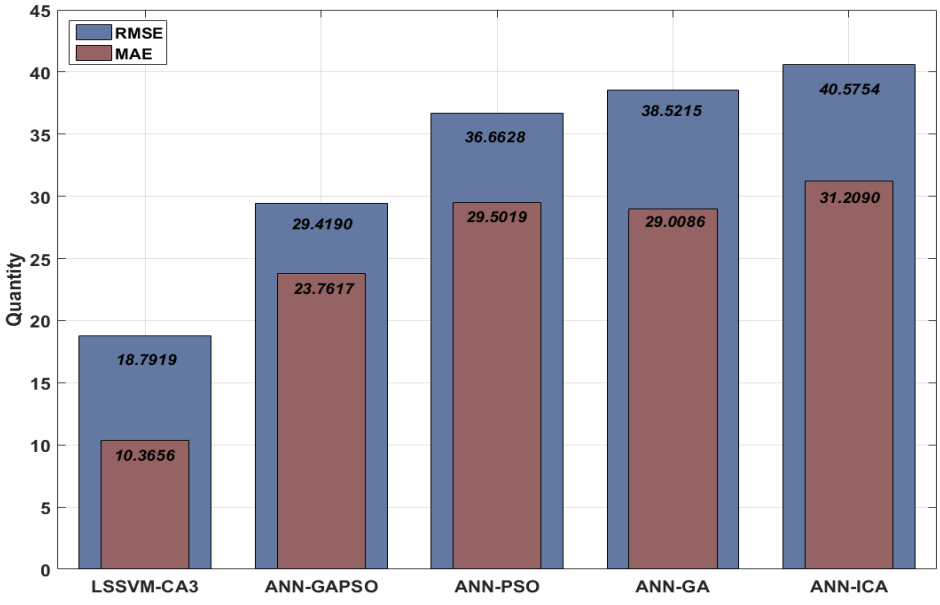

Fig. 3.17.a Evaluation of RMSE and MAE for the first predicted load point (36500 MW)

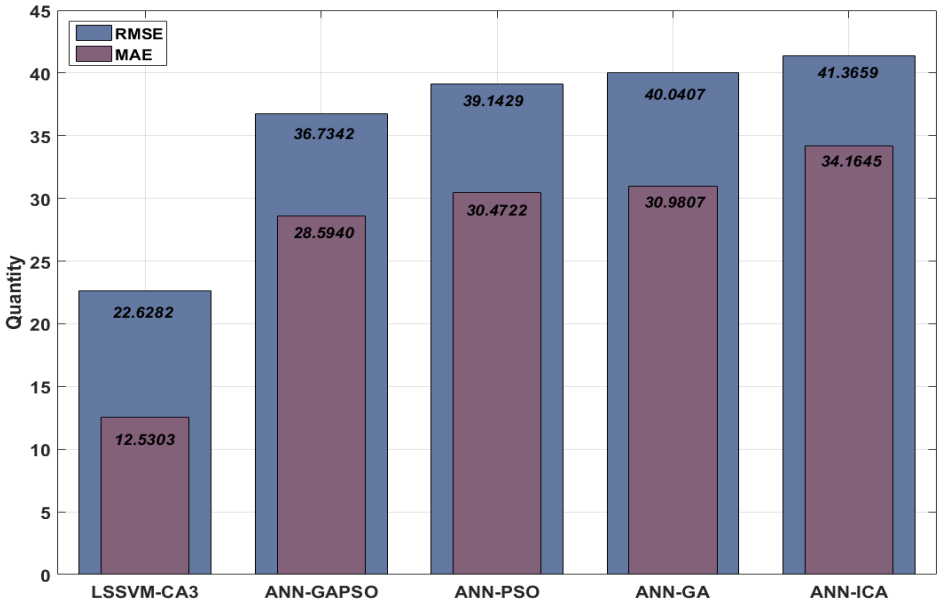

Fig. 3.17.b Evaluation of RMSE and MAE for the second predicted load point (41800 MW)

Fig 3.18 represents an overall comparison of NRMSE for all three studied test cases with respect to different load points. For simplicity of understanding the values are shown in descending order. As is seen, the LSSVM-CA3 has an outstanding performance in comparison to the other methods for all the different load points. The colour-bar on the right-hand side of Fig 3.18 represents the details of measured values.

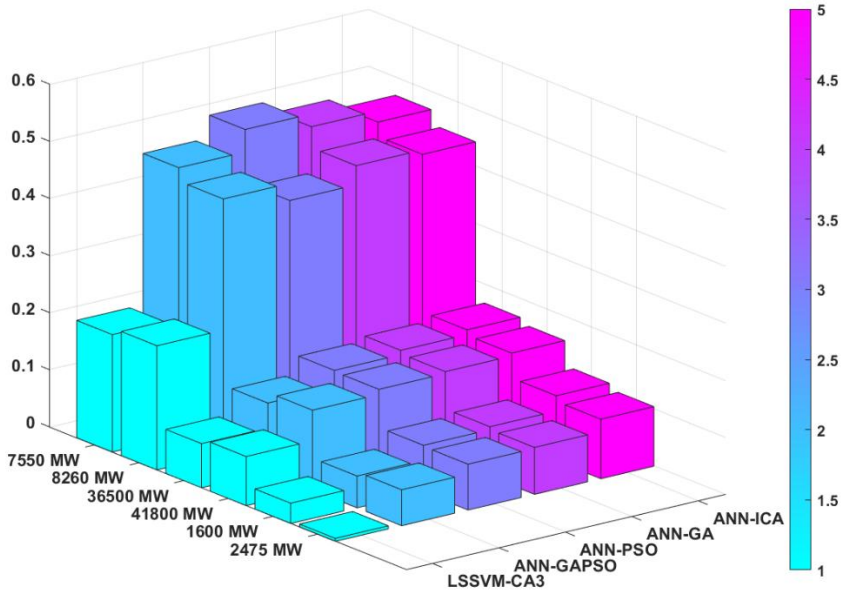

Fig. 3.18 Evaluation of NRMSE for all the studied cases

3.6.4 Test Case 4

To demonstrate the practicality of the proposed method for a real-time analysis on a large-scale of a realistic power system, the proposed method is investigated on the largest ever reported test system with a non-convex objective function. This test system consists of 420 generation units, which is comprised of 120 coal units, 153 LNG units, 60 nuclear units, and 87 oil units. This test system has been made by three times replication of the 140-unit system of case 3. The considerable increase in the number of generation units, considering the physical constraints of the generators, imposes a substantial complexity into the real-time analysis of the CEED problem due to the high number of discontinuities caused by POZs, as this leads to the increased number of possible local minima.

Table 3.7 lists the hourly load demand of the system (all the values are expressed in MW), where the lowest load of the day and peak demand are equal to 105000 MW and 150000 MW, respectively. Two random load points which have been used for the prediction purposes are equal to 125000 MW and 139000 MW. Fig 3.19 and 3.20 show the residuals representation of all the compared the methods for both the load points. Among all the compared methods, the proposed method represents the highest accuracy for both load points. The placement of the residuals within the confidence bound for the different subsets of the two selected load points are, 89.82% for the training phase, 96.40% for the testing phase for the first load point. In the case of the second load point, the performance of the proposed method is considerably noticeable by having 96.10% precision of prediction for the training phase and 96.40% for the testing phase.

Table 3.7 Hourly load data for 420 units system

1	2	3	4	5	6	7	8	9	10	11	12
105000	112500	118500	123000	127500	130500	133500	141000	144000	147000	148500	150000
13	14	15	16	17	18	19	20	21	22	23	24
144900	136500	130500	127800	126000	129000	135000	138000	144600	128400	120000	108000

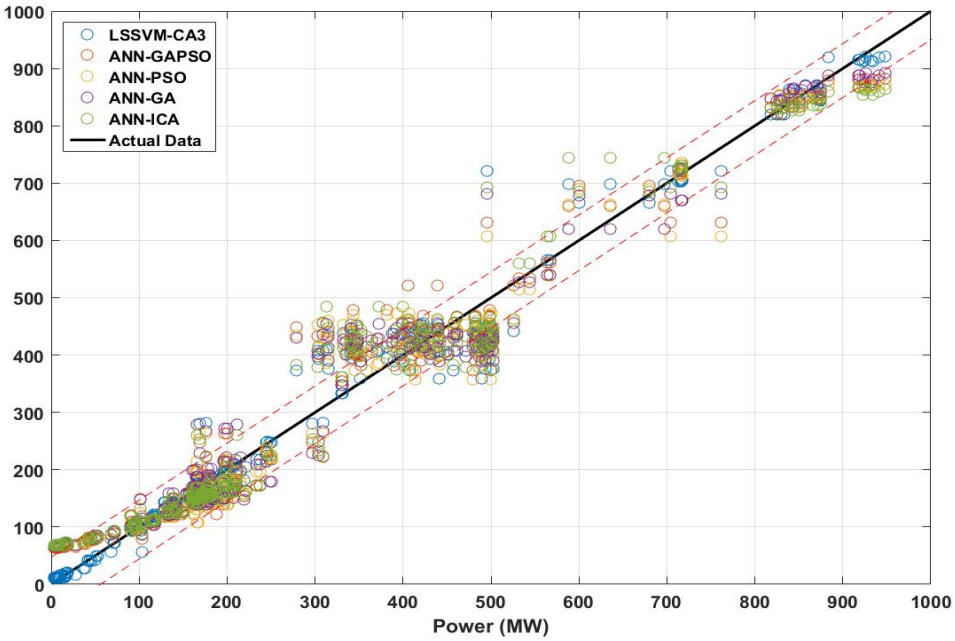

Fig. 3.19.a Residual representation for the first predicted load point (125000 MW) of case 4, Training Phase

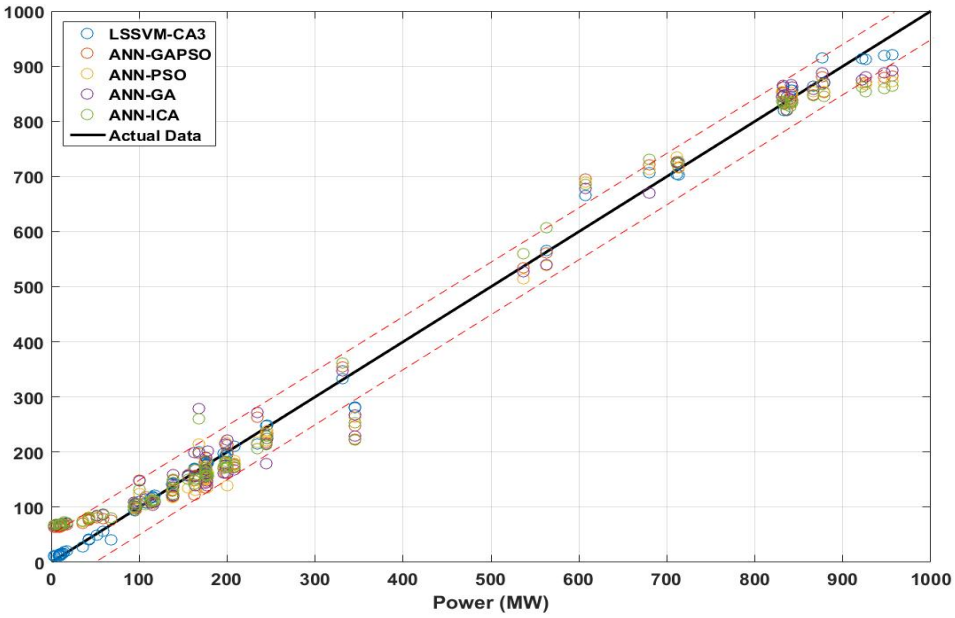

Fig. 3.19.b Residual representation for the first predicted load point (125000 MW) of case 4, Testing Phase

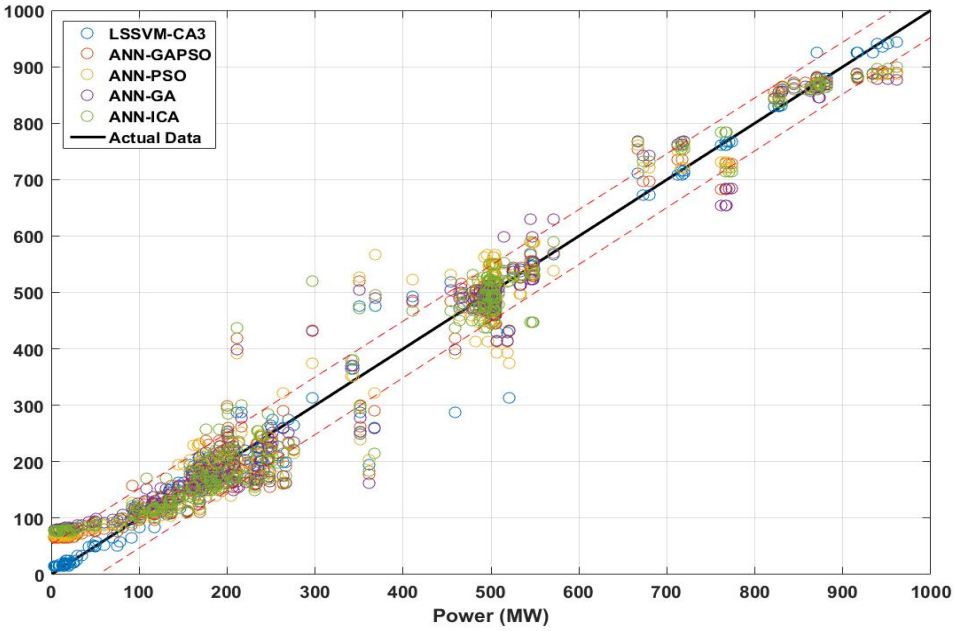

Fig. 3.20.a Residual representation for the second predicted load point (139000 MW) of case 4, Training Phase

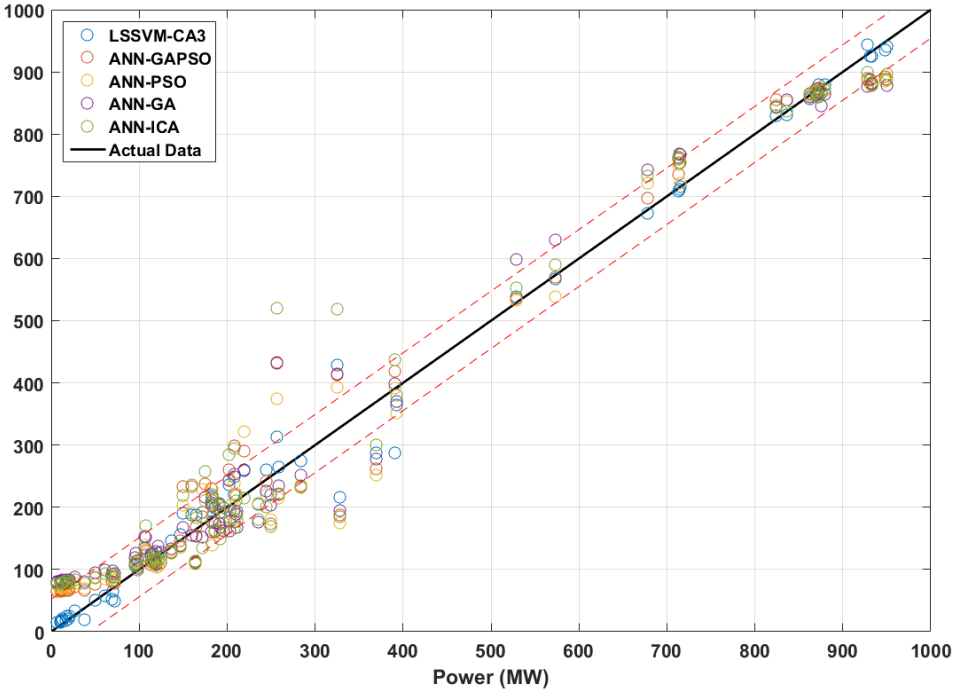

Fig. 3.20.b Residual representation for the second predicted load point (139000 MW) of case 4, Testing Phase

Table 3.8 arranges the best-achieved values of the adjusting parameters for the LSSVM-CA3. Table 3.9 presents the detailed analysis of all the compared methods. From Table 3.9, it is

obvious that the LSSVM-CA3 has acquired the lowest average and minimum total generation cost if compared to other methods in a very fast running time considering the higher complication of the analysis for this large system. The fast convergence and evaluation of the proposed method in solving the large-scale of CEED problem indicates its capability to be used by the system operators in any real-time electricity market.

Table 3.8 Final optimized values for LSSVM-CA3 adjusting parameters (420 units system)

Load Point (MW)	γ	σ^2
125000	14.37	7.29
139000	16.75	13.58

Table 3.9 Comparison of the obtained results for MSE (420 units system)

125000 MW	Min	Avg	Max	Avg Elapsed Time (s)
LSSVM-CA3	1127.21	1228.66	1271.39	12.24
ANN-GAPSO	1999.19	2145.31	2489.54	269.73
ANN-PSO	2036.18	2245.84	2781.65	37.21
ANN-GA	2058.44	2325.28	2844.63	38.33
ANN-ICA	2146.91	2574.25	3122.88	254.78
MIQP	…	…	…	945.28
139000 MW				
LSSVM-CA3	860.52	918.28	960.56	12.35
ANN-GAPSO	1765.95	2001.85	2102.25	273.25
ANN-PSO	1998.77	2135.14	2345.57	38.01
ANN-GA	2075.43	2185.47	2441.43	38.55
ANN-ICA	2284.82	2236.49	2564.78	261.05
MIQP	…	…	…	967.48

Lastly, the performance of all methods are studied by three other statistical methods; RMSE, NRMSE, and MAE, where their results have been tabulated in Table 3.10. From Table 3.10, it is very clear that the LSSVM-CA3 has obtained the lowest error among the others by a

significant amount, which emphasizes the superiority of the proposed method in a real-time analysis.

Table 3.10 Comparison of the obtained results for the error analysis (420 units system)

125000 MW	MAE	RMSE	NRMSE
LSSVM-CA3	18.69	33.57	0.1306
ANN-GAPSO	33.48	44.71	0.1739
ANN-PSO	34.25	45.12	0.1755
ANN-GA	35.22	45.37	0.1765
ANN-ICA	35.51	46.33	0.1802
139000 MW			
LSSVM-CA3	17.34	29.33	0.1106
ANN-GAPSO	30.31	42.02	0.1584
ANN-PSO	33.63	44.71	0.1685
ANN-GA	33.54	45.56	0.1718
ANN-ICA	35.44	47.79	0.1831

3.6.5 Test Case 5

To further clarify on the performance of the proposed method, several scenarios from the different technical point of view have been considered. For the first scenario, to demonstrate the replicability of the proposed method of the study, for each studied test case, the proposed algorithm has been randomly executed four times for each load point of the test system, where the results are tabulated in Table 3.11 to Table 3.13.

Table 3.11 Results of random execution of the proposed algorithm (15 units system).

15 Units, LSSVM-CA3								
	1600 MW				2475 MW			
	1	2	3	4	1	2	3	4
γ	134.62	89.66	109.49	97.58	651618.64	593539.57	564871.98	581544.05
σ^2	2.59	2.47	2.80	2.61	49.85	48.29	53.17	46.37
MSE	43.47	9.13	8.05	11.86	8.20	16.89	5.53	6.98
Time (s)	0.15	0.28	0.35	0.41	0.54	0.19	0.11	0.21

Table 3.12 Results of random execution of the proposed algorithm (40 units system).

40 Units, LSSVM-CA3								
	7550 MW				8260 MW			
	1	2	3	4	1	2	3	4
γ	24.20	23.38	27.29	29.56	76952.81	65268.83	54821.75	74512.04
σ^2	4.22	4.89	5.51	6.57	3.61	7.04	5.29	4.63
MSE	1072.31	948.55	642.44	725.00	1137.85	2868.31	1831.42	1629.26
Time (s)	1.35	2.35	1.30	1.27	2.33	2.84	1.37	1.04

Table 3.13 Results of random execution of the proposed algorithm (140 units system).

140 Units, LSSVM-CA3								
	36500 MW				41800 MW			
	1	2	3	4	1	2	3	4
γ	81268.28	53283.26	48517.25	63152.58	27.28	43.50	37.91	109.82
σ^2	45257.32	29061.55	18572.36	27345.85	5.76	6.49	4.74	7.35
MSE	402.81	386.16	354.74	369.22	520.67	494.13	509.15	491.17
Time (s)	3.21	1.77	2.10	1.95	2.45	1.44	1.87	1.23

From the acquired results in Table 3.11 to Table 3.13, it can be seen that, all of the solutions are within the range of the presented results in the previous sections.

For the second scenario, due to different characteristics of the optimization algorithms, the best population size, and parameters of various optimization methods could be different. As ANN-GAPSO has shown the best performance among all the other ANN based methods according to the results in the previous test cases, the population size of GAPSO has been adjusted to obtain its best performance. Therefore, to investigate the ability of ANN-GAPSO with a higher number of swarms or agents in the search space, its population size has been increased to 80,100 and 150, while its results have been compared to LSSVM-CA3 (for comparable results, ANN-GAPSO has been performed 20 times). The results of this scenario are presented in Table 3.14 to Table 3.16.

Table 3.14 Comparison of the proposed algorithm with the higher number of the population size of ANN-GAPSO (15 units system).

15 Units								
	1600 MW				2475 MW			
	LSSVM-CA3	80	100	150	LSSVM-CA3	80	100	150
MSE	12.72	30.80	30.27	21.23	0.78	89.52	63.11	13.31
Avg Elapsed Time (s)	0.13	18.45	25.38	45.12	0.14	19.25	26.54	44.75

Table 3.15 Comparison of the proposed algorithm with the higher number of the population size of ANN-GAPSO (40 units system).

40 Units								
	7550 MW				8260 MW			
	LSSVM-CA3	80	100	150	LSSVM-CA3	80	100	150
MSE	753.99	1569.92	1491.57	1100.91	1090.65	3088.06	2814.72	1249.17
Avg Elapsed Time (s)	1.55	25.32	36.45	85.37	1.29	23.61	41.25	91.54

Table 3.16 Comparison of the proposed algorithm with the higher number of the population size of ANN-GAPSO (140 units system).

140 Units								
	36500 MW				41800 MW			
	LSSVM-CA3	80	100	150	LSSVM-CA3	80	100	150
MSE	353.14	383.27	374.53	373.05	512.04	1077.49	983.83	949.66
Avg Elapsed Time (s)	1.87	57.02	94.83	178.77	1.95	53.11	110.46	195.26

As it can be seen from the results, by increasing the population size of the GAPSO, the total performance of ANN-GAPSO has been considerably improved, however, due to the increment in population size of GAPSO, the total running time of the ANN-GAPSO has also been significantly increased, which does not make the approach suitable for real-time analysis. Whereas, the proposed method has achieved a better solution in a lower time.

For the third scenario, to demonstrate the advantage of LSSVM-CA3 in comparison to the combination of the other algorithms with LSSVM, the GAPSO has been combined with LSSVM (GAPSO has been selected to be compared with LSSVM for the same reason as the previous scenario). To have comparable results, the population sizes of both optimizers were set to 50 and have been executed 20 times. The results are charted in Table 3.17 to Table 3.19.

Table 3.17 Comparison of the proposed algorithm with LSSVM-GAPSO (15 units system).

15 Units				
	1600 MW		2475 MW	
	LSSVM-CA3	LSSVM-GAPSO	LSSVM-CA3	LSSVM-GAPSO
γ	114.21	118.06	743710.44	610051.29
σ^2	3.24	3.21	68.84	108.84
MSE	12.72	12.79	0.78	12.23
Avg Elapsed Time (s)	0.13	0.99	0.14	1.23

Table 3.18 Comparison of the proposed algorithm with LSSVM-GAPSO (40 units system).

40 Units				
	7550 MW		8260 MW	
	LSSVM-CA3	LSSVM-GAPSO	LSSVM-CA3	LSSVM-GAPSO
γ	26.88	29.19	74390.99	65450.24
σ^2	7.4	8.01	5.99	11.79
MSE	753.99	1077.79	1090.65	1174.67
Avg Elapsed Time (s)	1.55	2.73	1.29	7.84

Table 3.19 Comparison of the proposed algorithm with LSSVM-GAPSO (140 units system).

140 Units				
	36500 MW		41800 MW	
	LSSVM-CA3	LSSVM-GAPSO	LSSVM-CA3	LSSVM-GAPSO
γ	63381.17	59346.85	23.56	307.87
σ^2	26822.02	24136.10	4.71	18.95
MSE	353.14	365.57	512.04	721.53
Avg Elapsed Time (s)	1.87	2.47	1.95	3.41

From Table 3.17 to Table 3.19, it is evident that the proposed method (LSSVM-CA3) outperforms LSSVM-GAPSO with a considerable difference in all the studied cases.

3.7 Conclusions

An accurate, fast and reliable method of dispatching generating resources is a critical tool in the real-time electricity market to ensure the delivery of consistent and economic electricity services to all the grid-connected customers. In this paper, a hybrid mathematical model based on LSSVM and CA3 for optimal scheduling of generation units in the context of a real-time electricity market has been proposed. Several physical constraints and environmental impacts of the generation units through different test systems were considered and analysed to demonstrate the practicality and efficiency of the proposed model. The optimal scheduling for the hourly load curve of the test systems has been prepared by the MIQP for training purposes. The comparison cases were performed between LSSVM-CA3 and other ANN coupled prediction methods. According to the obtained results of the proposed method the following conclusions can be drawn:

- The proposed model demonstrated superior stable performance in optimal scheduling of the generation units and achieved the lowest values of MSE, RMSE, and MAE compared to

other hybrid well-established ANN methods which are widely used for power market forecasting.

- The proposed method acquired the lowest residual values with the highest placement of the predictions within the confidence bound in a very fast processing time in comparison to all other methods of ANN, and where the reduction percentage in processing time compared to MIQP is almost equal to 99% for the first and the third test case and 60% for the second test case.
- Analysis of the NRMSE shows the excellent performance of LSSVM-CA3 compared to other methods for all the studied cases.
- The proposed method is capable of understanding the equality and inequality constraints of generation units as well as adhering to their physical and environmental constraints.
- The proposed method has adopted a tuning optimizer for its adjusting parameters (γ and σ^2) to obtain the best possible solution without the interference of the human experience during the optimization process.

According to all above mentioned facts and the considerable accuracy of the obtained results, it implies that the proposed model of the study is applicable to the real-time power market.

3.8 References

[1] S. I. Vagropoulos, E. G. Kardakos, C. K. Simoglou et al., “ANN-based scenario generation methodology for stochastic variables of electric power systems,” *Electric Power Systems Research*, vol. 134, pp. 9-18, May, 2016.

[2] E. C. (EU), "Energy Roadmap, 2050," 2012.

[3] V. N. Dieu, and P. Schegner, “Augmented Lagrange Hopfield network initialized by quadratic programming for economic dispatch with piecewise quadratic cost functions and prohibited zones,” *Applied Soft Computing*, vol. 13, no. 1, pp. 292-301, Jan, 2013.

[4] A. A. A. Mousa, “Hybrid ant optimization system for multiobjective economic emission load dispatch problem under fuzziness,” *Swarm and Evolutionary Computation*, vol. 18, pp. 11-21, Oct, 2014.

[5] E. Afzalan, and M. Joorabian, “An improved cuckoo search algorithm for power economic load dispatch,” *International Transactions on Electrical Energy Systems*, vol. 25, no. 6, pp. 958-975, Jun, 2015.

[6] N. E. Koltsaklis, and M. C. Georgiadis, “A multi-period, multi-regional generation expansion planning model incorporating unit commitment constraints,” *Applied Energy*, vol. 158, pp. 310-331, Nov 15, 2015.

[7] N. E. Koltsaklis, A. S. Dagoumas, M. C. Georgiadis et al., “A midterm market-based power systems planning model,” *Applied Energy*, vol. 179, pp. 17-35, 2016.

[8] T. Niknam, A. Khodaei, and F. Fallahi, “A new decomposition approach for the thermal unit commitment problem,” *Applied Energy*, vol. 86, no. 9, pp. 1667-1674, Sep, 2009.

[9] C. K. Simoglou, P. N. Biskas, and A. G. Bakirtzis, “Optimal Self-Scheduling of a Thermal Producer in Short-Term Electricity Markets by MILP,” *IEEE Transactions on Power Systems*, vol. 25, no. 4, pp. 1965-1977, Nov, 2010.

[10] E. Delarue, and W. D'haeseleer, “Adaptive mixed-integer programming unit commitment strategy for determining the value of forecasting,” *Applied Energy*, vol. 85, no. 4, pp. 171-181, Apr, 2008.

[11] R. M. Lima, and A. Q. Novais, “Symmetry breaking in MILP formulations for Unit Commitment problems,” *Computers & Chemical Engineering*, vol. 85, pp. 162-176, Feb 2, 2016.

[12] J. Wang, A. Botterud, R. Bessa et al., “Wind power forecasting uncertainty and unit commitment,” *Applied Energy*, vol. 88, no. 11, pp. 4014-4023, Nov, 2011.

[13] J. D. Wang, J. H. Wang, C. Liu et al., "Stochastic unit commitment with sub-hourly dispatch constraints," *Applied Energy*, vol. 105, pp. 418-422, May, 2013.

[14] S. Baskar, P. Subbaraj, and M. V. C. Rao, "Hybrid real coded genetic algorithm solution to economic dispatch problem," *Computers & Electrical Engineering*, vol. 29, no. 3, pp. 407-419, May, 2003.

[15] B. Mohammadi-ivatloo, A. Rabiee, and M. Ehsan, "Time-varying acceleration coefficients IPSO for solving dynamic economic dispatch with non-smooth cost function," *Energy Conversion and Management*, vol. 56, pp. 175-183, Apr, 2012.

[16] D. C. Secui, "A new modified artificial bee colony algorithm for the economic dispatch problem," *Energy Conversion and Management*, vol. 89, pp. 43-62, Jan 1, 2015.

[17] E. Khorram, and M. Jaberipour, "Harmony search algorithm for solving combined heat and power economic dispatch problems," *Energy Conversion and Management*, vol. 52, no. 2, pp. 1550-1554, Feb, 2011.

[18] S. Khamsawang, and S. Jiriwibhakorn, "DSPSO-TSA for economic dispatch problem with nonsmooth and noncontinuous cost functions," *Energy Conversion and Management*, vol. 51, no. 2, pp. 365-375, Feb, 2010.

[19] D. C. Secui, "A method based on the ant colony optimization algorithm for dynamic economic dispatch with valve-point effects," *International Transactions on Electrical Energy Systems*, vol. 25, no. 2, pp. 262-287, Feb, 2015.

[20] A. Rajagopalan, V. Sengoden, and R. Govindasamy, "Solving economic load dispatch problems using chaotic self-adaptive differential harmony search algorithm," *International Transactions on Electrical Energy Systems*, vol. 25, no. 5, pp. 845-858, May, 2015.

[21] G. Xiong, D. Shi, and X. Duan, "Multi-strategy ensemble biography-based optimization for economic dispatch problems," *Applied Energy*, vol. 111, pp. 801-811, 2013.

[22] J. S. Alsumait, J. K. Sykulski, and A. K. Al-Othman, "A hybrid GA-PS-SQP method to solve power system valve-point economic dispatch problems," *Applied Energy*, vol. 87, no. 5, pp. 1773-1781, May, 2010.

[23] M. T. Tsai, and C. W. Yen, "The influence of carbon dioxide trading scheme on economic dispatch of generators," *Applied Energy*, vol. 88, no. 12, pp. 4811-4816, Dec, 2011.

[24] W. Wei, F. Liu, J. Wang et al., "Robust environmental-economic dispatch incorporating wind power generation and carbon capture plants," *Applied Energy*, vol. 183, pp. 674-684, 2016.

[25] T. Niknam, "A new fuzzy adaptive hybrid particle swarm optimization algorithm for non-linear, non-smooth and non-convex economic dispatch problem," *Applied Energy*, vol. 87, no. 1, pp. 327-339, Jan, 2010.

[26] P. K. Roy, and S. Bhui, "A multi-objective hybrid evolutionary algorithm for dynamic economic emission load dispatch," *International Transactions on Electrical Energy Systems*, vol. 26, no. 1, pp. 49-78, Jan, 2016.

[27] M. Mandala, and C. P. Gupta, "Combined economic emission dispatch based transmission congestion management under deregulated electricity market," *in International Conference on Computing, Electronics and Electrical Technologies*, Kumaracoil, 2012, pp. 122-127.

[28] D. N. Vo, and W. Ongsakul, "Economic dispatch with multiple fuel types by enhanced augmented Lagrange Hopfield network," *Applied Energy*, vol. 91, no. 1, pp. 281-289, Mar, 2012.

[29] B. Canizes, J. Soares, P. Faria et al., "Mixed integer non-linear programming and Artificial Neural Network based approach to ancillary services dispatch in competitive electricity markets," *Applied Energy*, vol. 108, pp. 261-270, Aug, 2013.

[30] J. A. Momoh, and S. S. Reddy, "Combined Economic and Emission Dispatch using Radial Basis Function," *in IEEE PES General Meeting, National Harbor*, MD, 2014, pp. 1-5.

[31] C. M. Huang, and F. L. Wang, "An RBF network with OLS and EPSO algorithms for real-time power dispatch," *IEEE Transactions on Power Systems*, vol. 22, no. 1, pp. 96-104, Feb, 2007.

[32] B. Kar, K. K. Mandal, D. Pal et al., "Combined Economic and Emission Dispatch by ANN with backprop algorithm using variant learning rate & momentum coefficient," *in International Power Engineering Conference*, Singapore, 2005, pp. 230-235.

[33] W. M. Lin, C. S. Tu, R. F. Yang et al., "Particle swarm optimisation aided least-square support vector machine for load forecast with spikes," *IET Generation Transmission & Distribution*, vol. 10, no. 5, pp. 1145-1153, Apr 7, 2016.

[34] G. S. dos Santos, L. G. J. Luvizotto, V. C. Mariani et al., "Least squares support vector machines with tuning based on chaotic differential evolution approach applied to the identification of a thermal process," *Expert Systems with Applications*, vol. 39, no. 5, pp. 4805-4812, Apr, 2012.

[35] j. e. a. Nagi, "Detection of Abnormalities and Electricity Theft using Genetic Support Vector Machines," *in TENCON - IEEE Region 10 Conference*, Heyderabad, 2008, pp. 1-6.

[36] Z. Mustafa, Y. Yusof, and S. S. Kamaruddin, “Application of LSSVM by ABC in Energy Commodity Price Forecasting,” *in IEEE 8th International Power Engineering and Optimization Conference*, Langkawi, 2014, pp. 94-98.

[37] J. Zhang, Y. Lin, and P. Lu, “Short-term Electricity load Forecasting Based on ICA and LSSVM*,” in International Conference on Computational Intelligence and Software Engineering*, Wuhan, 2009, pp. 1-4.

[38] M. Shabanzadeh. "Business processes in wholesale market operation," 23 June 2016; http://mortezash.blogfa.com/cat-5.aspx.

[39] E. S. Limited, "Capacity Market," 2016.

[40] M. Kazemi, P. Siano, D. Sarno et al., “Evaluating the impact of sub-hourly unit commitment method on spinning reserve in presence of intermittent generators,” *Energy*, vol. 113, pp. 338-354, Oct 15, 2016.

[41] G. L. Decker, and A. D. Brooks, “Valve Point Loading of Turbines,” *Electrical Engineering*, vol. 77, no. 6, pp. 50, 2013.

[42] I. Ciornei, and E. Kyriakides, “Recent methodologies and approaches for the economic dispatch of generation in power systems,” *International Transactions on Electrical Energy Systems*, vol. 23, no. 7, pp. 1002-1027, Oct, 2013.

[43] U. e. a. Govenc, “Combined economic and emission dispatch using gravitational search algorithm,” *Scientia Iranica. Transaction D*, vol. 19, no. 6, pp. 1754-1762, 2012.

[44] V. K. Jadoun, N. Gupta, K. R. Niazi et al., “Dynamically controlled particle swarm optimization for large-scale nonconvex economic dispatch problems,” *International Transactions on Electrical Energy Systems*, vol. 25, no. 11, pp. 3060-3074, Nov, 2015.

[45] S. K. Wang, J. P. Chiou, and C. W. Liu, “Non-smooth/non-convex economic dispatch by a novel hybrid differential evolution algorithm,” *IET Generation Transmission & Distribution*, vol. 1, no. 5, pp. 793-803, Sep, 2007.

[46] A. Goudarzi, A. Ahmadi, G. A. Swanson et al., “Non-Convex Optimisation of Combined Environmental Economic Dispatch through Cultural Algorithm with the Consideration of the Physical Constraints of Generation units and Price Penalty Factors,” *Africa Research Journal, SAIEE*, vol. 107, no. 3, pp. 146- 166, 2016.

[47] H. F. Zhang, J. Z. Zhou, N. Fang et al., “Daily hydrothermal scheduling with economic emission using simulated annealing technique based multi-objective cultural differential evolution approach,” *Energy*, vol. 50, pp. 24-37, Feb 1, 2013.

[48] B. Bhattacharya, D. Mandal, and N. Chakraborty, “A multi-objective optimization based on cultural algorithm for economic dispatch with environmental constraints,” *International Journal of Scientific and Engineering Research*, vol. 3, pp. 1-8, 2012.

[49] J. A. K. Suykens, “Least Squares Support Vector Machines,” World Scientific Publishing Company, 2002.

[50] J. A. K. Suykens, J. De Brabanter, L. Lukas et al., “Weighted least squares support vector machines: robustness and sparse approximation,” *Neurocomputing*, vol. 48, pp. 85-105, Oct, 2002.

[51] J. A. K. Suykens, and J. Vandewalle, “Least squares support vector machine classifiers,” *Neural Processing Letters*, vol. 9, no. 3, pp. 293-300, Jun, 1999.

[52] R. Tapia, “Practical Methods of Optimization, Vol 2, Constrained Optimization - Fletcher,R,” *Siam Review*, vol. 26, no. 1, pp. 143-144, 1984.

[53] A. Goudarzi, I. E. Davidson, A. Ahmadi et al., “Intelligent Analysis of Wind Turbine Power Curve,” *in IEEE Symposium Series on Computational Intelligence*, Orlando, Florida, 2014, pp. 1-7.

[54] M. Grigoriu, Stochastic Calculus: Applications in Science and Engineering, Boston: Birkhäuser, 2002.

[55] j. Novak, and P. Chalupa, “Implementation of Mixed-Integer Programming on Embedded System,” *in 25th DAAAM International Symposium on Intelligent Manufacturing and Automation*, Daaam, 2015, pp. 1649-1656.

[56] T. Niknam, R. Azizipanah-Abarghooee, and J. Aghaei, “A New Modified Teaching-Learning Algorithm for Reserve Constrained Dynamic Economic Dispatch,” *IEEE Transactions on Power Systems*, vol. 28, no. 2, pp. 749-763, May, 2013.

[57] Z. L. Gaing, “Particle swarm optimization to solving the economic dispatch considering the generator constraints,” *IEEE Transactions on Power Systems*, vol. 18, no. 3, pp. 1187-1195, Aug, 2003.

[58] J. B. Park, Y. W. Jeong, J. R. Shin et al., “An Improved Particle Swarm Optimization for Nonconvex Economic Dispatch Problems,” *IEEE Transactions on Power Systems*, vol. 25, no. 1, pp. 156-166, Feb, 2010.

[59] J. P. S. Catalão, Smart and Sustainable Power Systems: Operations, Planning, and Economics ofinsular electricity grids, pp. 439: Taylor and Francis Group.

3.9 Appendix

For ease of reference all the system specifications which have been used in the studied cases is given in this section.

3.9.1 Appendix A

In this appendix all the required data for the 15 units system is given (all the units are thermal). This data is based in [57]. Unit data can be found in Tables A. 1and A.2.

Table A.1 15 units system characteristics

Unit No.	P_i^{min} (MW)	P_i^{max} (MW)	a_i ($/h)	b_i ($/MWh)	c_i ($/MW^{2}h)	P_i^0 (MW)	UR_i (MW)	DR_i (MW)
1	150	455	671	10.1	0.000299	400	80	120
2	150	455	574	10.2	0.000183	300	80	120
3	20	130	374	8.8	0.001126	105	130	130
4	20	130	374	8.8	0.001126	100	130	130
5	150	470	461	10.4	0.000205	90	80	120
6	135	460	630	10.1	0.000301	400	80	120
7	135	465	548	9.8	0.000364	350	80	120
8	60	300	227	11.2	0.000338	95	65	100
9	25	162	173	11.2	0.000807	105	60	100
10	25	160	175	10.7	0.001203	110	60	100
11	20	80	186	10.2	0.003586	60	80	80
12	20	80	230	9.9	0.005513	40	80	80
13	25	85	225	13.1	0.000371	30	80	80
14	15	55	309	12.1	0.001929	20	55	55
15	15	55	323	12.4	0.004447	20	55	55

Table A.2 Prohibited operating zones of 15 units system

Unit No.	Prohibited Operating Zones (MW)
2	[185 225][305 335][420 450]
5	[180 200][305 335][390 420]
6	[230 255][365 395][430 455]
12	[30 40][55 65]

3.9.2 Appendix B

In this appendix all the required data for the 40 units system is given (all the units are thermal). This data is based in [43]. Unit data is given in Table B. 1.

Table B.1 40 units system characteristics

Unit No.	P_i^{min} (MW)	P_i^{max} (MW)	a_i ($/h)	b_i ($/MWh)	c_i ($/MW^{2}h)	d_i ($/h)	e_i (rad/MW)	α_i (ton/h)	β_i (ton/MWh)	γ_i (ton/MW^{2}h)	η_i (ton/h)	δ_i (1/MW)
1	36	114	94.705	6.73	0.0069	100	0.084	60	-2.22	0.048	1.31	0.0569
2	36	114	94.705	6.73	0.0069	100	0.084	60	-2.22	0.048	1.31	0.0569
3	60	120	309.54	7.07	0.02028	100	0.084	100	-2.36	0.0762	1.31	0.0569
4	80	190	369.03	8.18	0.00942	150	0.063	120	-3.14	0.054	0.9142	0.0454
5	47	97	148.89	5.35	0.0114	120	0.077	50	-1.89	0.085	0.9936	0.0406
6	68	140	222.33	8.05	0.01142	100	0.084	80	-3.08	0.0854	1.31	0.0569
7	110	300	287.71	8.03	0.00357	200	0.042	100	-3.06	0.0242	0.655	0.02846
8	135	300	391.98	6.99	0.00492	200	0.042	130	-2.32	0.031	0.655	0.02846
9	135	300	455.76	6.6	0.00573	200	0.042	150	-2.11	0.0335	0.655	0.02846
10	130	300	722.82	12.9	0.00605	200	0.042	280	-4.34	0.425	0.655	0.02846
11	94	375	635.2	12.9	0.00515	200	0.042	220	-4.34	0.0322	0.655	0.02846
12	94	375	654.69	12.8	0.00569	200	0.042	225	-4.28	0.0338	0.655	0.02846
13	125	500	913.4	12.5	0.00421	300	0.035	300	-4.18	0.0296	0.5035	0.02075
14	125	500	1760.4	8.84	0.00752	300	0.035	520	-3.34	0.0512	0.5035	0.02075
15	125	500	1760.4	8.84	0.00752	300	0.035	510	-3.55	0.0496	0.5035	0.02075
16	125	500	1760.4	8.84	0.00752	300	0.035	510	-3.55	0.0496	0.5035	0.02075
17	220	500	647.85	7.97	0.00313	300	0.035	220	-2.68	0.0151	0.5035	0.02075
18	220	500	649.69	7.95	0.00313	300	0.035	222	-2.66	0.0151	0.5035	0.02075
19	242	550	647.83	7.97	0.00313	300	0.035	220	-2.68	0.0151	0.5035	0.02075
20	242	550	647.81	7.97	0.00313	300	0.035	220	-2.68	0.0151	0.5035	0.02075
21	254	550	785.96	6.63	0.00298	300	0.035	290	-2.22	0.0145	0.5035	0.02075
22	254	550	785.96	6.63	0.00298	300	0.035	285	-2.22	0.0145	0.5035	0.02075
23	254	550	794.53	6.66	0.00284	300	0.035	295	-2.26	0.0138	0.5035	0.02075
24	254	550	794.53	6.66	0.00284	300	0.035	295	-2.26	0.0138	0.5035	0.02075
25	254	550	801.32	7.1	0.00277	300	0.035	310	-2.42	0.0132	0.5035	0.02075
26	254	550	801.32	7.1	0.00277	300	0.035	310	-2.42	0.0132	0.5035	0.02075
27	10	150	1055.1	3.33	0.52124	120	0.077	360	-1.11	1.842	0.9936	0.0406
28	10	150	1055.1	3.33	0.52124	120	0.077	360	-1.11	1.842	0.9936	0.0406
29	10	150	1055.1	3.33	0.52124	120	0.077	360	-1.11	1.842	0.9936	0.0406
30	47	97	148.89	5.35	0.0114	120	0.077	50	-1.89	0.085	0.9936	0.0406
31	60	190	222.92	6.43	0.0016	150	0.063	80	-2.08	0.0121	0.9142	0.0454
32	60	190	222.92	6.43	0.0016	150	0.063	80	-2.08	0.0121	0.9142	0.0454
33	60	190	222.92	6.43	0.0016	150	0.063	80	-2.08	0.0121	0.9142	0.0454
34	90	200	107.87	8.95	0.0001	200	0.042	65	-3.48	0.0012	0.655	0.02846
35	90	200	116.58	8.62	0.0001	200	0.042	70	-3.24	0.0012	0.655	0.02846
36	90	200	116.58	8.62	0.0001	200	0.042	70	-3.24	0.0012	0.655	0.02846
37	25	110	307.45	5.88	0.0161	80	0.098	100	-1.98	0.095	1.42	0.0677
38	25	110	307.45	5.88	0.0161	80	0.098	100	-1.98	0.095	1.42	0.0677
39	25	110	307.45	5.88	0.0161	80	0.098	100	-1.98	0.095	1.42	0.0677
40	242	550	647.83	7.97	0.00313	300	0.035	220	-2.68	0.0151	0.5035	0.02075

3.9.3 Appendix C

In this appendix all the required data for the 140 units system is given. This data is based in [58]. Unit data can be found in Tables C. 1, C. 2 and C. 3.

Table C.1 140 units system characteristics

Unit No.	P_i^{min} (MW)	P_i^{max} (MW)	a_i ($/h)	b_i ($/MWh)	c_i ($/MW^{2}h)	P_i^0 (MW)	UR_i (MW)	DR_i (MW)
Coal#01	71	119	1220.645	61.242	0.032888	98.4	30	120
Coal#02	120	189	1315.118	41.095	0.00828	134	30	120
Coal#03	125	190	874.288	46.31	0.003849	141.5	60	60
Coal#04	125	190	874.288	46.31	0.003849	183.33	60	60
Coal#05	90	190	1976.469	54.242	0.042468	125	150	150
Coal#06	90	190	1338.087	61.215	0.014992	91.3	150	150
Coal#07	280	490	1818.299	11.791	0.007039	401.1	180	300
Coal#08	280	490	1133.978	15.055	0.003079	329.5	180	300
Coal#09	260	496	1320.636	13.226	0.005063	356.1	300	510
Coal#10	260	496	1320.636	13.226	0.005063	427.3	300	510
Coal#11	260	496	1320.636	13.226	0.005063	412.2	300	510
Coal#12	260	496	1106.539	14.498	0.003552	370.1	300	510
Coal#13	260	506	1176.504	14.651	0.003901	301.8	600	600
Coal#14	260	509	1176.504	14.651	0.003901	368	600	600
Coal#15	260	506	1176.504	14.651	0.003901	301.9	600	600
Coal#16	260	505	1176.504	14.651	0.003901	476.4	600	600
Coal#17	260	506	1017.406	15.669	0.002393	283.1	600	600
Coal#18	260	506	1017.406	15.669	0.002393	414.1	600	600
Coal#19	260	505	1229.131	14.656	0.003684	328	600	600
Coal#20	260	505	1229.131	14.656	0.003684	389.4	600	600
Coal#21	260	505	1229.131	14.656	0.003684	354.7	600	600
Coal#22	260	505	1229.131	14.656	0.003684	262	600	600
Coal#23	260	505	1267.894	14.378	0.004004	461.5	600	600
Coal#24	260	505	1229.131	14.656	0.003684	371.6	600	600
Coal#25	280	537	975.926	16.261	0.001619	462.6	300	300
Coal#26	280	537	1532.093	13.362	0.005093	379.2	300	300
Coal#27	280	549	641.989	17.203	0.000993	530.8	360	360
Coal#28	280	549	641.989	17.203	0.000993	391.9	360	360
Coal#29	260	501	911.533	15.274	0.002473	480.1	180	180
Coal#30	260	501	910533	15.212	0.002547	319	180	180
Coal#31	260	506	1074.81	15.033	0.003542	329.5	600	600
Coal#32	260	506	1074.81	15.033	0.003542	333.8	600	600
Coal#33	260	506	1074.81	15.033	0.003542	390	600	600
Coal#34	260	506	1074.81	15.033	0.003542	432	600	600
Coal#35	260	500	1278.46	13.992	0.003132	402	660	660
Coal#36	260	500	861.742	15.679	0.001323	428	900	900
Coal#37	120	241	408.834	16.542	0.00295	178.4	180	180
Coal#38	120	241	408.834	16.542	0.00295	194.1	180	180
Coal#39	423	774	1288.815	16.518	0.000991	474	600	600
Coal#40	423	769	1436.251	15.815	0.001581	609.8	600	600
LNG#1	3	19	669.988	75.464	0.90236	17.8	210	210
LNG#2	3	28	134.544	129.544	0.110295	6.9	366	366
LNG-CC#1	160	250	3427.912	56.613	0.024493	224.3	702	702
LNG-CC#2	160	250	3751.722	54.451	0.029156	210	702	702
LNG-CC#3	160	250	3918.78	54.736	0.024667	212	702	702
LNG-CC#4	160	250	3379.58	58.034	0.016517	200.8	702	702
LNG-CC#5	160	250	3345.296	55.981	0.026584	220	702	702
LNG-CC#6	160	250	3138.754	61.52	0.00754	232.9	702	702
LNG-CC#7	160	250	3453.05	58.635	0.01643	168	702	702
LNG-CC#8	160	250	5119.3	44.647	0.045934	208.4	702	702
LNG-CC#9	165	504	1898.415	71.584	0.000044	443.9	1350	1350
LNG-CC#10	165	504	1898.415	71.584	0.000044	426	1350	1350
LNG-CC#11	165	504	1898.415	71.584	0.000044	434.1	1350	1350
LNG-CC#12	165	504	1898.415	71.584	0.000044	402.5	1350	1350
LNG-CC#13	180	471	2473.39	85.12	0.002528	357.4	1350	1350
LNG-CC#14	180	561	2781.705	87.682	0.000131	423	720	720
LNG-CC#15	103	341	5515.508	69.532	0.010372	220	720	720
LNG-CC#16	100	312	6240.909	58.172	0.012464	273.5	1500	1500
LNG-CC#17	153	471	9960.11	46.636	0.039441	336	1656	1656
LNG-CC#18	163	500	3671.977	76.947	0.007278	432	2160	2160
LNG-CC#19	95	302	1837.383	80.761	0.000044	220	900	900
LNG-CC#20	160	511	3108.395	70.136	0.000044	410.6	1200	1200
LNG-CC#21	160	511	3108.395	70.136	0.000044	422.7	1200	1200
LNG-CC#22	196	490	7095.484	49.84	0.018827	351	1014	1014
LNG-CC#23	196	490	3392.732	65.404	0.010852	296	1014	1014
LNG-CC#24	196	490	7095.484	49.84	0.018827	411.1	1014	1014
LNG-CC#25	196	490	7095.484	49.84	0.018827	263.2	1014	1014
LNG-CC#26	130	432	4288.32	66.645	0.03456	370.3	1350	1350
LNG-CC#27	130	432	13813.001	22.941	0.08154	418.7	1350	1350
LNG-CC#28	137	455	4435.493	64.314	0.023534	409.6	1350	1350
LNG-CC#29	137	455	9750.75	45.017	0.035475	412	1350	1350
LNG-CC#30	195	541	1042.366	70.644	0.000915	423.2	780	780
LNG-CC#31	175	536	1159.895	70.959	0.000044	428	1650	1650
LNG-CC#32	175	540	1159.895	70.959	0.000044	436	1650	1650
LNG-CC#33	175	538	1303.99	70.302	0.001307	428	1650	1650
LNG-CC#34	175	540	1156.193	70.662	0.000392	425	1650	1650
LNG-CC#35	330	574	2118.968	71.101	0.000087	497.2	1620	1620

LNG-CC#36	160	531	779.519	37.854	0.000521	510	1482	1482
LNG-CC#37	160	531	829.888	37.768	0.000498	470	1482	1482
LNG-CC#38	200	542	2333.69	67.983	0.001046	464.1	1668	1668
LNG-CC#39	56	132	2028.954	77.838	0.13205	118.1	120	120
LNG-CC#40	115	245	4412.017	63.671	0.096968	141.3	180	180
LNG-CC#41	115	245	2982.219	79.458	0.054868	132	120	180
LNG-CC#42	115	245	2982.219	79.458	0.054868	135	120	180
LNG-CC#43	207	307	3174.939	93.966	0.014382	252	120	180
LNG-CC#44	207	307	3218.359	94.723	0.013161	221	120	180
LNG-CC#45	175	345	3723.822	66.919	0.016033	245.9	318	318
LNG-CC#46	160	531	779.519	37.854	0.000521	510	1482	1482
LNG-CC#47	175	345	3551.405	68.185	0.013653	247.9	318	318
LNG-CC#48	175	345	4322.165	60.821	0.028148	183.6	318	318
LNG-CC#49	175	345	3493.739	68.551	0.01347	288	318	318
NUCLEAR#01	360	580	226.799	2.842	0.000064	557.4	18	18
NUCLEAR#02	415	645	382.932	2.946	0.000252	529.5	18	18
NUCLEAR#03	795	984	156.987	3.096	0.000022	800.8	36	36
NUCLEAR#04	795	978	154.484	3.04	0.000022	801.5	36	36
NUCLEAR#05	578	682	332.834	1.709	0.000203	582.7	138	204
NUCLEAR#06	615	720	326.599	1.668	0.000198	680.7	144	216
NUCLEAR#07	612	718	345.306	1.789	0.000215	670.7	144	216
NUCLEAR#08	612	720	350.372	1.815	0.000218	651.7	144	216
NUCLEAR#09	758	964	370.377	2.726	0.000193	921	48	48
NUCLEAR#10	755	958	367.067	2.732	0.000197	916.8	48	48
NUCLEAR#11	750	1007	124.875	2.651	0.000324	911.9	36	54
NUCLEAR#12	750	1006	130.785	2.798	0.000344	898	36	54
NUCLEAR#13	713	1013	878.746	1.595	0.00069	905	30	30
NUCLEAR#14	718	1020	827.959	1.503	0.00065	846.5	30	30
NUCLEAR#15	791	954	432.007	2.425	0.000233	850.9	30	30
NUCLEAR#16	786	952	445.606	2.499	0.000239	843.7	30	30
NUCLEAR#17	795	1006	467.223	2.674	0.000261	841.4	36	36
NUCLEAR#18	795	1013	475.94	2.692	0.000259	835.7	36	36
NUCLEAR#19	795	1021	899.462	1.633	0.000707	828.8	36	36
NUCLEAR#20	795	1015	1000.367	1.816	0.000786	846	36	36
OIL#01	94	203	1269.132	98.83	0.014355	179	120	120
OIL#02	94	203	1269.132	89.83	0.014355	120.8	120	120
OIL#03	94	203	1269.132	89.83	0.014355	121	120	120
OIL#04	244	379	4965.124	64.125	0.030266	317.4	480	480
OIL#05	244	379	4965.124	64.125	0.030266	318.4	480	480
OIL#06	244	379	4965.124	64.125	0.030266	335.8	480	480
OIL#07	95	190	2243.185	76.129	0.024027	151	240	240
OIL#08	95	189	2290.381	81.805	0.00158	129.5	240	240
OIL#09	116	194	1681.533	81.14	0.022095	130	120	120
OIL#10	175	321	6743.302	46.665	0.07681	218.9	180	180
OIL#11	2	19	394.398	78.412	0.953443	5.4	90	90
OIL#12	4	59	1243.165	112.088	0.000044	45	90	90
OIL#13	15	83	1454.74	90.871	0.072468	20	300	300
OIL#14	9	53	1011.051	97.116	0.000448	16.3	162	162
OIL#15	12	37	909.269	83.244	0.599112	20	114	114
OIL#16	10	34	689.378	95.665	0.244706	22.1	120	120
OIL#17	112	373	1443.792	91.202	0.000042	125	1080	1080
OIL#18	4	20	535.553	104.501	0.085145	10	60	60
OIL#19	5	38	617.734	83.015	0.524718	13	66	66
OIL#20	5	19	90.966	127.795	0.176515	7.5	12	6
OIL#21	50	98	974.447	77.929	0.063414	53.2	300	300
OIL#22	5	10	263.81	92.779	2.740485	6.4	6	6
OIL#23	42	74	1335.594	80.95	0.112438	69.1	60	60
OIL#24	42	74	1033.871	89.073	0.041529	49.9	60	60
OIL#25	41	105	1391.325	161.288	0.000911	91	528	528
OIL#26	17	51	4477.11	161.829	0.005245	41	300	300
OIL#27	7	19	57.794	84.972	0.234787	13.7	18	30
OIL#28	7	19	57.794	84.972	0.234787	7.4	18	30
OIL#29	26	40	1258.437	16.087	1.111878	28.6	72	120

Table C.2 Valve-point data of 140 units system with unit characteristics

Unit No.	a_i ($/h)	b_i ($/MWh)	c_i ($/MW^{2}h)	d_i ($/h)	e_i (rad/MW)
COAL#05	1976.469	54.242	0.042468	700	0.080
COAL#10	1320.636	13.226	0.005063	600	0.055
COAL#15	1176.504	14.651	0.003901	800	0.060
COAL#22	1229.131	14.656	0.003684	600	0.050
COAL#33	1074.810	15.033	0.003542	600	0.043
COAL#40	1436.251	15.815	0.001581	600	0.043
LNG_CC#10	1898.415	71.584	0.000044	1100	0.043
LNG_CC#28	13813.001	22.941	0.081540	1200	0.030
LNG_CC#30	9750.750	45.017	0.035475	1000	0.050
LNG_CC#42	2982.219	79.458	0.054868	1000	0.050
OIL#08	2290.381	81.805	0.001580	600	0.070
OIL#10	6743.302	46.665	0.076810	1200	0.043

Table C.3 Prohibited operating zones of 140 units system

Unit No.	Prohibited Operating Zones (MW)
COAL#08	[250 280][305 335][420 450]
COAL#32	[220 250][320 350][390 420]
LNG_CC#32	[230 255][365 395][430 455]
OIL#25	[50 75][85 95]

4. CHAPTER 4

Paper Number 4

Evaluating the Impact of Sub-hourly Unit Commitment Method on Spinning Reserve in Presence of Intermittent Generators

Evaluating the Impact of Sub-hourly Unit Commitment Method on Spinning Reserve in Presence of Intermittent Generators

Abstract- This paper presents an algorithm to deal with thermal Unit Commitment which takes into account the intermittency and volatility of renewable energies such as wind and solar energies. Dynamic Programming (DP) integrating Priority Listing order (PL) based on Best Per Unit Cost (BP) was applied to commit the thermal units in an isolated island with generators based on renewable sources. In this work, the effects of a high time resolutions such as 60, 30, 15, 10 and 5 min on production costs, reserves and intermittent generators are investigated. In order to demonstrate the capability of the proposed algorithm, two cases were studied. Firstly, a test system composed of ten diesel generators, three wind turbines and one Photovoltaic (PV) power plant is examined and then the IEEE 118-bus test system, integrating wind and PV power plants, is considered. The results show that a sufficient schedule for each generation unit can be reached at a time resolution closer to real-time unit commitment and economic dispatch while a high level of reliability is guaranteed by fulfilling practical constraints.

Keywords: Dynamic programming (DP), priority listing order, renewable energy sources, unit commitment (UC).

4.1 Introduction

One of the most important issues regarding power system operation is the optimal scheduling of the diesel units. The Unit Commitment (UC) in an autonomous grid becomes more complicated when including renewable energies, such as wind and solar energies, as they are intermittent and volatile in nature. Renewable energies are an attractive alternative to generate the electricity allowing the reduction of the greenhouse gases and emissions. They introduce more constraints in the problem formulation, such as minimum diesel loading and ramp-up and down rates, and imply the enlargement of physical reserves to cope with the uncertainty and unpredictability of renewable energy in order to maintain a high level of reliability of the system. With the inherent intermittency and volatility of renewable resources affecting renewable energy production, in order to increase the penetration of these resources and maintain the reliability of the system, more flexible units with fast response are required. In this regard, the system operators rely on power plants that can supply demand on the same timescale as variations of renewable outputs and therefore generator manufacturers are trying to improve the abilities of generation units such as ramp rate limits and minimum generation levels [1]. The operation objective is to find the best trade-off between production costs and reliability of the system, even limiting the penetration of renewable energy which is proportional to the reserves' requirements.

The UC problem can be solved by using different methods included in two main categories, namely heuristic methods and evolutionary algorithms. Priority List, Augmented Lagrangian Relaxation, Dynamic Programming (DP) and the Branch-and-Bound algorithm, belonging to the first optimization group, have been used to solve the classic UC problem. Since the beginning of the last decade, methods classified in the second group, such as Genetic Algorithms (GAs), Simulated Annealing (SA), Analytic Hierarchy Process (AHP), and Particle Swarm Optimization (PSO) have also been used to solve the UC problem [2].

A methodology based on GAs has been presented by T. Senjyu et al. to solve the UC of thermal units integrated with wind and solar power in which the Best Per Unit Cost (BP), that is a function of production cost coefficients, was used to sort the generators' order [3].

A hybrid approach which is a combination of branch and bound algorithm with a Dynamic Programming (DP) has been presented by Chun-Lung Chen et al. to commit the thermal units in an isolated hybrid power system consisting of wind and thermal plants [4].

It has also been demonstrated by J. Wang [5] that the cumulative wind power might not be intermittent even if the single wind farm is intermittent within a day period. The electric power generated by a wind farm and even the aggregated wind power output of a wider system can vary significantly on sub-hourly time scales, particularly at high wind penetrations and for small isolated system [6]. A limitation of previous research is that the intra-hour impact of renewable energies has not been considered in UC and economic load dispatch (ELD) which leads to inaccurate operational cost computing.

An approach which is focused on the ramp capability with an interval resolution of 5 min has been proposed by N. Navid, and G. Rosenwald and utilized in security constrained economic dispatch (SCED) study for both single period (SP) and time coupled multi period (TCMP). In this approach the amount of ramp capability can be adjusted based on forecasted deviations and historical uncertainties in order to respond to the net load. The authors demonstrated that the proposed approach is a viable option to provide increased response capability from the same set of supplies for both SP and TCMP [7]. A comparison has been made by E. Ela, and M. O'Malley between TCMP and SP in a Real Time Market (RTM) and it has been shown that the TCMP has a better solution for efficiency, reliability and reduction of production price [8].

In a recent work UC and ELD problems were solved stochastically for a 6-hour time horizon. Improved bender decomposition is deployed to show the impacts of increased temporal resolution of 10, 15, 30 and 60 min on the operational cost. A comparison has been made between deterministic and stochastic UC-ELD with hourly and sub-hourly resolutions. It has been illustrated that sub-hourly resolution can reduce the dispatch cost if the UC is solved stochastically [9].

J.P. Deane et al. utilized the power systems modelling tool PLEXOS to show the variability of the renewable generation and it has been illustrated that the inability of thermal units can be captured by means of a more accurate resolution. A time resolution of 5, 15, 30 and 60 min in UC and ELD was considered for one year and it has been depicted that a higher resolution implies a higher generation cost [10].

The importance of energy storage in reducing cycling burden has been explored by C. O'Dwyer, and D. Flynn [11]. The authors deployed PLEXOS in UC and ELD to investigate the impact of a high wind energy penetration (with a capacity of 42%) on a conventional plant cycling in sub-hourly (15-min) resolution and they have found that energy storage can reduce cycling and improve the performance of the system while a significant cost saving can be obtained [11]. Key limitations derived from the above literature are given below:

- Minimum diesel loading has not been considered.
- Ramp rates taken into account in previous studies are based on [12].
- Sub-hourly variability of the spinning reserve in presence of renewable energies has not been investigated.

The previously mentioned limitations have been taken into account in the proposed method. Another important innovative of the proposed method is the combined use of dynamic programming (DP) integrated with priority listing order (PL) based on best per unit cost (BP), it's worth noting that this hybrid method has not been utilized into any other published article.

The new method is, in fact, based on combination of DP and PL in accordance with best per unit cost ($2\sqrt{a_i c_i} + b_i$) and is called DP-BP. In order to show the capability of the presented method to solve UC and ED on an hourly basis, a comparison has been made with different methods such as complete enumeration DP (DP-CE) and full load average cost DP (DP-FA) with the same exact conditions for a given case study. After illustrating the capability of the suggested method, different time resolutions (5, 10, 15, 30, 60 min) have been considered to simultaneously optimise the UC and ELD and facilitate the integration of renewable energies into the grid.

4.2 Problem formulation

4.2.1 Statement of the problem

The main objective of the proposed method is to schedule diesel units, solar and wind based generators in an optimal manner in order to reduce the total production costs while satisfying physical and operation constraints. Fig 4.1 depicts an autonomous hybrid power plant which is composed of a diesel unit, a wind turbine and a PV generator.

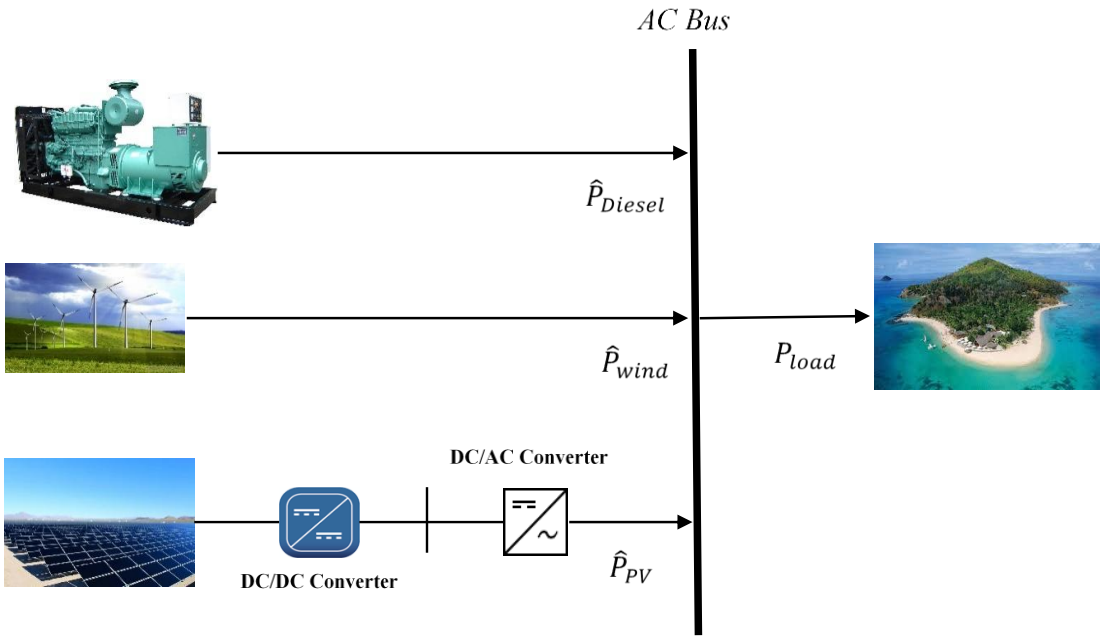

Fig. 4.1 Autonomous hybrid system

Short-term scheduling problem can be mathematically formulated by means of equations (1) - (5) as an optimization problem as follows [12]:

$$FC = \sum_{t=1}^{To} \sum_{i=1}^{N_D} F_i \left(P_{D_i}(t)\right) e_i(t)\, e_i^D(t) + S_i(t) \tag{1}$$

The final production cost (FC) is due to production and transition state costs of diesel generators over a planning horizon (*To)* (24, 48, 72, 144, 288), with time intervals of t. In this study, t was considered to be 5, 10, 15, 30 and 60 min. $e_i(t)$ is a vector which describes the status of i^{th} diesel generator and $e_i^D(t)$ denotes the availability of the diesel generator and is a function of time calculated using Monte Carlo method or preventive maintenance (PM) schedule. The

study considered that after running Monte Carlo method all components are available and working in a good manner:

$$e_i(t) = \begin{cases} 1 \\ 0 \end{cases}, i = 1,2,\dots,N_D, \qquad t = 1,2,\dots,To \tag{2}$$

where, 1 means the i^{th} diesel unit is committed and 0 is not.

$$e_i^D(t) = \begin{cases} 1 \\ 0 \end{cases}, i = 1,2,\dots,N_D, \qquad t = 1,2,\dots,To \tag{3}$$

where, 1 means the i^{th} diesel unit is available and 0 is not.

$F_i\left(P_{D_i}(t)\right)$ in equation (1) is the production cost of i^{th} diesel generator at duration *t*, which is called cost function ($\frac{\$}{hr}$), and is calculated as the product of the heat rate ($\frac{MBTU}{hr}$) and the unit fuel cost ($\frac{\$}{MBTU}$). In some cases, input-output characteristics of the diesel generators can be described as quadratic function which is as follows:

$$F_i\left(P_{D_i}(t)\right) = a_i + b_i P_{D_i}(t) + c_i P_{D_i}^2 \tag{4}$$

where $a_i\left(\frac{\$}{hr}\right)$, $b_i\left(\frac{\$}{kWhr}\right)$ and $c_i\left(\frac{\$}{kW^2hr}\right)$ are the cost coefficients. For simplicity and for enhancing the speed of the calculation this function can be linearized by means of piecewise linear approximation [13]. $S_i(t)$ in equation (1) is the transition cost from one stage to another and consists of start-up (SU) and shut-down (SD) costs.

$$S_i(t) = SU\big(1 - e_i(t-1)\big)e_i(t) + SD\big(1 - e_i(t)\big)e_i(t-1) \tag{5}$$

In this work, SU cost is considered as time dependent and is defined as follows:

$$SU_i(t) = \begin{cases} hc_i : T_i^{off} \le X_i^{off} \le T_i^{off} + csh_i \\ cc_i : T_i^{off} \le X_i^{off} > T_i^{off} \end{cases} \tag{6}$$

In this research, the concept has been used to linearize the SU cost function is basically based on [14]. Jiří Šumbera has used three start up states which are hot, warm and cold start up. However, for simplicity cold and hot states have been considered in this work and SD cost is assumed to be constant with no price. Equation (1) can be minimized subject to system and unit constraints which are listed below.

4.2.2 System constraints

4.2.2.1 System power balance

$$P_D(t) + P_R(t) - P_L(t) = 0 \tag{7}$$

where $P_D(t)$, $P_R(t)$ and $P_L(t)$ are the actual diesel generators power output, actual renewable power output and total system load demand, respectively [4]. In particular:

$$P_R(t) = P_W(t) + P_{PV}(t) \tag{8}$$

where $P_W(t)$ and $P_{PV}(t)$ are the actual wind farm and PV plant power outputs, respectively.

$$P_{NetLoad}(t) = P_L(t) - P_R(t) \tag{9}$$

where $P_{netload}(t)$ is considered as re-dispatchable load while intermittent generations are integrated into the grid.

4.2.2.2 System spinning reserve

Spinning reserve (SR) requirement is typically defined as a base component plus a percentage of the load and a percentage of the highest operation limit of the largest on-line unit [4]. In this work, SR was assumed as a percentage of the total system load (the load before injecting the renewable sources) in order to maintain the system in a high level of reliability against frequent load fluctuations.

In equations (10) and (11), $RU_i(t)$ and $RD_i(t)$ are the required spinning up and down reserves, respectively and $\propto$ is a reliability level parameter which is equal to 10% without taking into account the renewable power according to [3].

$$\sum_{i=1}^{N_D} e_i(t)\, e_i^D(t)\; RU_i(t) \geq \propto * P_L(t) + P_R(t) \tag{10}$$

$$\sum_{i=1}^{N_D} e_i(t)\, e_i^D(t)\, RD_i(t) \geq P_R(t) \tag{11}$$

4.2.3 Diesel unit constraints

Diesel plant generation limits are [4]:

$$\sum_{i=1}^{N_D} P_{D_i}^{min}(t)\ e_i(t)\ e_i^D(t) \leq P_L(t) - \sum_{i=1}^{N_D} e_i(t)\ e_i^D(t)\ RD_i(t) \tag{12}$$

$$\sum_{i=1}^{N_D} P_{D_i}^{max}(t)\ e_i(t)\ e_i^D(t) \geq P_L(t) + \sum_{i=1}^{N_D} e_i(t)\ e_i^D(t)\ RU_i(t) \tag{13}$$

Total available diesel generation is referred to the sum of the maximum power output of available diesel units which are committed to generate the actual power in a specific period of time [4]:

$$P_D^*(t) = \sum_{i=1}^{N_D} e_i(t)\ e_i^D(t)\ P_{D_i}^{max}(t) \tag{14}$$

The total actual diesel generation is limited by the available generation:

$$P_D(t) \leq P_D^*(t) \tag{15}$$

The diesel generation of each unit has the following limits [4]:

$$P_{D_i}^{min}(t) \leq P_{D_i}(t) \leq P_{D_i}^{max}(t) \tag{16}$$

The diesel minimum up/down times constraints are [13]:

$$(X_i^{on}(t-1) - T_i^{on})\ \left(e_i(t-1) - e_i(t)\right) \geq 0 \tag{17}$$

$$\left(X_i^{off}(t-1) - T_i^{off}\right)\left(e_i(t) - e_i(t-1)\right) \geq 0 \tag{18}$$

$X_i^{\frac{on}{off}}$ is the time for which i^{th} diesel unit has been on/off at stage *t* and $T_i^{\frac{on}{off}}$ is minimum up/down time of i^{th} diesel unit. Ramp rate limits are:

$$\begin{aligned} P_{D_i}(t) - P_{D_i}(t-1) &\leq UR_i(t-1)\ subject\ to\ UR_i(t-1) \\ &\leq min\begin{cases} UR_i \\ P_{D_i}^{max} - P_{D_i}(t-1) \end{cases} \end{aligned} \tag{19}$$

$$\begin{aligned} P_{D_i}(t-1) - P_{D_i}(t) &\leq DR_i(t-1)\ subject\ to\ DR_i(t-1) \\ &\geq min\begin{cases} DR_i \\ P_{D_i}(t-1) - P_{D_i}^{min} \end{cases} \end{aligned} \tag{20}$$

where UR_i and DR_i are the fixed ramp-up and ramp-down of the diesel generator, respectively and are set at 60% of its rated capacity [4]. Whereas, $UR_i(t)$ and $DR_i(t)$ are the time dependent ramp-up and down at stage t. In this research to include more feasible states ramp rate limits were considered as time dependent which were proportion of maximum output power at time *t*.

The total available SR (or SR capacity) of a diesel unit is the difference between the maximum power output of each diesel unit that can operate and the generated power [4]. It differs from required reserve, which is a percentage of the hourly or sub-hourly demanded power to cover the fluctuation of the load:

$$RU_i(t) = P_{D_i}^{max}(t) - P_{D_i}(t) \tag{21}$$

$$RD_i(t) = P_{D_i}(t) - P_{D_i}^{min}(t) \tag{22}$$

The minimum diesel plant output is:

$$\sum_{i=1}^{N_D} P_{D_i}^{min}(t) \leq P_L(t) - P_R(t) \tag{23}$$

Various operating limits are considered to maintain sufficient level of loading on the diesel generators for safe and reliable operation in terms of autonomous hybrid system which relies on continuous use of diesel generators without energy storage. Therefore, excess intermittent energy must be dumped while diesel generators operate at minimum loading [15]. In this study minimum diesel loading is considered as an important factor to prevent the most expensive units from frequent on and off and let them work at their optimum level. The minimum diesel loading, according to [15], is:

$$\underline{P_L}(t) \geq \sum_{i=1}^{N_D} P_{D_i}^{min}(t) \tag{24}$$

4.2.4 Renewable system constraints

The renewable generation fluctuation constraints are [4]:

$$P_R(t) - P_R(t-1) \leq DR(t), \text{ if } P_R(t-1) \leq P_R(t) \tag{25}$$

$$P_R(t-1) - P_R(t) \leq UR(t), \text{ if } P_R(t-1) \geq P_R(t) \tag{26}$$

where $P_R(t)$, $UR(t)$ and $DR(t)$ represent the total actual renewable generation, total diesel generators ramp-up and down, respectively.

4.2.4.1 Wind farm power generation constraints

In order to overcome intermittency and volatility of the renewable power, wind farms are installed in different areas and total available wind generation is taken from Chun-Lung Chen et al. literature [4]. Due to unavailability of data, generated random numbers based on Gaussian random distribution are used to simulate intra-hour data for a 24-hour period based on given hourly wind data with intervals of 5, 10, 15, 30 min:

$$P_W^*(t) = \sum_{j=1}^{N_{WT}} P_{W_j}^*(t)\ e_j(t)\ e_j^W(t) \tag{27}$$

$$e_j(t) = \begin{cases} 1 \\ 0 \end{cases}, j = 1,2,\dots,N_{WT}, \qquad t = 1,2,\dots,To \tag{28}$$

$$e_j^W(t) = \begin{cases} 1 \\ 0 \end{cases}, j = 1,2,\dots,N_{WT}, \qquad t = 1,2,\dots,To \tag{29}$$

In the above equations, $e_j(t)$ is a vector which describes the status of j^{th} wind turbine (WT), $e_j^W(t)$ denotes the availability of the WT and is a function of time calculated using Monte Carlo method or the PM schedule, and N_{WT} is the number of WTs. In equation (29), 1 means the j^{th} WT is online and 0 is not. Total actual wind generation is limited as follows [4]:

$$0 \le P_W(t) \le P_W^*(t) \tag{30}$$

4.2.4.2 PV generator constraints

Total available PV generation can be rewritten by using equation (27):

$$P_{PV}^*(t) = \sum_{k=1}^{N_{PV}} P_{PV_k}^*(t)\ e_k(t)\ e_k^{PV}(t), \qquad k = 1,2,\dots,N_{PV} \tag{31}$$

$$e_k(t) = \begin{cases} 1 \\ 0 \end{cases}, k = 1,2,\dots,N_{PV}, \qquad t = 1,2,\dots,To \tag{32}$$

$$e_k^{PV}(t) = \begin{cases} 1 \\ 0 \end{cases}, k = 1,2,\dots,N_{PV}, \qquad t = 1,2,\dots,To \tag{33}$$

In the above equations $e_k(t)$ is a vector which describes the status of $k^{th}PV$ generator, e_k^{PV} (t) denotes the availability of the PV panels and is a function of time calculated using Monte Carlo method or schedule of PM, N_{PV} is the number of PV generators, 1 means the $k^{th}PV$ generator is online and 0 is not. Total actual PV generation limits are [4]:

$$0 \le P_{PV}(t) \le P_{PV}^*(t) \tag{34}$$

4.3 Proposed method for unit commitment (UC)

The objective function (equation (1)) subjected to equations (6) - (24) is a non-linear mixed integer optimization which consists of integer variables for diesel UC and continuous variables for ELD. This problem becomes more complex when renewable power with intermittency and volatility is incorporated and needs more constraints to limit the renewable power penetration to reach a compromise between system security and total operating cost. The method utilized to handle the UC is DP, which is a recursive procedure that determines at each stage (or time period) the optimum UC and minimizes its corresponding cost. Conventional DP [16], which depicts in Fig 4.2, with complete enumeration has $2^{N_D} - 1$ combination where N_D is the number of diesel generators and takes long computation time if either the number of units or time horizon is large [17]. For this reason, sequential DP [18] with strict priority listing order based on $(2\sqrt{a_i c_i} + b_i)$, which is known as BP cost function where a_i,b_i, and c_i are the coefficients of cost function [3], can be used to reduce the computational time. For instance, Table 4.1 shows the list of states for three generators where each state has one committed unit more than the previous state. In this example, which has been created based on BP, if the order of generators' BP costs gives G3, G1 and G2, then it can be seen that the least expensive generators are coming first. The list is column based, the first column contains only the cheapest generator, the second column contains two cheapest generators and the last one contains all generators. Fig 4.3 illustrates the overall process of the proposed method and being discussed in the next sections. All the algorithms are implemented in MATLAB and executed by a personal computer with the following spec, 1.6GHZ CPU and 2.5GB RAM.

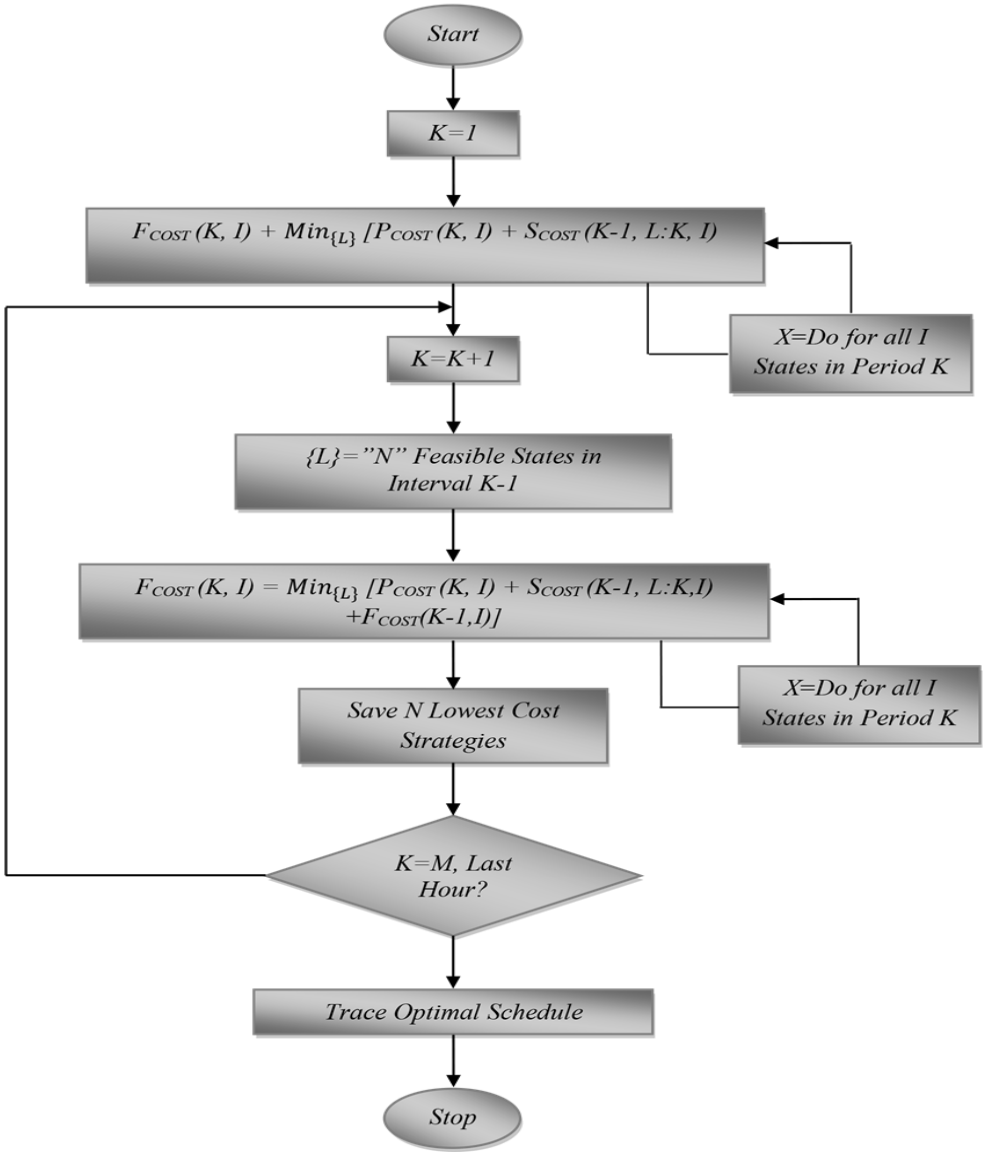

Fig. 4.2 UC via forward DP

where,

$Fcost\ (K,I)$ is least total cost to arrive at state (K, I)

$Pcost\ (K,I)$ is production cost for state (K, I)

$Scost\ (K-1,L{:}\ K,I)$ is transition cost from state (K-1,L) to state (K, I)

$State\ (K,I)$ is I^{th} combination in K^{th} hour

X = number of states to search each period

N = number of strategies, or paths, to save at each step

M = total period

K = current period

Table 4.1 Example of unit combination based on priority listing order

Gen-No.	Gen-cost [$]	No. of State		
		1	2	3
1	5	0	1	1
2	7	0	0	1
3	3	1	1	1

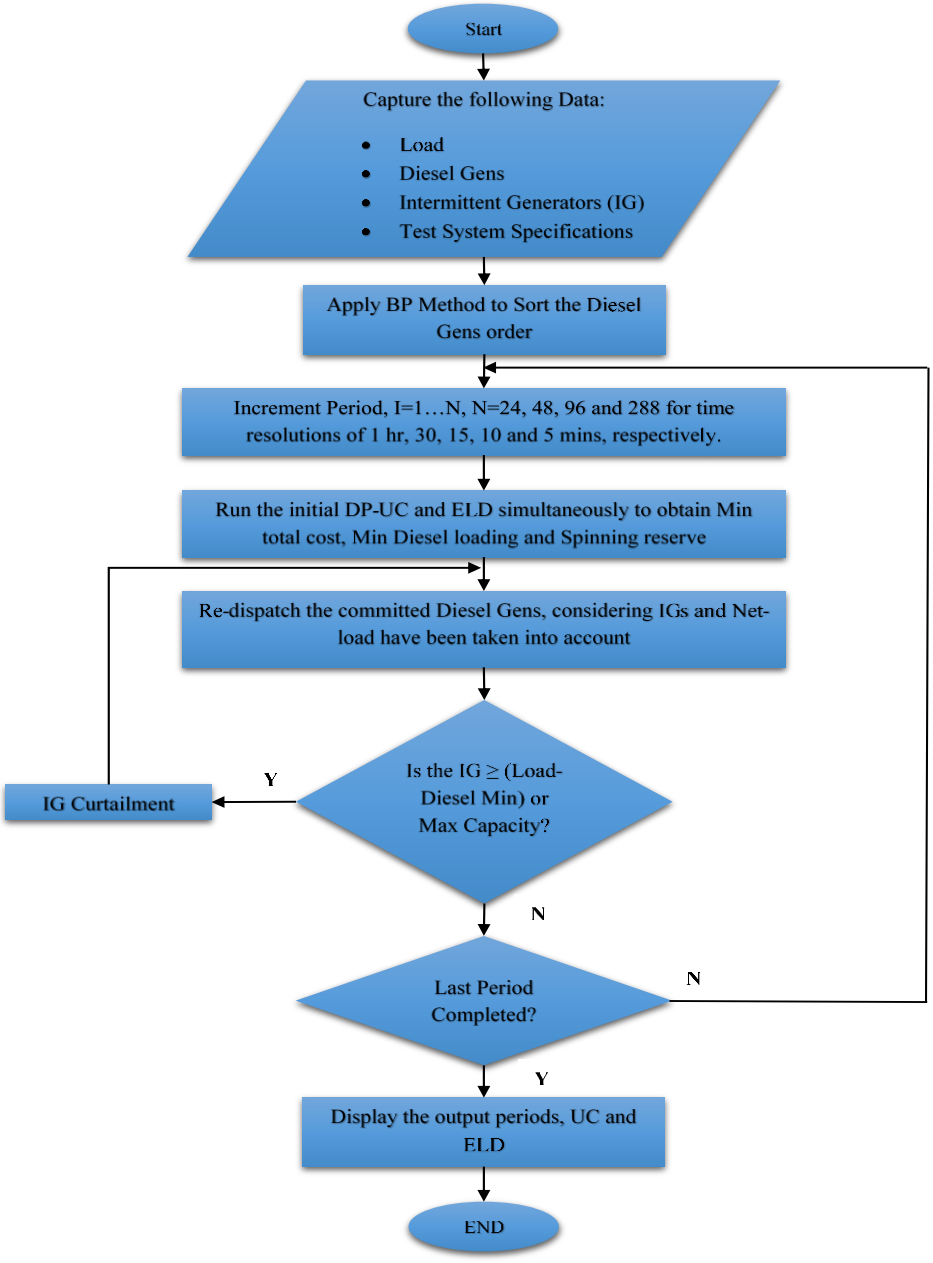

Fig. 4.3 Overall schematic of proposed method

4.3.1 Initial diesel UC and ELD

The main elements of the power grid which have significant influence to deliver power generation at the least cost are optimum scheduling of generation units, fuel cost, and transmission line losses. The most effective generating unit in the power grid does not guarantee to decrease and to minimize the total generation cost as it may be located far away from the load demand which will effectively lead to more transmission line losses or it is possible that the fuel cost can vary according on the geographical location of generation units. The main aim of ELD method is to minimize the total cost and meet the load demand of system simultaneously by determining the optimum amount of generation units' schedules and reducing the power losses [19]. Transmission line losses were not consider in this study. The purpose of this calculation is to find minimum diesel production which allows keeping reliability of the system. For this reason, in order to minimize equation (1) subject to (6) - (24) DP with PL order according to BP is utilized to perform UC and ELD simultaneously without considering wind and PV power for a 24-hour of time horizon with different time resolutions (5, 10, 15, 30, 60 min). Since, the nature of quadratic programing (QP) allows us to find the best solution (which can be maximization or minimization of objective function) for a quadratic objective function while considering a limited number of decision variables subject to a limited number of linear equality and/or inequality constraints [20].

Details of ELD based on QP which utilized to handle the production function are given below:

$$f(x) = \alpha + \sum_{i=1}^{n} c_i x_i + \frac{1}{2}\sum_{k=1}^{n}\sum_{i=1}^{n} q_{ki} x_k x_i \tag{35}$$

By utilizing matrix notation, the above mentioned objective function can be simplified to

$$f(x) = \alpha + c^T x + \frac{1}{2} x^T Q x \tag{36}$$

where

$$c = \begin{bmatrix} c_1 \\ c_2 \\ \vdots \\ c_n \end{bmatrix} \tag{37}$$

$$Q = \begin{bmatrix} q_{11} & q_{12} & \cdots & q_{1n} \\ q_{21} & q_{22} & \cdots & q_{2n} \\ \vdots & \vdots & \ddots & \vdots \\ q_{n1} & q_{n2} & \cdots & q_{nn} \end{bmatrix} \tag{38}$$

With considering no loss in general, we can assume that the matrix Q is symmetric since

$$x^T Qx = (x^T Qx)^T = x^T Q^T x = \frac{1}{2}(x^T Qx + x^T Q^T x) = x^T(\frac{Q + Q^T}{2})x \quad (39)$$

It is possible to replace the matrix Q by the symmetric matrix $\frac{Q+Q^T}{2}$. Henceforward, we assume the matrix Q is symmetric and the standard form of QP can be formulated as follows:

$$Q_{min}: c^T x + \frac{1}{2}x^T Qx \quad \text{subject to} \quad \begin{cases} Ax \leq b \\ x \geq 0 \end{cases} \quad (40)$$

where $A \in R^{m \times n}$ and $B \in R^m$. The standard form of QP can be solved by employing the optimality conditions of Karush-Kuhn-Tucker (KKT) that we derived to handle the constrained optimization. Thereafter, the Lagrangian function for Q can be given per below:

$$L(x, y, z) = c^T x + \frac{1}{2}x^T Qx + y^T(Ax - b) - z^T x \ \text{ subject to } \begin{cases} y \geq 0 \\ z \geq 0 \end{cases} \quad (41)$$

The optimality conditions of KKT can be expressed in the following order:

$$\begin{cases} (I) Ax \leq b \ and \ x \geq 0 \\ (II) y \geq and \ z \geq 0 \\ (III) y^T(Ax - b) = 0 \ and \ z^T x = 0 \\ (IV) \nabla_x L(x, y, z) = Qx + c + A^T y - z = 0 \end{cases} \quad (42)$$

The conditions I, II, II and IV express the primal feasibility, dual feasibility, complementarity conditions and stationarity conditions, respectively. In order to reduce the complexity of the conditions, it is possible to rewrite the condition (IV) in order to omit the variable *z* through to $z = Qx + c + A^T y$.

c = is an n-dimensional row vector describing the coefficients of the linear terms in the objective function

Q = is an $(n \times m)$ symmetric maxtrix describing of the quadratic terms.

x = the vector of decision variables of n-dimension column

A = linear equality constraint matrix

b = linear inequality constraint vector

$f(x)$ = strictly convex objective function for all the feasible points of the problem that has an unique local minimum

y = nonnegative surplus variables ($y \in R^n$)

z = nonnegative slack variables ($z \in R^m$)

In this way, minimum diesel loading, optimum power output and minimum production cost of assigned load to each diesel generators will be obtained. The purpose of finding minimum diesel loading which will be applied to the next step is to prevent not only frequent switching on and off of the generators but also enforce them to work above or close to their minimum. The main reason of considering different time resolutions in this section is to overcome the intra-hour occurrence of intermittent and volatile generation, which will be considered in to the next section, as well as maintaining the system reliability while the highest penetration level of renewable generation can be injected to the grid.

4.3.2 Diesel UC and ED incorporating wind and PV power

The presence of PV and wind energies with their natural intermittency aside from the load demand fluctuation, arise economic and reliability problems on the grid. It is costly to keep the diesel units online to reach a reliable system while the load is fluctuating. Conversely, the system becomes more unreliable when penetration of the PV and wind is very high just to have savings on fuel cost. Due to natural intermittency and unpredictability of the wind and PV power which both occur at multiple timescales (time resolution and time horizon) [21], more practical constraints and additional reserves are needed to have a system with a high level of reliability. For this reason, additional constraints such as minimum diesel loading (equation (24)) and ramp rates (equations (25) and (26)) should be taken into consideration. The variability and uncertainty of the renewable generation cannot be captured in an hourly calculation, and this leads to improper scheduling of thermal generators and underestimation of the production cost, as such an intra-hour calculation is essential. In this step, the optimum power output $P_{D_i}(t)$ that revealed from QP calculation and the minimum power output will be used as upper and lower bounds to find the linear production cost function. The concept of linearization is based on [14] with the difference that $P_{D_i}(t)$ in our study is changing at each stage based on optimum position and is shown in Fig 4.4.

$$F_t^p = A_0 + \sum_{k=1}^{K} B_k l_{kt} \ , \qquad \forall t \tag{43}$$

where F_t^p, A_0 and B_k are production cost, constant and linear coefficients of the unit production cost in the k^{th} segment of the piecewise linear approximation and l_{kt} is the corresponding generation variables. They have the following limitations:

$$l_{kt} \leq P_{D_i}(t) - P_{D_i}^{min}(t), \forall t, \forall k \tag{44}$$

The equation defining the total generation as sum of generation at each segment is also required:

$$P_{D_i}(t) = P_{D_i}^{min}(t) + \sum_{k=1}^{K} l_{kt}, \forall t \tag{45}$$

This approximation is always greater or equal to the quadratic approximation and is called upper piecewise linear approximation. Again, ELD will be performed linearly to re-dispatch the *Net-Load* (see equation (9)) to the committed diesel units with different time resolutions of 5, 10, 15, 30 and 60 min. In other words, the states of the diesel generators which obtained from the previous step will remain constant in the next step.

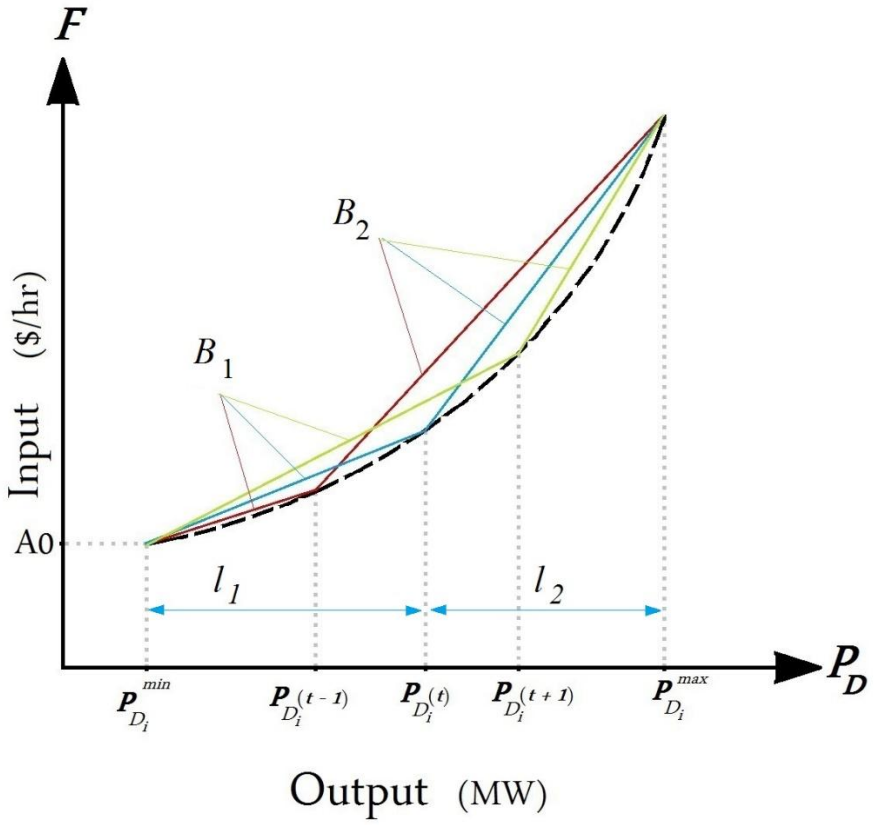

Fig. 4.4 Approximation (solid) of the quadratic cost function (dashed) vs. power output

4.3.3 Modelling choices and input data

4.3.3.1 Diesel generator model

The diesel generator has a speed and power control mechanism that can follow the load. The fuel consumption curve of the proposed diesel unit is a convex curve and is shown in Fig. 4. Equation (4) shows the production cost of the i^{th} diesel generator at duration t. The characteristics of ten-unit diesel generators which is used in Case Study 1 are derived from [22] while generators' data of Case Study 2 are taken from [13].

4.3.3.2 Wind energy model

The type of WT considered is variable-pitched and has an induction generator. Wind power curve was approximated as linear function of the wind speed. Hourly wind speed data, accessible from HOMER (a free optimization model for distributed power system introduced by U.S National Renewable Energy Laboratory (NREL) [23]) is converted into its corresponding wind power using the performance curve of the proposed WT and equation (35). Wind power curve constraints are [4]:

$$P_{W_j}^{*}(t) = \begin{cases} 0, & V(t) \le V_{I_j}, V(t) > V_{O_j} \\ \Phi_j\big(V(t)\big), & V_{I_j} < V(t) \le V_{R_j} \\ P_{W_j}^{max}(t), & V_{R_j} < V(t) \le V_{O_j} \end{cases} \tag{46}$$

In equation (31), $\Phi_j\big(V(t)\big)$ is wind power output and usually approximated by a linear or quadratic function of $V(t)$, $P_{W_j}^{max}(t)$ is the maximum wind generator power output and V_{I_j}, V_{R_j}, V_{O_j} are the wind generator cut-in, rated and cut-out wind speeds, respectively. In this case, linear least square approximation method is utilized to find the power output of the WTs in hourly and sub-hourly basis [24]. The relationship between the wind speed and power output of the turbine is presented by wind turbine power curve which are mainly used in planning, forecasting, performance monitoring and control of the wind turbines and provided by wind turbine manufacturers [25]. The power output can be controlled to any desired value through blade pitch control. The performance curve of the Enercon E33-330 which is used in Case Study 1 is shown in Fig 4.5 [4].

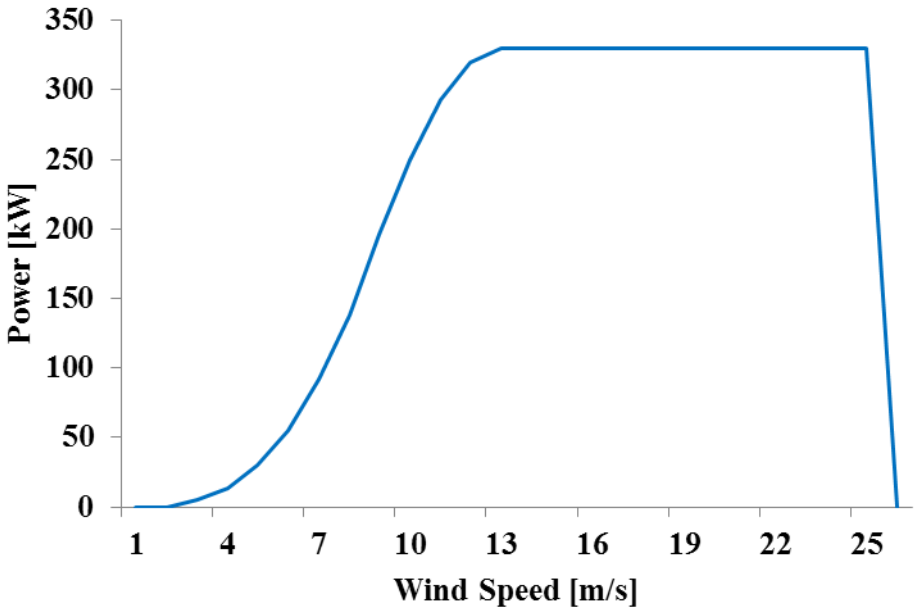

Fig. 4.5 Performance curve of the Enercon 330 turbine

4.3.3.3 Photovoltaic Cell Model

The Photovoltaic (PV) power curve is a function of radiation and temperature as depicted in Fig 4.6 and can be calculated by means of equation (36). The relationship is non-linear, but for practical purposes the linearized relationship can be used. The characteristics of the PV cell are the same as in research which has been done by M.K.C. Marwali et al. [12].

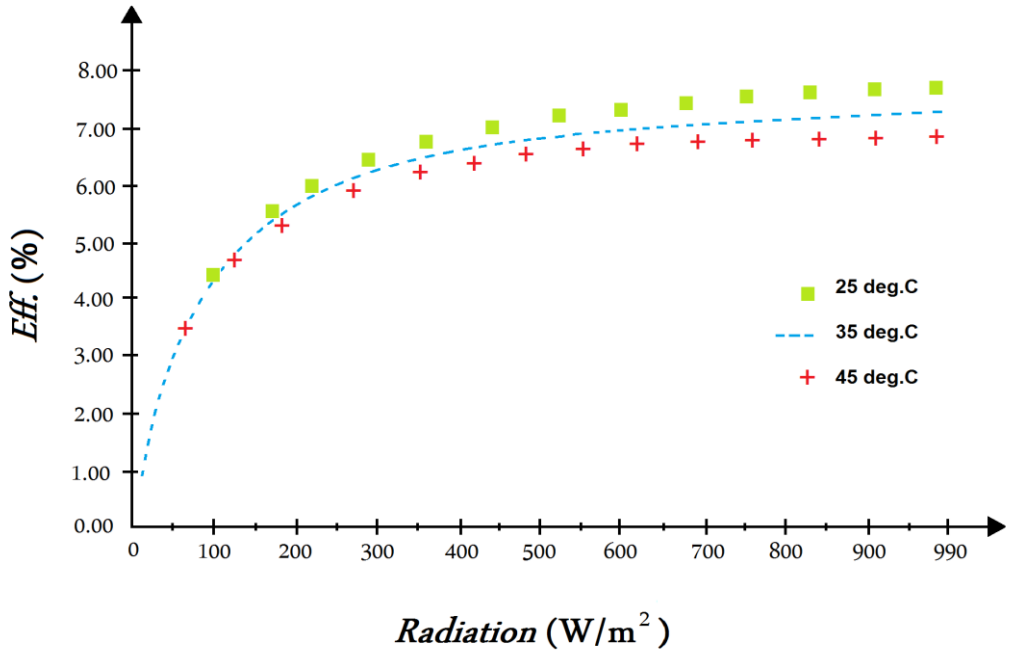

Fig. 4.6 PV efficiency vs. radiation

PV power curve constraints are [12]:

$$P_{PV}^{*}(t) = \begin{cases} \frac{\eta_c}{K_c}({G_t}^2), & 0 < G_t < K_c \\ \eta_c G_t, & G_t > K_c \end{cases} \quad (47)$$

where $K_c\left(\frac{W}{m^2}\right)$, $G_t\left(\frac{W}{m^2}\right)$ and η_c are the certain radiation point, forecasted radiation and corresponding efficiency, respectively.

$$P_{PV}^{*}(t) = f\big(G_t(t),\, T_c(t)\big), \quad t = 1,2,\dots,To \quad (48)$$

where $T_c(t)$ is the ambient temperature.

4.4 Numerical experiments

To demonstrate the capability of the proposed algorithm, two cases as benchmarks were studied. Case test system one comprises of 10 Diesel generators [22], one PV power plant [12] which was limited to 100kW and three 330kW WTs. Ramp rate limits for both up and down were considered as 60% of maximum rated power and spinning reserve level was assumed to be 10% of the hourly load [3]. Case test system two considers an IEEE 118-bus test system [13] with 54 units, two PV power plants limited to 500MW and two wind farms limited by a maximum power output of 2400MW and spinning reserve level of 10% of the hourly load [13]. The hourly solar radiation (taken from HOMER) and its corresponding power output for case one is given in Table 4.2. The hourly wind speed data obtained from HOMER was then converted to its corresponding wind power using the Linear least square method and performance curve of the proposed WT [24]. Table 4.3 depicts the wind speed data and its corresponding power output of one WT of case one.

In this study, it was assumed that renewable power generators are owned by the public utility who wants to determine the renewable capacity that can be incorporated into the system. The basic requirement of this scenario was to achieve the maximum fuel saving and guarantee a reliable power supply. The generation cost of the renewable power from the public utility was the cheapest because it needs no fuel and there was no fuel cost. It should be noted that the conditions and constraints which have been applied in all methods to make such comparison were exactly the same as benchmark references ([13] and [22] as benchmarks) which data derived from.

Table 4.2 Solar radiation and corresponding power data

Hour	G(W/m^2)	Power(kW)	Hour	G(W/m^2)	Power(kW)
1	0	0	13	834	69.5
2	0	0	14	586	34.3
3	0	0	15	554	30.7
4	0	0	16	551	30.4
5	0	0	17	305	9.3
6	5	0	18	138	1.9
7	113	1.3	19	7	0
8	278	7.7	20	0	0
9	553	30.6	21	0	0
10	760	57.8	22	0	0
11	889	79	23	0	0
12	901	81.2	24	0	0

Table 4.3 Hourly wind speed and wind power data

Hour	Speed(m/s)	Power(kW)	Hour	Speed(m/s)	Power(kW)
1	2.4	0	13	7.9	135.1
2	4.47	25.8	14	8.1	143.5
3	4.89	28.2	15	7.6	119.8
4	5.1	32.4	16	7.3	104.2
5	5.79	50	17	6.9	88.5
6	7.43	112	18	8.3	155.6
7	6.93	89.5	19	9.2	208.8
8	8.12	144	20	8.8	185.6
9	7.34	107.6	21	9.6	226.4
10	5.17	34.2	22	6.4	68.6
11	5.75	48.9	23	4.6	23.3
12	6.23	63.6	24	3.1	5.9

4.4.1 Case study 1: Ten-unit thermal system UC and ELD with and without WT and PV power plants

In first case study, hourly and sub-hourly UC and ELD were performed for a period of one day. The hourly load distribution over 24-hour time horizon and generation units' data are given in Tables 4.4 and 4.5. Table 4.6 depicts an hourly basis comparison which has been made among DP with complete enumeration (DP-CE) [16], DP with PL order based on full load average cost (DP-FA) [15], DP-BP and the reference [22] which data obtained from. Tables 4.7 and 4.8 present the units' output powers for 24-hour time horizon without and with renewable power, respectively. Results show that DP-BP achieved better solution than DP-FA in terms of computation time and production cost.

Table 4.4 Load demand of 10-unit base problem

Hour	1	2	3	4	5	6
Load[kW]	2000	1980	2000	1900	1840	1870
Hour	7	8	9	10	11	12
Load[kW]	1820	1700	1510	1410	1320	1260
Hour	13	14	15	16	17	18
Load[kW]	1200	1160	1140	1160	1260	1380
Hour	19	20	21	22	23	24
Load[kW]	1560	1700	1820	1900	1950	1990

Table 4.5 Diesel unit characteristics of 10-unit base problem

Unit	1	2	3	4	5	6	7	8	9	10
Pmin[kW]	10	20	30	25	50	75	120	125	250	250
Pmax[kW]	60	80	100	120	150	280	320	445	520	550
Coef_A[$]	15	25	40	32	29	72	49	82	105	100
Coef_B[$/kWhr]	2.2034	1.9161	1.8518	1.6966	1.8015	1.5354	1.2643	1.2163	1.1954	1.1285
Coef_C[$/kW^{2}hr]	0.0051	0.004	0.0039	0.0038	0.0021	0.0026	0.0029	0.0015	0.0013	0.0014
Min up[hr]	3	3	2	3	3	6	8	10	12	12
Min down[hr]	2	5	2	2	2	6	2	5	7	3
Cold start cost[$]	10	12	12	13	11	18	13	15	14	20
Hot start cost[$]	4500	5000	550	560	900	170	260	30	30	30
Cold start[hr]	5	5	4	4	4	2	2	0	0	0
Ini status[hr]	-20	-20	-20	10	10	10	10	20	20	20
Ramp up[kW]	50	60	70	80	100	200	200	300	200	200
Ramp down[kW]	50	60	70	80	100	200	200	300	200	200

Table 4.6 Comparison of hourly results of various DP-UC for 10-Diesel case

UC	DP-CE	DP-BP	DP-FA	Ref. [22]
FC [$]	79043	79050	79165	79169
Time [s]	1066	0.4	4.3	6.92

Table 4.7 10-Diesel system initial UC and ELD power [kW]

Unit	Hour 1 to 24																							
	1	2	3	4	5	6	7	8	9	10	11	12	13	14	15	16	17	18	19	20	21	22	23	24
1	0	0	0	0	0	0	0	0	0	0	0	0	0	0	0	0	0	0	0	0	0	0	0	0
2	0	0	0	0	0	0	0	0	0	0	0	0	0	0	0	0	0	0	0	0	0	0	0	0
3	0	0	0	0	0	0	0	0	0	0	0	0	0	0	0	0	0	0	0	0	0	0	0	0
4	96	95	96	89	97	100	96	0	0	0	0	0	0	0	0	0	0	0	0	72	96	89	93	96
5	149	146	149	136	150	150	148	144	114	0	0	0	0	0	0	0	0	0	90	133	148	136	142	147
6	172	170	172	161	0	0	0	0	0	0	0	0	0	0	0	0	0	0	0	0	0	161	167	171
7	202	200	202	193	204	207	201	198	177	179	166	158	150	145	142	145	159	175	187	190	201	193	197	201
8	411	407	411	392	413	421	409	404	361	365	341	325	309	299	294	299	325	357	381	388	409	392	402	409
9	487	483	487	466	490	498	485	479	429	433	406	387	369	356	350	356	387	424	452	460	485	466	476	485
10	483	479	483	463	486	494	481	475	429	433	407	390	372	360	354	360	389	424	450	457	481	463	473	481
Final Cost = $79050																								

Table 4.8 10-Diesel system UC and ELD power output [kW] incorporating renewable power plants

Unit	Hour 1 to 24																							
	1	2	3	4	5	6	7	8	9	10	11	12	13	14	15	16	17	18	19	20	21	22	23	24
1	0	0	0	0	0	0	0	0	0	0	0	0	0	0	0	0	0	0	0	0	0	0	0	0
2	0	0	0	0	0	0	0	0	0	0	0	0	0	0	0	0	0	0	0	0	0	0	0	0
3	0	0	0	0	0	0	0	0	0	0	0	0	0	0	0	0	0	0	0	0	0	0	0	0
4	96.3	89.4	90.3	782.2	85.3	72.9	74.3	0	0	0	0	0	0	0	0	0	0	0	0	41.7	41.5	74.5	87.8	94.3
5	149	136.3	137.9	123.4	129	106.7	109.1	76	63.8	0	0	0	0	0	0	0	0	0	50	50.4	50.1	109.5	133.4	145.3
6	172	161.7	163	151.2	0	0	0	0	0	0	0	0	0	0	0	0	0	0	0	0	0	139.9	159.3	169
7	202	192.9	194.1	183.5	187.6	171.2	173	148.7	139.7	164.7	146.6	132.4	120	120	120	120	122.2	120	120	129.9	129.7	173.3	190.8	199.5
8	411	392.9	395.3	374.5	382.5	350.5	353.9	306.6	289.1	337.7	302.3	274.7	174.7	125	160	210.5	254.9	230.7	221.6	125	269.4	354.5	388.8	405.8
9	487	466.1	468.9	444.7	454	416.7	420.7	365.6	345.1	401.8	360.5	328.3	250	250	250	253.6	305.3	277	266.5	269.9	322.2	421.4	461.3	481.1
10	483	63.3	465.9	443.1	452	416.8	420.5	368.6	349.4	402.8	363.9	333.7	250	250	250	263.3	312	285.4	275.5	322.8	327.9	421.2	458.8	477.4
IG	0	77.7	84.7	97.3	149.5	335.1	268.5	434.7	322.9	103	146.7	191	405.3	415	359.4	312.5	265.6	466.9	626.3	556.7	679.1	205.8	69.8	17.7
IG= Intermittent Generation													Final cost = $64846.8											

Fig 4.7 and 4.8 show the hourly diesel contribution for a 24-hour of time horizon without and with wind and PV power, respectively. Comparing these two figures, it can be seen that diesel generators status (only online generators), maximum and minimum generations were exactly the same which means that the minimum diesel loading and ramp rate limits were satisfied. The maximum generation capacity remained constant and has covered demand load and the required reserve before and after integrating renewable energies.

The level of available reserve has increased when demand load decreased and vice versa. Fig 4.7 and 4.9 illustrate the hourly available and required reserves for a 24-hour of time horizon before and after renewable energies injection, respectively and it can be seen that available reserve covers the amount of required reserve. Comparing trends of Fig 4.6 and 4.7 the much renewable power injected the much available and required reserves are achieved.

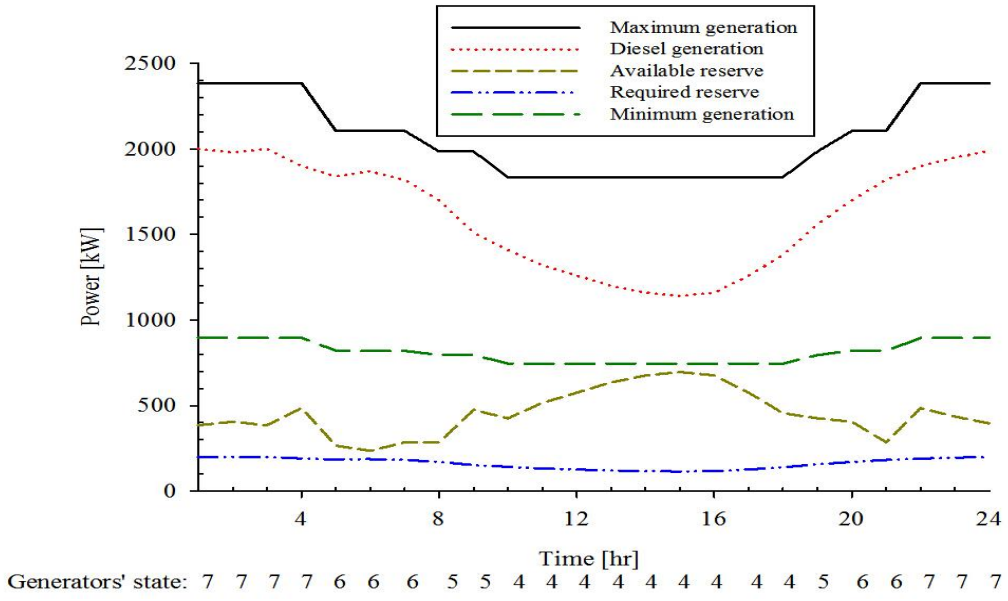

Fig. 4.7 Hourly generators' behaviour and required reserve

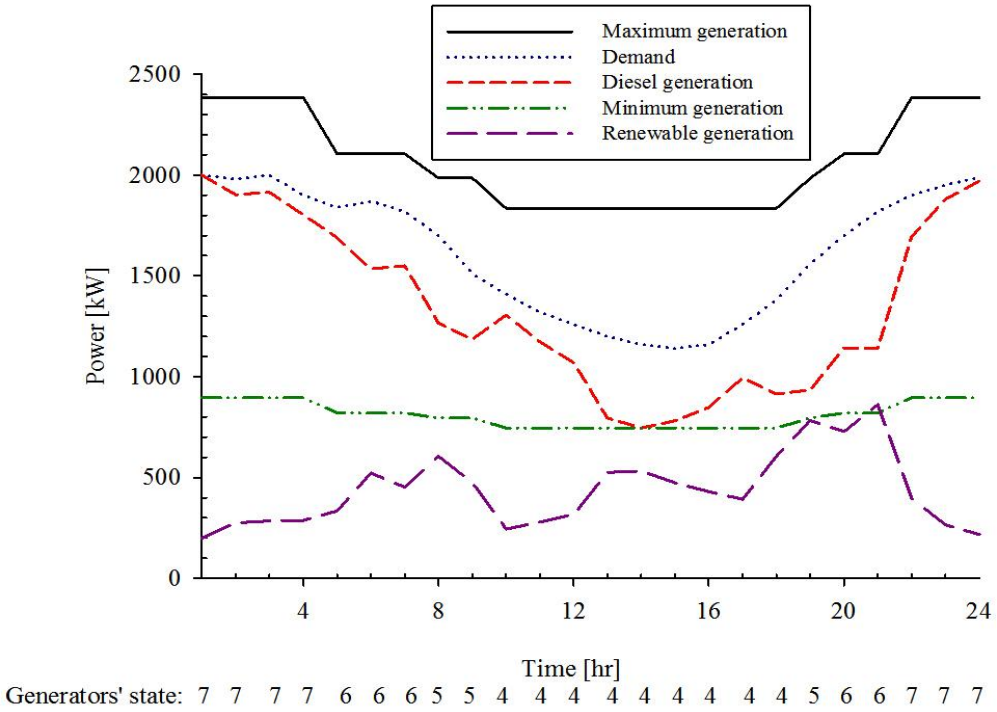

Fig. 4.8 Hourly contributions of diesel and renewable power plants

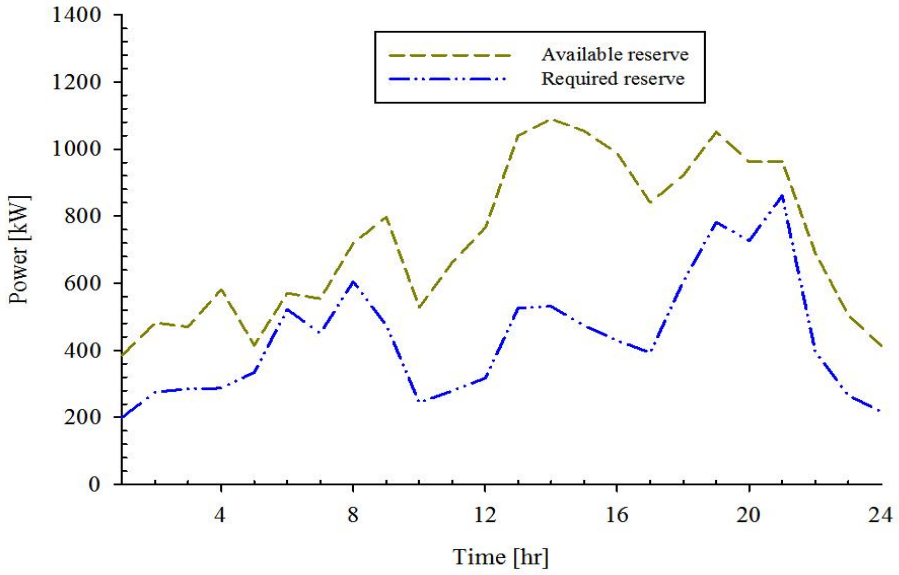

Fig. 4.9 Comparison of hourly available and required spinning reserves after applying renewable power

Table 4.9 shows a brief overview of production cost with and without wind and PV power plants at different time resolutions. It is noted that higher time resolution has higher production cost compared to an hourly time resolution which means intermittency and volatility of renewable energies can be captured by running UC and ELD at a higher time resolution. The initial UC-ELD

cost and re-dispatched cost (considering renewable) difference between 60 and 5 min is about 0.7% and 1.8%, respectively which indicates that generators' status will change with higher time resolution. In other words, more start up and shut down would occur in the case of involvement of different time resolutions into UC and ELD. Table 4.10 depicts a comparison of the mean value of available and required spinning reserves at different time resolutions for a 24-hour of time horizon before and after concerning intermittent generations. It can be seen that the level of available reserve will increase by increasing the time resolution despite that the level of required spinning reserve was constant.

Table 4.9 Total production costs of various time resolutions with and without renewable power

	60 min Resolution	30 min Resolution	15 min Resolution	10 min Resolution	5 min Resolution
FC without renewable power [$]	79050	79067	79066	79066	79613
FC with renewable power [$]	64847	64645	65393	64951	66041

Table 4.10 Comparison of available and required reserves' mean values with and without renewable power

	60 min Resolution	30 min Resolution	15 min Resolution	10 min Resolution	5 min Resolution
Available reserve before renewable power [kW]	452	455	458	459	551
Required reserve before renewable power[kW]	161.8	161.8	161.8	161.8	161.8
Available reserve after renewable power[kW]	727	727	721	731	816
Required reserve after renewable power[kW]	436	439	427	434	427

4.4.2 Case study 2: IEEE 118-Bus test system thermal system UC and ELD with and without WT and PV power plants

In this case, in order to demonstrate the capability and robustness of the proposed method, DP-BP was implemented to schedule the components of IEEE 118-Bus Test System which was taken from reference [13] for a 24-hour period. In this section, for simplicity and better understanding of the method time resolution with 60, 30, and 5 min has been considered. Table 4.11 compares this study with reference [13] and it is shown that computation time of these two are the same but the production cost of our method is about 0.7% cheaper than reference [13] for a 24-hour of time horizon while the considered conditions are exactly the same for both studies. Tables 4.12 and 4.13 list the units' output powers for 24-hour time horizon before and after integrating renewable power, respectively.

Table 4.11 Comparison of hourly results of DP-BP and [13] for IEEE 118-bus case

UC	DP-BP	Ref. [13]
FC [$]	1632000	1643000
Time [s]	6.3	6.5

Table 4.12 IEEE 118-bus test system initial UC and ELD power output [MW]

Unit	Hour 1 to 24																							
	1	2	3	4	5	6	7	8	9	10	11	12	13	14	15	16	17	18	19	20	21	22	23	24
3-1	0	0	0	0	0	0	0	0	0	0	0	0	0	0	0	0	0	0	0	0	0	0	0	0
4	201	179	150	150	150	150	201	255	260	277	281	263	242	212	269	275	260	272	286	296	300	273	264	213
5	201	179	133	100	100	146	201	255	260	277	281	263	242	212	269	275	260	272	286	296	300	273	264	213
6	0	0	0	0	0	0	0	0	0	0	0	0	0	0	0	0	0	0	0	0	0	0	0	0
7	0	0	0	0	0	0	0	25	28	43	46	31	25	25	36	41	29	38	51	59	63	39	32	0
9-8	0	0	0	0	0	0	0	0	0	0	0	0	0	0	0	0	0	0	0	0	0	0	0	0
10	201	179	133	100	100	146	201	255	260	277	281	263	242	212	269	275	260	272	286	296	300	273	264	213
11	350	350	350	314	350	350	350	350	350	350	350	350	350	350	350	350	350	350	350	350	350	350	350	350
13-12	0	0	0	0	0	0	0	0	0	0	0	0	0	0	0	0	0	0	0	0	0	0	0	0
14	0	0	0	0	0	0	0	25	28	43	46	31	25	25	36	41	29	38	51	59	63	39	32	0
15	0	0	0	0	0	0	0	0	0	0	0	0	0	0	0	0	0	0	0	0	0	0	0	0
16	0	0	0	0	0	0	0	0	28	43	46	31	25	25	36	41	29	38	51	59	63	39	32	0
18-17	0	0	0	0	0	0	0	0	0	0	0	0	0	0	0	0	0	0	0	0	0	0	0	0
19	0	0	0	0	0	0	0	0	28	43	46	31	25	25	36	41	29	38	51	59	63	39	32	0
20	250	250	250	125	250	250	250	250	250	250	250	250	250	250	250	250	250	250	250	250	250	250	250	250
21	250	250	250	125	250	250	250	250	250	250	250	250	250	250	250	250	250	250	250	250	250	250	250	250
22	0	0	0	0	0	0	0	0	28	43	46	31	25	25	36	41	29	38	51	59	63	39	32	0
23	0	0	0	0	0	0	0	0	28	43	46	31	25	25	36	41	29	38	51	59	63	39	32	0
24	200	200	200	100	150	200	200	200	200	200	200	200	200	200	200	200	200	200	200	200	200	200	200	200
25	200	200	200	100	150	200	200	200	200	200	200	200	200	200	200	200	200	200	200	200	200	200	200	200
26	0	0	0	0	0	0	0	0	28	43	46	31	25	25	36	41	29	38	51	59	63	39	32	0
27	420	399	351	203	296	365	420	420	420	420	420	420	420	420	420	420	420	420	420	420	420	420	420	420
28	420	399	351	203	296	365	420	420	420	420	420	420	420	420	420	420	420	420	420	420	420	420	420	420
29	201	179	133	80	80	146	201	255	260	277	281	263	242	212	269	275	260	272	286	296	300	273	264	213
30	0	0	0	0	0	0	0	0	0	0	0	0	0	0	0	0	0	0	0	40	43	37	35	0
33-31	0	0	0	0	0	0	0	0	0	0	0	0	0	0	0	0	0	0	0	0	0	0	0	0
34	0	0	0	0	0	0	0	0	28	43	46	31	25	25	36	41	29	38	51	59	63	39	32	0
35	0	0	0	0	0	0	0	0	28	43	46	31	25	25	36	41	29	38	51	59	63	39	32	0
36	201	179	150	150	150	150	201	255	260	277	281	263	242	212	269	275	260	272	286	296	300	273	264	213
37	0	0	0	0	0	0	0	0	0	43	46	31	25	25	36	41	29	38	51	59	63	39	32	0
38	0	0	0	0	0	0	0	0	0	0	0	0	0	0	0	0	0	0	0	0	0	0	0	0
39	300	300	300	300	300	300	300	300	300	300	300	300	300	300	300	300	300	300	300	300	300	300	300	300
40	200	179	133	50	79	146	200	200	200	200	200	200	200	200	200	200	200	200	200	200	200	200	200	200
41	0	0	0	0	0	0	0	0	0	0	0	0	0	0	0	0	0	0	0	0	0	0	0	0
42	0	0	0	0	0	0	0	0	0	0	0	0	0	0	0	0	0	0	0	0	20	0	0	0
43	201	179	133	100	100	146	201	255	260	277	281	263	242	212	269	275	260	272	286	296	300	273	264	213
44	201	179	133	100	100	146	201	255	260	277	281	263	242	212	269	275	260	272	286	296	300	273	264	213

45	201	179	133	100	100	146	201	255	260	277	281	263	242	212	269	275	260	272	286	296	300	273	264	213
46	0	0	0	0	0	0	0	0	0	0	0	0	0	0	0	0	0	0	0	0	0	0	0	0
47	0	0	0	0	0	0	0	0	0	43	46	31	25	25	36	41	29	38	51	59	63	39	32	0
48	0	0	0	0	0	0	0	0	0	0	0	0	0	0	36	41	29	38	51	59	63	39	32	0
50-49	0	0	0	0	0	0	0	0	0	0	0	0	0	0	0	0	0	0	0	0	0	0	0	0
51	0	0	0	0	0	0	0	0	0	0	0	0	0	0	36	41	29	38	51	59	63	39	32	0
52	0	0	0	0	0	0	0	0	0	0	0	0	0	0	36	41	29	38	51	59	63	39	32	0
53	0	0	0	0	0	0	0	0	0	0	0	0	0	0	36	41	29	38	51	59	63	39	32	0
54	0	0	0	0	0	0	0	0	0	0	0	0	0	0	0	0	0	0	0	0	0	0	0	0
Final Cost $1632257																								

Table 4.13 IEEE 118-bus test system UC and ELD power output [MW] incorporating renewable power plants

Unit	Hour 1 to 24																							
	1	2	3	4	5	6	7	8	9	10	11	12	13	14	15	16	17	18	19	20	21	22	23	24
1-3	0	0	0	0	0	0	0	0	0	0	0	0	0	0	0	0	0	0	0	0	0	0	0	0
4	201	161	150	150	150	150	150	150	174	262	259	211	150	150	185	208	189	167	156	193	170	236	255	206
5	201	161	109	100	100	100	143	143	174	262	259	211	139	106	185	208	189	167	156	193	170	236	255	206
6	0	0	0	0	0	0	0	0	0	0	0	0	0	0	0	0	0	0	0	0	0	0	0	0
7	0	0	0	0	0	0	0	25	25	30	27	25	25	25	25	25	25	25	25	25	25	25	25	0
8-9	0	0	0	0	0	0	0	0	0	0	0	0	0	0	0	0	0	0	0	0	0	0	0	0
10	201	161	109	100	100	100	143	143	174	262	259	211	139	106	185	208	189	167	156	193	170	236	255	206
11	350	350	350	211	350	350	350	350	350	350	350	350	350	350	350	350	350	350	350	350	350	350	350	350
12-13	0	0	0	0	0	0	0	0	0	0	0	0	0	0	0	0	0	0	0	0	0	0	0	0
14	0	0	0	0	0	0	0	25	25	30	27	25	25	25	25	25	25	25	25	25	25	25	25	0
15	0	0	0	0	0	0	0	0	0	0	0	0	0	0	0	0	0	0	0	0	0	0	0	0
16	0	0	0	0	0	0	0	0	25	30	27	25	25	25	25	25	25	25	25	25	25	25	25	0
17-18	0	0	0	0	0	0	0	0	0	0	0	0	0	0	0	0	0	0	0	0	0	0	0	0
19	0	0	0	0	0	0	0	0	25	30	27	25	25	25	25	25	25	25	25	25	25	25	25	0
20	250	250	250	125	228	250	250	250	250	250	250	250	250	250	250	250	250	250	250	250	250	250	250	250
21	250	250	250	125	228	250	250	250	250	250	250	250	250	250	250	250	250	250	250	250	250	250	250	250
22	0	0	0	0	0	0	0	0	25	30	27	25	25	25	25	25	25	25	25	25	25	25	25	0
23	0	0	0	0	0	0	0	0	25	30	27	25	25	25	25	25	25	25	25	25	25	25	25	0
24	200	200	200	100	50	80.7	181	200	200	200	200	200	200	200	200	200	200	200	200	200	200	200	200	200
25	200	200	200	100	50	80.7	181	200	200	200	200	200	200	200	200	200	200	200	200	200	200	200	200	200
26	0	0	0	0	0	0	0	0	25	30	27	25	25	25	25	25	25	25	25	25	25	25	25	0
27	420	380	326	174	240	267	361	361	393	420	420	420	357	323	405	420	409	386	375	413	389	420	420	420
28	420	380	326	174	240	267	361	361	393	420	420	420	357	323	405	420	409	386	375	413	389	420	420	420
29	201	161	109	80	80	80	143	143	174	262	259	211	139	106	185	208	189	167	156	193	170	236	255	206
30	0	0	0	0	0	0	0	0	0	0	0	0	0	0	0	0	0	0	0	30	30	30	32	0
31-33	0	0	0	0	0	0	0	0	0	0	0	0	0	0	0	0	0	0	0	0	0	0	0	0
34	0	0	0	0	0	0	0	0	25	30	27	25	25	25	25	25	25	25	25	25	25	25	25	0
35	0	0	0	0	0	0	0	0	25	30	27	25	25	25	25	25	25	25	25	25	25	25	25	0
36	201	161	150	150	150	150	150	150	174	262	259	211	150	150	185	208	185	167	156	193	170	236	255	206
37	0	0	0	0	0	0	0	0	0	30	27	25	25	25	25	25	25	25	25	25	25	25	25	0
38	0	0	0	0	0	0	0	0	0	0	0	0	0	0	0	0	0	0	0	0	0	0	0	0
39	300	300	300	211	300	300	300	300	300	300	300	300	300	300	300	300	300	300	300	300	300	300	300	300
40	200	161	109	50	50	51.2	143	143	174	200	200	200	139	106	185	200	185	167	156	193	170	200	200	200
41	0	0	0	0	0	0	0	0	0	0	0	0	0	0	0	0	0	0	0	0	0	0	0	0
42	0	0	0	0	0	0	0	0	0	0	0	0	0	0	0	0	0	0	0	0	20	0	0	0
43	201	161	109	100	100	100	143	143	174	262	259	211	139	106	185	208	185	167	156	193	170	236	255	206
44	201	161	109	100	100	100	143	143	174	262	259	211	139	106	185	208	185	167	156	193	170	236	255	206
45	201	161	109	100	100	100	143	143	174	262	259	211	139	106	185	208	185	167	156	193	170	236	255	206
46	0	0	0	0	0	0	0	0	0	0	0	0	0	0	0	0	0	0	0	0	0	0	0	0
47	0	0	0	0	0	0	0	0	0	30	27	25	25	25	25	25	25	25	25	25	25	25	25	0
48	0	0	0	0	0	0	0	0	0	0	0	0	0	0	25	25	25	25	25	25	25	25	25	0
49-50	0	0	0	0	0	0	0	0	0	0	0	0	0	0	0	0	0	0	0	0	0	0	0	0
51	0	0	0	0	0	0	0	0	0	0	0	0	0	0	25	25	25	25	25	25	25	25	25	0
52	0	0	0	0	0	0	0	0	0	0	0	0	0	0	25	25	25	25	25	25	25	25	25	0
53	0	0	0	0	0	0	0	0	0	0	0	0	0	0	25	25	25	25	25	25	25	25	25	0
54	0	0	0	0	0	0	0	0	0	0	0	0	0	0	0	0	0	0	0	0	0	0	0	0
IG	0	0	218	250	383	823	666	1059	794	264	376	484	988	1049	880	770	660	1139	1557	1362	1718	519	183	50
IG= Intermittent Generation													Final Cost $1346806.6											

Hourly diesel contributions for a day of time horizon without and with wind and PV power are illustrated in Fig 4.10 and 4.11. As expected, diesel generators status, maximum and minimum generations are the same which means minimum diesel loading and ramp rate limits have been

respected. Fig 4.10 and 4.12 illustrate the hourly available and required reserves for a 24-hour of time horizon before and after considering intermittent generations, respectively.

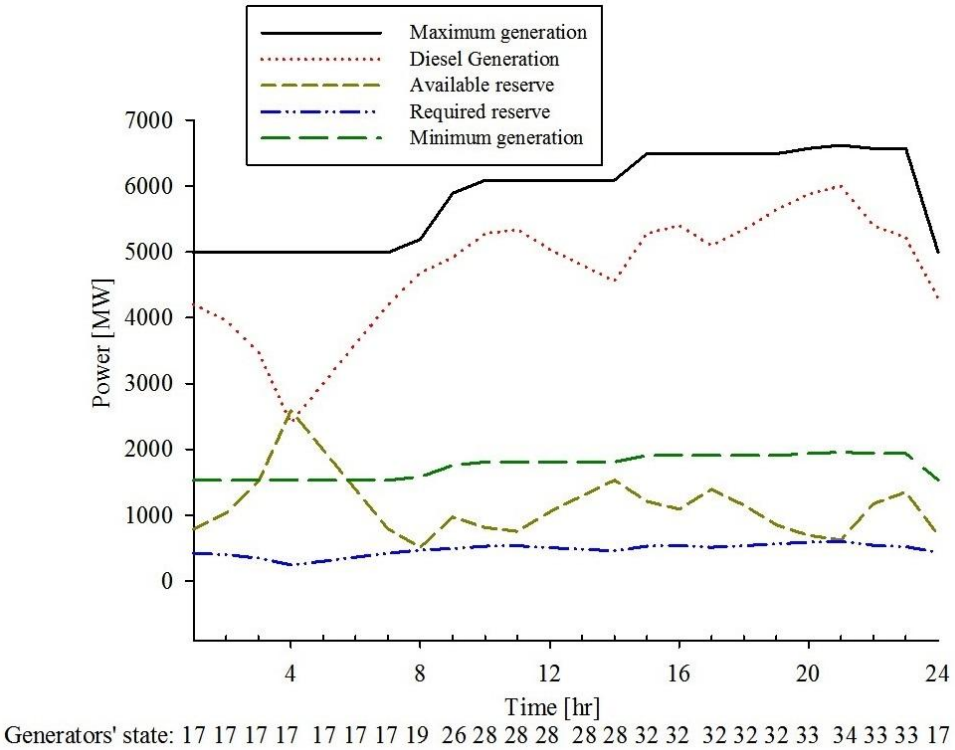

Fig. 4.10 Hourly generators' behaviour and required reserve

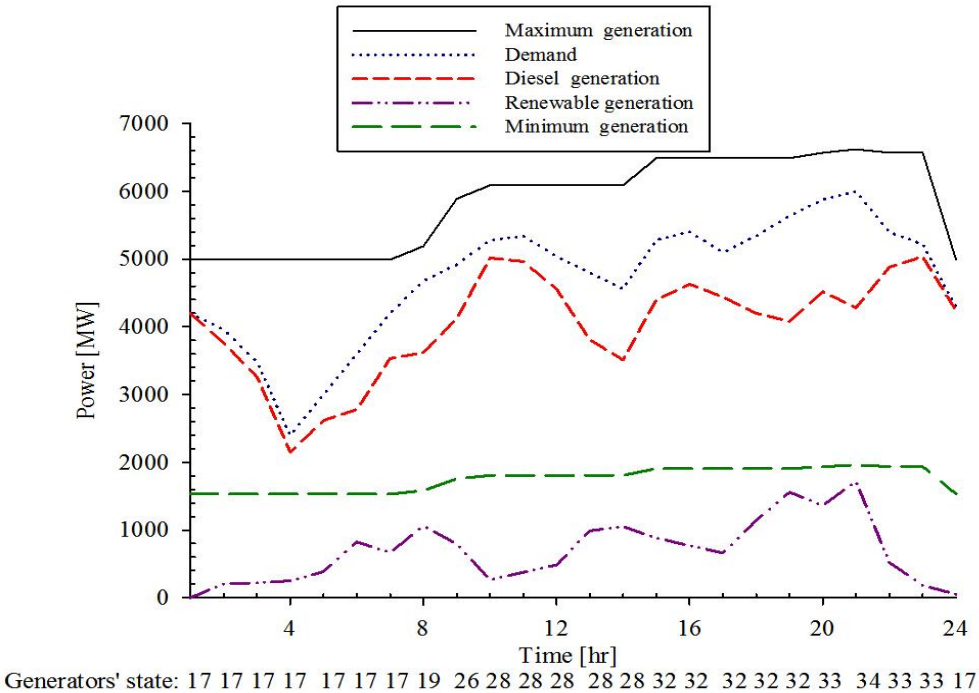

Fig. 4.11 Hourly contributions of diesel and renewable power plants

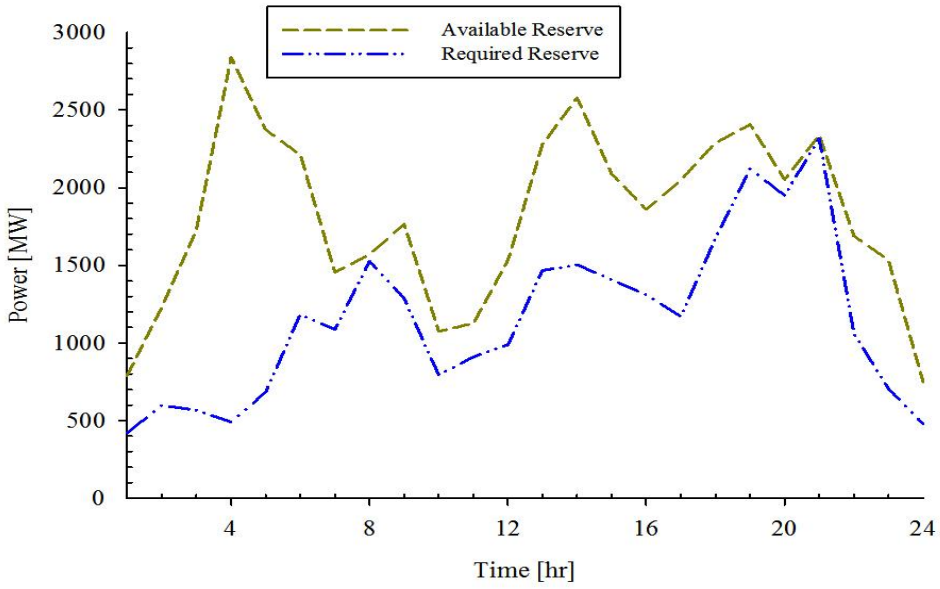

Fig. 4.12 Comparison of hourly available and required spinning reserves after applying renewable power

Table 4.14 demonstrates a brief overview of generation cost before and after incorporation of wind and PV power plants at different time resolutions. It can be observed that higher time resolution has higher production cost compared to an hourly time horizon which means uncertainty and unpredictability of intermittent generations can be captured by running UC and ELD in higher time resolution. The initial UC-ELD cost and re-dispatched cost (considering renewable) difference between 60 and 5 min is about 0.5% and 1%, respectively, which implies occurrence of more start up and shut down cost of the generators while UC and ELD is running in higher time resolutions closer to real time. Table 4.15 briefly compares the mean value of available and required spinning reserves at different time resolutions for a 24-hour of time horizon with and without integration of intermittent generations. From this case study it can be inferred that the amount of reserve tends to be reduced while time resolution is closer to real time. In other meanings, cost of reserve can be reduced if higher time resolution is applied to schedule the diesel generators.

Table 4.14 Total production costs of various time resolutions with and without renewable power

	60 min resolution	30 min resolution	5 min resolution
FC without renewable power [$]	1632257	1633171	1640762
FC with renewable power [$]	1346807	1341745	1360699

Table 4.15 Comparison of available and required reserves' mean values with and without renewable power

	60 min resolution	30 min resolution	5 min resolution
Available reserve before renewable power [MW]	1134	1100	939
Required reserve before renewable power [MW]	471	471	471
Available reserve after renewable power [MW]	1817	1793	1613
Required reserve after renewable power [MW]	1153	1169	1144

4.5 Conclusions

Starting from the formulation of the UC problem, an algorithm based on heuristic method was proposed to solve the UC and ELD integrated renewable sources such as wind and solar energies simultaneously. Priority listing (PL) order based on best per unit cost (BP) was applied to form the generators' order and involved in the dynamic programming (DP) to handle the UC and ELD. In order to implement UC-ELD in presence of intermittent generations more practical and operation constraints such as minimum diesel loading, ramp rate limits and spinning reserve are vital. For this reason, initial UC-ELD has run while ELD performed based on quadratic programming at each stage (60, 30, 15, 10, 5 min). After obtaining minimum diesel loading, renewable generations have been considered in to the ELD and at each stage *Net-Load* re-dispatched to the committed diesel units based on assumption of linearizing the production cost function.

To find out the capability of the suggested method two case studies have been investigated at different time resolutions (60, 30, 15, 10, 5 min) with and without considering intermittent generators. First, from the hourly initial UC-ELD, DP-BP found a better solution approach than two presented benchmarks from the simplicity of the formulation (refs. [13] and [22]) and DP based on full load average cost in terms of both accelerating the computation time and reaching less production cost simultaneously. Because of the natural intermittency and restrained predictability of the wind and solar powers, intra-hour time resolution aside from additional constraints should be taken into account to reach a compromise between system security and total production cost. After demonstrating the robustness of the proposed method, DP-BP has been fulfilled to schedule the diesel generators before and after concerning renewable energies at different time resolutions to investigate the behaviour of spinning reserve.

In this study, any certain renewable energy penetration factors were not discussed to limit the wind and solar powers. The only limitation is based on ramp rates and minimum diesel loading formulations which discussed in problem formulation. As seen from the results, maximum penetrations for cases 1 and 2, are almost 40% and 29% of the instantaneous load at hours19 and 21, respectively (Figs. 8 and 11). This amount of penetration was obtained while constraints considered in this research were satisfied. In some hours, the algorithm curtailed the renewable power (dumping power) to the limited amount which achieved maximum penetration of instantaneous load. Nevertheless, higher penetration will affect the power quality and stability. In this manner, dumping load such as machines is one of the solutions, while another one could be dumping power, which is used in this research.

The results of these cases revealed that, UC and ELD should be implemented in higher time resolution to overcome the intra-hour occurrence of intermittent and volatile generations while having a system with high level of reliability and penetration level of renewable generation. Available spinning reserve was increased by increasing the penetration of wind and solar power. These increases were followed by the amount of renewable power and did not exceed the available amount (maximum power output minus operated power). It also has been seen, that in our second case study, which is robust and strong in terms of load and generation, the amount of spinning reserve has been decreased with higher time resolution closer to real time UC. To generalize this, less reserve cost of a robust and strong grid with strong load will be the result of running the UC-ELD in higher time resolution closer to real-time.

4.6 References

[1] E. Cutter, B. Haley, J. Hargreaves et al., “Utility scale energy storage and the need for flexible capacity metrics,” *Applied Energy*, vol. 124, pp. 274-282, Jul 1, 2014.

[2] Z. Zhu, Optimization of Power System Operation, Canada: Wiley and Sons, Inc, 2009.

[3] T. Senjyu, S. Chakraborty, A. Y. Saber et al., "Thermal unit commitment strategy with solar and wind energy systems using genetic algorithm operated particle swarm optimization.” *2nd IEEE International Conference on Power and Energy*, pp. 866 – 871.

[4] C. L. Chen, S. C. Hsieh, T. Y. Lee et al., “Optimal integration of wind farms to isolated wind-Diesel energy system,” *Energy Conversion and Management*, vol. 49, no. 6, pp. 1506-1516, Jun, 2008.

[5] J. H. Wang, M. Shahidehpour, and Z. Y. Li, “Security-constrained unit commitment with volatile wind power generation,” *IEEE Transactions on Power Systems*, vol. 23, no. 3, pp. 1319-1327, Aug, 2008.

[6] N. Troy, D. Flynn, and M. O’Malley, "The importance of sub-hourly modeling with a high penetration of wind generation.", *IEEE Power and Energy Society General Meeting*, pp. 1-6.

[7] N. Navid, and G. Rosenwald, “Market Solutions for Managing Ramp Flexibility With High Penetration of Renewable Resource,” *IEEE Transactions on Sustainable Energy*, vol. 3, no. 4, pp. 784-790, Oct, 2012.

[8] E. Ela, and M. O'Malley, “Scheduling and Pricing for Expected Ramp Capability in Real-Time Power Markets,” *IEEE Transactions on Power Systems*, vol. 31, no. 3, pp. 1681-1691, May, 2016.

[9] J. D. Wang, J. H. Wang, C. Liu et al., “Stochastic unit commitment with sub-hourly dispatch constraints,” *Applied Energy*, vol. 105, pp. 418-422, May, 2013.

[10] J. P. Deane, G. Drayton, and B. P. O. Gallachoir, “The impact of sub-hourly modelling in power systems with significant levels of renewable generation,” *Applied Energy*, vol. 113, pp. 152-158, Jan, 2014.

[11] C. O'Dwyer, and D. Flynn, “Using Energy Storage to Manage High Net Load Variability at Sub-Hourly Time-Scales,” *IEEE Transactions on Power Systems*, vol. 30, no. 4, pp. 2139-2148, Jul, 2015.

[12] M. K. C. Marwali, H. L. Ma, S. M. Shahidehpour et al., “Short term generation scheduling in photovoltaic-utility grid with battery storage,” *IEEE Transactions on Power Systems*, vol. 13, no. 3, pp. 1057-1062, Aug, 1998.

[13] S. H. Hosseini, A. Khodaei, and F. Aminifar, “A novel straightforward unit commitment method for large-scale power systems,” *IEEE Transactions on Power Systems*, vol. 22, no. 4, pp. 2134-2143, Nov, 2007.

[14] J. Sumbera, Modelling generator constraints for the self-scheduling problem, University of Economics. Prague Technical Report, Econometrics and Operational Research, 2011.

[15] F. Katiraei, and C. Abbey, "Diesel plant sizing and performance analysis of remote wind-diesel microgrid." *IEEE Power and Energy Society General Meeting*, pp. 1-8.

[16] A. J. Wood, and B. F. Wollenberg, Power generation, operation and control, 2nd ed., New York: Wiley, 1996.

[17] J. H. Park, S. K. Kim, G. P. Park et al., "Modified dynamic programming based unit commitment technique." IEEE Power and Energy Society General Meeting, pp. 1-7.

[18] C. S. Wang, Y. Zhou, J. D. Wang et al., “A novel Traversal-and-Pruning algorithm for household load scheduling,” *Applied Energy*, vol. 102, pp. 1430-1438, Feb, 2013.

[19] A. Goudarzi, and S. A. K., "Comparison of evolutionary optimization techniques on economic load dispatch with transmission line constraints." *South African Universities Power Engineering Conference*, pp. 212-217.

[20] P. Boggs, and J. Tolle, “Sequential quadratic programming,” *Acta Numer*, vol. 4, no. 1, pp. 1-51, 1996.

[21] M. Huber, D. Dimkova, and T. Hamacher, “Integration of wind and solar power in Europe: Assessment of flexibility requirements,” *Energy*, vol. 69, pp. 236-246, May 1, 2014.

[22] C. L. Chen, and S. C. Wang, “Branch-and-Bound Scheduling for Thermal Generating-Units,” IEEE Transactions on Energy Conversion, vol. 8, no. 2, pp. 184-189, Jun, 1993.

[23] HOMER, "The optimization model for distributed power getting started guide v2.0," U. N. R. E. Laboratories, ed., 2003.

[24] M. Kazemi, and A. Goudarzi, “A Novel method for estimating wind turbines power output based on least square approximation,” *International Journal of Engineering and Advanced Technology*, vol. 2, no. 1, pp. 97-101, 2012.

[25] A. Goudarzi, I. E. Davidson, A. Ahmadi et al., "Intelligent analysis of wind turbine power curve." *IEEE Symposium Series on Computational Intelligence*, pp. 1-7.

5. CHAPTER 5
Conclusion

5.1 Conclusions

The work presented in this thesis investigated several complex concerns for the real-time energy management, system operation, and reserve requirement services in deregulated power systems. The work contributed to and developed improvements to the operational tools for electricity markets and power systems operators from different perspectives as follows:

The first part of the work focused on the development of a method for the CEED problem and used a more accurate and optimal solution over other existing methods. Four optimisation algorithms based on the concept of culture algorithm were proposed, where the solution considered several physical constraints of generation units. The main conclusions of this study were as follows:

- The third version of proposed cultural algorithm (CA3) was the most efficient version in comparison to the other proposed versions.
- The results confirmed the superiority of CA3 in finding the optimal solutions in comparison to the other studied optimisation algorithms.
- The results demonstrated the fast convergence of CA3 in the solution space in comparison to the other algorithms.
- The Min-Max price penalty factors delivered the minimum total generation cost for conversion of multi-objective CEED problem to a single-objective CEED problem.

The second part of the work concentrated on finding a smart solution of real-time CEED problem by the precise prediction of generator schedules, instead of solving the CEED problem for a large interconnected power system which requires a long computation time. The proposed method was based on the combination of least square support vector machine and the third version of cultural algorithm (LSSVM-CA3). The main conclusions of this study were as follows:

- A hybrid formulation (LSSVM-CA3) for real-time scheduling of generation units was proposed.
- The proposed method (LSSVM) was capable of understanding the physical and environmental constraints of generation units on a real-time basis.
- The proposed method was capable of accurately predicting the power generation unit's behaviour in a dynamic environment.

The integration of weather-sensitive and intermittent power generation resources has caused a greater volatility in power generation and these are required to be accommodated by the optimal dispatch of thermal generation units. By increasing the worldwide concerns about the global warming and the production of pollutant gasses has pushed researchers towards further utilization of clean energies and focusing on smart management of conventional resources. These

issues would be more complicated when considering the settlement period between the consecutive scheduling of generators closer to the time of delivery as it happens in real-time electricity markets.

To address these concerns, the third part of the work was dedicated to formulating a hybrid method based on dynamic programming and priority list ordering method (DP-BP) for optimal allocation of generation units in the context of sub-hourly (real-time) UC. The Proposed method considered the variability of renewable resources like wind and solar on the cost of generation and power reserve determination. The best per unit cost method was employed to facilitate the fast convergence of the algorithms in real-time analysis of the system. The following conclusions were drawn from the work:

- The proposed a robust mathematical formulation for real-time UC-ELD with consideration of physical constraint of thermal generators.
- The proposed method accommodated a high level of renewable energy penetration (up to 40% of total load) in sub-hourly UC and ELD.
- The proposed method considered the availability and intermittency of renewable energies power output in real-time power generation dispatches.
- The proposed method is capable of optimal determination of spinning reserve in the real-time basis considering mixed generation resources.

5.2 Recommendations

The recommended areas of future work are as follows:

- The global search engine of CA3 could be modified and coupled with another optimisation algorithm such as invasive weed optimizer (IWO).
- The future CEED problem could consider the optimal regulation of more pollutant gasses such as $S0_x$ and CO_2.
- The new types of price penalty factor could be studied based on a weighted sum method.
- The RBF-kernel function of LSSVM could be modified to approximate an initial guess with a higher precision for real-time big data applications.
- The LSSVM method could be coupled with other optimisation algorithms to enhance its prediction capabilities in dynamic environments.
- The proposed Sub-hourly UC and ELD method could be reformulated based on mixed integer quadratic programming (MIQP) while clustering on super computers for extremely large sale of interconnected power systems.

- The proposed Sub-hourly UC and ELD method could be modified in order to consider other types of renewable energies such as biomass and ocean energy while considering their generation behaviours.